

***ABLATION OF LIVER TISSUE: A COMPARISON
BETWEEN MICROWAVE, CRYOTHERAPY AND
RADIOFREQUENCY***

Thesis submitted for the degree of

Doctor of Medicine

At the University of Leicester

By

Neil Bhardwaj

University of Leicester

November 2010

This work is dedicated to mum and dad.

You made it possible.

Abstract

Ablation of liver tissue: A comparison between Microwave, cryotherapy and radiofrequency

Author: Neil Bhardwaj

Introduction

The majority of primary and secondary liver tumours are inoperable. 'In situ' thermal destruction techniques such as radiofrequency, microwave ablation and cryotherapy have been employed to treat these inoperable tumours. Despite recent advances in these technologies, large and perivascular tumours still suffer from a relatively high recurrence rate post ablation. This is thought to be due to the loss of thermal energy to surrounding vasculature, known as the heat sink effect. The aim of this project was to investigate the effect of surrounding vasculature on ablation morphology and success and compare the three most popular ablation modalities.

Methods

Standard sized ablations were created in rat liver at various distances from the hilum with all three methods. At various time points, tissue samples were retrieved and underwent histological (H&E) and immuno-cytochemical (Hsp70 and Caspase 3) staining in order to assess lesion evolution and the effects of surrounding vasculature on ablation completeness.

Results

All rats survived. The greatest amount of activity was seen in the transition zone. H&E and immuno-cytochemical analyses of lesion evolution discovered previously unreported cellular changes, particularly in the transition zone. Cryotherapy ablation seemed to be the most irregular and unpredictable of the three. Radiofrequency ablation was uniform but showed evidence of extra-lesional apoptosis and perivascular cell survival in addition to Hsp 70 activity in the transition zone that was affected by surrounding vasculature. Microwave ablation seemed to be influenced least by surrounding vasculature and formed the most uniform lesion with very little extra-lesional collateral damage.

Conclusion

The success of ablation is dependent upon the adjacent blood vessels and microwave ablation seemed to form the most predictable burn and be least affected by surrounding vasculature compared to radiofrequency. Cryotherapy should not be used as first line treatment to treat unresectable liver tumours. In addition the exact role of HSP 70 on the fate of cells in the transition zone, and the subsequent final ablation size and morphology is yet to be determined. Larger ablations in larger animal models may help answer some of these questions.

ACKNOWLEDGEMENTS

This work would not have been possible without the support and dedication of many individuals. The majority of work was undertaken at the Department of Biomedical sciences, University of Leicester and the Department of Histopathology at the Leicester Royal Infirmary.

I am extremely grateful to **Mr. David Lloyd** for giving me the opportunity to undertake this work. It would not have been possible without his encouragement and support. I would also like to thank **Mr. Andrew Strickland**, who through his pioneering work in the field of microwave ablation has made this project possible today. Similarly I am indebted to **Professor Nick London** for his input into thesis format and meticulously and painstakingly proofreading the finished article. I also hope I have done justice to **Mr Ashley Dennison's** enthusiasm towards this project and his faith in my abilities.

I am greatly indebted to **Dr Kevin West** and **Dr John Dormer** at the Department of Histopathology, Leicester Royal Infirmary for their guidance and meticulous pathological analyses. I am greatly indebted to staff at the Department of Biomedical Sciences, University of Leicester for their technical ability and resources. Similarly I am grateful to **Dr Howard Pringle** and **Mrs Angela Gillies** for welcoming me into their lab and providing excellent technical support.

PUBLICATIONS AND PRESENTATIONS

Publications

Bhardwaj N, Strickland AD, Ahmad F, Atanesyan L, West K, Lloyd DM. A Comparative Histological Evaluation of the Ablations Produced by Microwave, Cryotherapy and Radiofrequency in the Liver. *Pathology* 2009; 41(2):168-172.

Bhardwaj N, Strickland AD, Ahmad F, Dennison AR, Lloyd MD. Liver ablation techniques: a review. *Surgical Endoscopy* 2010 Feb; 24(2): 254-65.

Bhardwaj N, Gravante G, Lloyd DM, Dennison ARD. Cryoablation: a Histological review. *Cryobiology* 2010 Aug;61(1):1-9.

Bhardwaj N, Dormer J, Ahmad F, Strickland AD, Gravante G, Beckingham I, West K, Dennison AR, Lloyd DM. Heat shock protein 70 expression following hepatic radiofrequency ablation is affected by adjacent vasculature. (accepted-Journal of Surgical Research).

Bhardwaj N, Dormer J, Ahmad F, Strickland AD, Gravante G, Beckingham I, West K, Dennison AR, Lloyd DM. A Histological evaluation of radiofrequency ablation in the liver;

description of lesion evolution with time and a review of the literature (submitted – Journal of Experimental Pathology).

Bhardwaj N, Dormer J, Ahmad F, Strickland AD, Gravante G, West K, Dennison AR, Lloyd DM. A Histological evaluation of cryotherapy ablation in the liver; description of lesion evolution over time and a review of the literature. (submitted- cryobiology).

Bhardwaj N, Dormer J, Ahmad F, Strickland AD, Gravante G, West K, Dennison AR, Lloyd DM. A Histological evaluation of microwave ablation in the liver; description of lesion evolution over time and a review of the literature. (submitted- Pathology)

Presentations and published abstracts

**The Centenary Pathological meeting of the society of Great Britain and Ireland
4th-7th July 2006, Manchester.**

The heat sink effect may cause inadequate tissue ablation: a histological evaluation of microwave, radiofrequency and Cryoablation in the rat liver.

Bhardwaj N, Strickland AD, Atenesyan L, Ahmad F, West K, Lloyd DM

Journal of Pathology 2006;210(1):55

IHPBA 3rd-7th September 2006, Edinburgh

Incomplete tissue ablation: a histological comparison between microwave, radiofrequency and Cryoablation in the rat liver.

Bhardwaj N, Strickland AD, Atenesyan L, Ahmad F, West K, Lloyd DM.

HPB (2006),8 No 4 (S2) 120.

Symposium on Biomedical Optics (BiOS), 20-25 January 2007, San Jose, CA.

(Invited speaker)

The heat sink effect on ablation morphology: a study comparing microwave, radio-frequency, and cryotherapy.

Bhardwaj N, Strickland AD, Atenesyan L, Ahmad F, West K, Lloyd DM.

AHPBA, 19-22 April, 2007, Las Vegas, Nevada.

The heat sink effect may lead to local recurrence: a comparative study of Radiofrequency, cryotherapy and microwave in the liver

Bhardwaj N, Strickland AD, Atenesyan L, Ahmad F, West K, Lloyd DM.

HPB (2007), No 1 (S2) 100.

ASGBI, 27th and 28th September 2007, Cardiff, Wales.

Radiofrequency and cryoablation may be more affected by the heat sink effect than microwave ablation.

Bhardwaj N, Strickland AD, Atanesyan L, Ahmad F, West K, Lloyd DM.

BJS (2007); 94(S5):35

IHPBA, 7th Feb – 2nd Mar 2008, Mumbai, India.

A comparison of lesions produced by radiofrequency, cryotherapy and microwave ablation in the liver.

Bhardwaj N, Strickland AD, Atanesyan L, Ahmad F, West K, Lloyd DM

HPB 2008; 10(S1)

1.	Chapter 1: Introduction	11
2.	Chapter 2: Methods.....	46
3.	Chapter 3. Survival, weight and bloods.....	67
4.	Chapter 4. Macroscopic lesion size and Haematoxylin & Eosin.....	82
5.	Chapter 5: Hsp 70	123
6.	Chapter 6: Caspase 3.....	146
7.	Chapter 7: Discussion	178

CHAPTER 1: INTRODUCTION

1. Chapter 1: Introduction	11
1.1. Radiofrequency	12
1.1.1. Mechanism of action.....	12
1.1.2. Complication rates	13
1.1.3. Recurrence rates.....	14
1.1.4. Survival.....	14
1.1.5. Limitations and effect of surrounding vasculature	17
1.1.6. Histological studies and lesion evolution	18
1.2. Cryotherapy.....	19
1.2.1. Mechanism of action.....	19
1.2.2. Complications	20
1.2.3. Recurrence rates.....	20
1.2.4. Survival.....	21
1.2.5. Limitations and effect of surrounding vasculature	23
1.2.6. Histological studies and lesion evolution	24
1.3. Microwave.....	26
1.3.1. Mechanism of action.....	26
1.3.2. Complication rate.....	27
1.3.3. Local recurrence.....	27
1.3.4. Survival.....	28
1.3.5. Limitations and effect of surrounding vasculature	31
1.3.6. Histological studies and lesion evolution	32
1.4. Ablation method limitations and unanswered questions.....	33
1.4.1. Previous research projects.....	33
1.4.2. Aims of study.....	34

1. Chapter 1: Introduction

The liver is a common site for both primary and secondary malignancies. Primary liver cancer in the form of Hepatocellular Carcinoma (HCC) is the third commonest cause of cancer deaths worldwide ¹ and around 3,200 new cases are registered in the UK each year ². Although rare in the UK, the incidence of primary liver carcinoma is predicted to rise in the future as a consequence of the Hepatitis C virus epidemic ³. The majority of liver tumours in this country are secondary. Colorectal carcinoma is the commonest gastrointestinal malignancy with over 32,000 cases diagnosed each year in the UK. The liver is often the first site of metastatic disease and Colorectal Liver Metastases (CRLM) are detectable in up to 25% of patients at presentation and approximately a further 50% will eventually develop liver metastases within three years of resection of the primary ⁴.

Untreated liver tumours have an extremely poor prognosis, with an estimated median survival of less than eight months. The best prognosis is in patients with isolated liver metastases ⁵. Liver resection for CRLM results in 5 year survival of 25-44%, with mortality rate of 0-6% and is considered the gold standard treatment ⁶⁻⁹. Unfortunately only 20-30% of patients with metastatic colorectal cancer that is confined to the liver are potentially resectable. This is due to tumour anatomical factors and/or significant patient co-morbidities ¹⁰. Liver transplantation and resection offer similar survival rates for even advanced HCC. However, the scarcity of donor livers and poor liver function reservoir, as HCC often develops on a background of liver cirrhosis, mean only 20-30% of patients are suitable ¹¹.

The search for an alternative treatment option for unresectable liver tumours has led to the development of various ‘in-situ’ tumour ablation techniques. The three main ones in use today are Radiofrequency, Cryotherapy and Microwave ablation. These treatments deploy cytotoxic thermal energy via a probe either in the form of heat (radiofrequency, microwave) or cold (cryotherapy) and cause irreversible cell death.

This chapter aims to describe the mechanism of action, associated complications, local recurrence rates, 3- and 5-year survival and limitations of each treatment modality. In addition, a review of all major studies which identify parameters which may contribute to the limitations will be presented. Pathological studies which describe the ablated lesion in detail and in particular evolution of the lesion are included.

1.1. Radiofrequency

1.1.1. Mechanism of action

The use of energy in the radiofrequency range (RF) as a means of heating tissue was first described in the 19th century ¹². RF ablation refers to coagulation resulting from all electromagnetic energy sources with a frequency less than 900 kHz, with most devices functioning in the range of 300-500 kHz ¹³. Many applications were envisaged for this technology and further studies examined potential areas of clinical application. This experimental work, principally with the use of alternating current sources culminated in the regular use of RF equipment in operating theatres by the late 1920’s.

Initially these devices were used to cauterise or cut tissue by varying the RF current but more recently there has been renewed interest in this technology and particularly its potential to produce a local area of destruction. This resulted in a variety of probes which

are capable of being used to deliver energy in a controlled, localised and predictable manner. This progress in RF technology resulted in electrodes which were capable of ablating tissue at significant distances from the energy source and opened the way for treatment of tumours in the centre of solid organs. Presently available electrodes can be inserted percutaneously, laparoscopically or at laparotomy and the tips of the probes allow an alternating electric field to be created within tissues. The ions in the tissue attempt to follow the direction of the rapidly changing alternating current and the frictional energy which is produced causes heating of the tissue and ultimately coagulative necrosis of a defined volume. With primary or secondary tumours in solid organs such as the liver or kidneys the volume of the ablated area is calculated to engulf the abnormality and produce a safe additional area to ensure that the entire tumour has been destroyed.

1.1.2. Complication rates

There are now a number of studies from around the world which have examined the complication rates and mortality associated RF ablation. In a large Korean survey the rate of major complications was 2.43% with the most common problems being hepatic abscess (0.66%), peritoneal haemorrhage (0.46%), biloma (0.20%), ground pad burns (0.20%), pneumothorax (0.20%) and vasovagal reflex (0.13%)¹⁴. A Belgian team estimated the combined mortality rate from laparoscopic, percutaneous and open RF to be 0.5%. In addition to these major complications abdominal bleeding (1.6%), abdominal infection (1.1%), biliary tract damage (1%), liver failure (0.8%), pulmonary complications (0.8%), dispersive pad burns (0.6%), hepatic vascular damage (0.6%), visceral damage (0.5%) and cardiac complications in 0.4% also occurred¹⁵. A

multicentre Italian study reported a mortality of 0.3% with the use of percutaneous RF and a major complication rate of 2.2% which was directly related to the number of treatment sessions ¹⁶. A group from the Netherlands reported an RF related complication rate of 9.8% and a mortality rate of 1.4% ¹⁷.

Minor side-effects include pain, peri-hepatic fluid collections and thermal damage to adjacent structures and in up to a third of patients there is a recognised phenomenon of post ablation syndrome characterised by fever, malaise, chills and delayed pain/nausea. This is proportional to the size of tumour treated and is usually self-limiting ¹⁸.

1.1.3. Recurrence rates

The recurrence rate following RF treatment is variable with figures ranging from 2 to 43% ¹⁹⁻²³, with the higher rates being associated with percutaneous treatments, larger and peri-vascular tumours ^{21, 23-27}. Needle tract seeding appears to be related to experience and although as high as 12.5% in smaller studies ²⁸ it falls to between 0% - 4% in larger studies. Seeding is more common in patients treated percutaneously for large subcapsular tumours or in patients who have undergone pre-operative biopsy ^{14, 16, 29, 30}.

1.1.4. Survival

There is a surprising paucity of data available for RF survival rates, with few studies quoting 3 year figures. These range between 25-80% and are summarised in Table 1-1 RF studies since 2001 with at least 3 year reported survival.

Table 1-1 RF studies since 2001 with at least 3 year reported survival.

	TUMOUR TYPE	RECURRENCE RATE	SURVIVAL 1YR	2YR	3YR	4YR	5YR
Buscarini ³¹ 2001	HCC	?	89%	62%	33%	n/a	n/a
Solbiati ²¹ 2001	CLM	39%	93%	69%	46%	n/a	n/a
Iannitti ³² 2002	CLM	n/a	87%	77%	50%	n/a	n/a
Guglielmi ³³ 2003	HCC	6.8%	87%	63%	45%	n/a	n/a
Abdalla ³⁴ 2004	CLM	9%	n/a	n/a	n/a	22%	n/a
Gillams ³⁵ 2005	CLM		91%	n/a	40%	n/a	17%
Lu M.-D ³⁶ 2005	HCC	20%	71%	47%	37%	24%	n/a
Tateishi ³⁷ 2005	HCC	n/a	Naive 94%	86%	77%	67%	54%
			Recurrence 91%	75%	62%	53%	38%
Lin S.-M ³⁸ 2005	HCC	14%	93%	81%	74%	n/a	n/a
Chen M ³⁹ 2005	mixed	HCC 10%	87%	67%	58%	n/a	n/a
		Met 14%	87%	48%	25%	n/a	n/a
Raut ⁴⁰ 2005	HCC	4.6%	84%		68%		53%
Machi ⁴¹ 2005	HCC	6.3%	n/a	n/a	n/a	n/a	39%
Navara ⁴² 2005	Mixed	n/a	72%	n/a	52%	n/a	n/a
Lencioni ⁴³ 2005	HCC	10%	97%	71%	57%	n/a	48%
Lermite ⁴⁴ 2006	Mixed	20.6% (overall)	HCC 84%	57%	34%		
			CLM 90%	54%	54%		
Choi D * ⁴⁵ 2007	HCC	11.9%	93%	83%	65%	56%	51%
Choi D # ⁴⁶ 2007	HCC	3%	87%	83%	80%	68%	55%
Zhai ²³ 2007	HCC	43%	(4-5 cm) 78%		48%		17%
			(5-6 cm) 66%		36%		9%

			(>6cm) 53%		28%		0%
Abitabile ₄₇ 2007	CLM	8%	88%	80%	57%	n/a	n/a
Lupo [~] ₄₈ 2007	HCC	n/a	96%	n/a	53%	n/a	32%

CLM – Colorectal metastases. Met- metastases. * RF ablation of recurrent HCC post resection. # RF ablation and hepatectomy. ^ Tumours > 4cm. ~ Tumours 3-5cm.

‡ Study divided results into 1st time ablations (Naïve) and recurrent ablations.

1.1.5. Limitations and effect of surrounding vasculature

Early radiofrequency were inefficient due to the effects of high temperatures in the tissue around the probe. As temperatures in the target tissue approached 100°C the increase in tissue impedance due to tissue desiccation and charring and the formation of electrically insulating gas between the electrode and the tissue due to boiling and evaporation of tissue fluid ^{49, 50} results in a marked reduction in the flow of current ⁵¹. This potentially limits the value of this technology particularly for the treatment of larger tumours but has been addressed to an extent by the use of electrodes with tips which are cooled. Unfortunately the main limitation of RF ablation remains the size of ablations that can be produced following a single insertion of the applicator. This is thought to be principally due to its mechanism of action as only tissue immediately adjacent to the applicator is heated by ionic agitation. The majority of the ablation in the surrounding tissue (the volume required to engulf the tumour) being produced by thermal conduction from this inner region which reduces exponentially as power density falls at increasing distances from the probe. Finite-element computer modelling suggests that this results in an inefficient transformation of electrical energy into heat, particularly at tissue-vessel interfaces where flowing blood thermally protects perivascular tissue and tumour ^{51, 52}.

This method of conductive heating makes it particularly susceptible to the corrupting effects of local large blood vessels where the high blood flow produces cooling referred to as the “heat sink effect”. This is defined as the tissue cooling occurring due to adjacent vessels of greater than one millimetre in diameter that cause deflection of the ablation zone away from the vessel ¹³. This phenomenon may be seen at the tumour tissue/vessel

where blood flow is at its highest ⁵³ and there is the potential for cancer cells to survive and recover, particularly in large tumours. In addition, tumours in the vicinity of large blood vessels may undergo inadequate ablation and may account for the increased rate of local recurrence observed at these sites. Liver parenchyma and primary and secondary liver tumours are water rich and invariably have an extensive vascular supply.

Many approaches have been investigated and developed over the last few years to overcome the problem of vascular mediated cooling by partial or complete inflow occlusion during ablation. This is usually achieved by temporarily occluding the portal vein and hepatic artery (the Pringle manoeuvre) which has been shown to increase the volume of ablation zones while preserving the consistent size of the treated areas ⁵⁴⁻⁵⁸. Unfortunately vascular occlusion obviates the protective effect of the high blood flow found in all areas of the liver and as a consequence increases the incidence of bile duct damage ⁵⁸⁻⁶⁰ and portal vein thrombosis ^{15, 61}. Strategies to reduce bile duct damage by instilling chilled saline in the ducts have been developed in experimental studies ⁶²⁻⁶⁴, but have only been used sporadically in the clinical setting ⁶⁵ and are yet to become part of regular clinical practice.

1.1.6. Histological studies and lesion evolution

Classically the ablated lesion is described as comprising three distinct zones; the ablated zone consists of disrupted cells with cytoplasmic eosinophilia indicative of coagulative necrosis. This is usually surrounded by a zone of either haemorrhage or inflammatory infiltration, commonly referred to as the 'transition zone'. This usually evolves to a

fibroblastic reaction dependent upon the time since the ablation. The outer rim is usually normal liver^{51, 56, 66-73}.

Despite RF being in use for over 20 years, very few studies have described lesion evolution in any great detail, particularly the effects of local or intra-lesional blood flow. Experimental and clinical studies quantifying the vessel size responsible for inadequate ablation are limited but suggest that vessels greater than 3mm in size tend to remain patent with evidence of viable hepatocytes in contact with the vessel^{24, 71, 74-76}.

1.2. Cryotherapy

1.2.1. Mechanism of action

Cryoablation uses repetitive freezing and thawing of tissue to produce necrosis and irreversible tissue destruction will occur between minus 20 and minus 40 °C. Liquid nitrogen and argon gas can both be used as coolants and are capable of producing temperatures of at least minus 40 °C^{12, 77}. The physiological basis of cryotherapy has been well investigated and is dependent upon the rapid formation of intracellular ice crystals during the freezing process. In addition, cellular hypoxia secondary to disruption of surrounding micro vascular structures also induces cell destruction and augments the direct damage resulting from intracellular ice crystal formation^{78, 79}. The completeness of cell destruction is directly proportional to the rapidity and duration of freezing and the rate of thawing. The temperature drops faster and to lower temperatures with decreasing distance from the cryoprobe⁸⁰. Close to the probe the main mechanisms of cell death consist of ice crystals which form within and around cells. These crystals rupture cell

membranes during thawing leading to rehydration and tissue death. Away from the probe ice crystals form only within arterioles and venules but not within cells. In this way the extracellular fluid becomes hypertonic and unfrozen cells dehydrate. Furthermore, the extracellular fluid accumulates within vessels which consequently break during thawing. The haemorrhages produce tissue hypoxia and loss of tissue nutrition ⁸¹.

1.2.2. Complications

The main disadvantage of cryotherapy is the development of the post treatment syndrome known as ‘cryoshock.’ This is a systemic response to ablation which consists of a marked thrombocytopenia (thought to be secondary to the repeated freeze thaw cycles) which leads to coagulopathies, pleural effusions, ARDS like syndrome and myoglobinuria. The incidence of ‘cryoshock’ is difficult to estimate but reports in the literature suggest mortality rate of 0- 8% although a large multicentre survey suggested it was responsible for 18% of the peri-operative deaths ⁸². There is also a surprisingly high rate of local complications such as haemorrhage (from cracking of frozen liver), sub-phrenic abscesses, bilomas and biliary fistulae. Biliary fistulae have been described in all series and occur in almost a third of patients ⁸³. There is a direct relationship between the volume of liver ablated and the incidence of complications ^{82, 84, 85}.

1.2.3. Recurrence rates

The rate of local recurrence following cryotherapy is estimated to be between 9 and 44% ⁸⁶⁻⁸⁸. One of the few trials comparing RF and cryotherapy estimate the recurrence rate for cryoablation to be 13.6% with two-thirds of the recurrence occurring in contact with or adjacent to a major hepatic vessel. Even though technically this is not a heat sink it is

postulated that inflowing warm blood has a protective effect and prevents adequate freezing and destruction of tumour cells directly adjacent to major blood vessels. In these series the combined rate of major and minor complications was 40.7% ²⁰. Large tumours (> 3cm) and tumours close to blood vessels suffer from a higher recurrence rate ⁸⁹. A study from Sloan Kettering compared RF with cryoablation and found a 12% recurrence rate with cryoablation and 14% with RF ⁹⁰.

1.2.4. Survival

Reports of three and five year survival rates following cryotherapy are scarce and ablation is frequently combined with other treatments including chemotherapy and surgery. In one large study, the majority of patients treated with cryoablation also underwent intra-arterial chemotherapy and had a recurrence rate of 33% ⁸⁹. In another study although 3 and 5 year survival rates of 40 and 27% respectively were reported the majority of patients were again treated with multimodal therapies including intra-arterial chemotherapy and hepatic artery ligation ⁹¹. Other studies quote similar figures with a 3 year survival of 48% and 5 year survivals of 28% ⁹² and 26% ⁹³. A significant study comparing laparoscopic and open cryoablation by a group in Italy reported no local recurrences at the treated site with a minor complication rate of 54%. There was a major complication rate of 26% in the open group and 6% in the laparoscopic group with a median survival of 22 months in the open group at a mean follow up period of 39 months ⁹⁴. These studies (summarised in Table 1-2. Large cryoablation studies with at least 3 year survival. illustrate the difficulties encountered when trying to compare the results of cryoablation with surgery or other ablative techniques as most authors report series where a variety of different treatment modalities are used in conjunction with cryoablation.

Table 1-2. Large cryoablation studies with at least 3 year survival.

Study	Tumour type	Recurrence	Survival 1yr	2yr	3yr	4yr	5yr
Weaver 1998 ⁹⁵	CLM	38% (same lobe as ablation)	80% [¥]		40% [¥]		20% [¥]
Zhou 1998 ⁹¹	HCC		n/a	n/a	40%	n/a	27%
Seifert # 1999 ⁸⁹	CLM	33%	46%	16%	8%		
Sheen 2002 ⁹⁶	Mixed		n/a	n/a	CLM 14%	n/a	n/a
Yan * 2003 ⁹⁷	CLM		89%	65%	41%	24%	19%
Kerkar 2004 ⁹²	Mixed	15%	81%	62%	48%	n/a	28%
Seifert 2005 ⁹³	CLM	24%	70% [¥]	n/a	42% [¥]	n/a	26%
Joosten ° 2005 ⁹⁸	CLM	Cryo 20%	76%	61%	40% [¥]		
		RF 14%	93%	75%	50% [¥]	n/a	n/a
Brooks ^ 2005 ⁹⁹	CLM	n/a	85%	n/a	43%	n/a	19%
Yan * 2006 ¹⁰⁰	CLM	39%	87%	65%	43%	28%	23%
Niu 2007 ¹⁰¹	CLM	78%	84%	n/a	43%	n/a	24%

* cryotherapy and hepatic arterial chemotherapy. (2006 study presumably includes patients from study published in 2003)

^ 85% had cryotherapy and hepatic arterial chemotherapy

91% had cryotherapy and hepatic arterial chemotherapy

¥ survival estimated from graph

° Cryotherapy vs RF

1.2.5. Limitations and effect of surrounding vasculature

With cryotherapy it is generally felt important to continue the treatment until at least 1 cm of normal liver parenchyma is included in the 'ice ball' although some users advocate ablating beyond the 1 cm boundary to ensure that lethal temperatures are achieved at the periphery of the tumour and ablation is complete ¹⁰². Unfortunately effective tissue freezing is dependent on adequate conduction of 'coldness' (distal energy transfer from the probe) and experimental data suggests that this reduces substantially as the distance from the probe increases ¹⁰³. This phenomenon may account for the higher tumour recurrences seen with large and perivascular tumours. Two or three freezing cycle approximately doubles the volume and the further addition of the Pringle manoeuvre quadruples it (two times more compared to the absence of vascular inflow occlusion) ^{80, 104, 105}. Same results are obtained with total vascular exclusion (clamping of the infra and suprahepatic vena cava along with the Pringle manoeuvre) ¹⁰⁶. The borders achieved during Pringle manoeuvre are more regular than those obtained without, in which indentations are observed ¹⁰⁴. Limited experimental work has attempted to prevent bile duct damage by the infusion of intra-ductal warm saline, however this has not become part of regular clinical practice ¹⁰⁷.

There are only a few studies which have attempted to describe the interaction between vascular structures and the cryoablated lesion. A unique study which ablated in close proximity to the vena cava under total vascular exclusion reported complete cellular destruction in all lesions ¹⁰⁶ but others have also reported concomitant venous thromboses associated with vascular exclusion ¹⁰⁸. Other studies report survival of ablated

hepatocytes in close proximity to the retro-hepatic vena cava in pigs with only minimal necrosis of the vessel intima ¹⁰⁹. A repeat experiment by the same group, with and without total vascular exclusion produced adventitial damage of the vena cava and transmural necrosis with intimal disruption following 83% and 67% of treatments respectively. However, without vascular exclusion comparable changes were found in 71% and 14% respectively. Significantly, no hepatocyte survival adjacent to the vena cava was evident in either case. This approach is clearly not possible in the clinical setting due to the problems associated with complete occlusion of both the inflow and outflow of the liver ¹⁰⁶. Other studies in a porcine model have compared vessel integrity in the centre of an ablated area and compared them with those at the periphery. All lesions examined showed necrosis up to the vessel wall with relative sparing of the adventitia. Vessels showed evidence of thromboses in 50% of vessels when they were centrally located and in 22% when they were peripheral. The ice-ball was seen to be deflected from patent blood vessels greater than 2 mm but crucially when tissue from non-deflected ice-balls which were macroscopically normal were examined, over 60% of blood vessels were thrombosed ¹¹⁰. Other studies have demonstrated evidence of hepatocyte survival at the periphery of treated areas when temperatures that were achieved did not fall below -15°C ^{105, 111}. These studies suggest that the vascular structures do substantiate hepatocyte survival, particularly at the periphery of lesions.

1.2.6. Histological studies and lesion evolution

Heard in 1955 was one of the first to describe the morphological appearances of a liver subjected to slow cooling by liquid nitrogen ¹¹². The ablated area usually consists of an

area of central necrosis^{113, 114}, which is usually heterogenous with leukocyte infiltration¹⁷ or complete loss of nuclear and cytoplasmic detail¹¹⁵. This is surrounded by sinusoidal congestion and haemorrhage, principally observed in the portal zone connective tissue and central veins^{116, 117}, similar to the ‘transition zone’ of RF ablation. By 24 hours, the lesion is divided into 3 zones; a central zone of pan-coagulative necrosis, an intermediate zone of infiltrating polymorphonuclear leukocytes and a thin outer zone of reactive hyperaemia^{80, 81, 105, 110, 111, 113, 118}. This clear demarcation continues up until 1 week post-ablation, where the hyperaemic area is largely replaced by granulation tissue and early changes associated with the formation of fibrosis (loose fibrous tissue with neo-vascularization, proliferating biliary ductules, hemosiderin-laden macrophages, foreign-body type giant cells and foci of calcification)^{116, 118}. However, in proximity to large blood vessels there is an increase in the ‘transition zone’ which causes distortion of the ablation¹⁰⁴ with a pronounced band of fibrosis at the deep margins of the lesion, capillary proliferation and mild inflammation extending from adjacent normal liver into the area of coagulation necrosis resulting in the scalloped appearance of the margin¹¹¹. Interestingly, medium- to large-size bile ducts and arteries were preserved in both the zones of coagulative necrosis and granulation tissue whereas smaller adjacent veins showed endothelial damage¹¹⁸.

In most studies by day 21 after cryoablation, two clear zones have developed with a central area of persistent necrosis and an outer area of granulation and fibrous tissue without an intervening inflammatory zone¹¹⁶. There are a smaller number of reports where the persistence of the initial three zones is described up to a month post ablation

¹¹⁹. From the outer zone, fibrous septa extend into the area of coagulative necrosis which appears significantly reduced in size ^{116, 118}. By week 4 the lesion consists principally of fibrous tissue, although with survival of large vessels and bile ducts ^{105, 111, 116, 118}. After more than sixty days following cryoablation, a small area of fibrosis was the only evidence of previous cellular destruction ^{111, 120}.

1.3. Microwave

1.3.1. Mechanism of action

Microwave ablation is the term usually reserved for all equipment inducing tumour destruction with frequencies in the range of 900-2450 MHz. Within this electromagnetic field, polar molecules (mainly water), try to align themselves in the direction of the current and as the direction changes constantly this continuous realignment causes a heating effect. Microwaves are tuned to the natural resonant frequency of water in order to enhance this interaction. Electromagnetic energy heats tissue by targeting the water molecules and like RF induces cell death by coagulative necrosis ^{121, 122}. The first clinical microwave generator was developed in 1979 and initially the technology was used as an aid to liver resection due to its ability to cut and coagulate liver parenchyma ¹²³. Over the years this initial design has been modified to encompass a wide range of clinical applications, from endometrial ablation for menorrhagia, to widespread use in ablating primary and secondary tumours in the liver and lungs. The equipment available today consists of a magnetron in a microwave generator and a coaxial cable and probe. Probes

are available in several different sizes depending on whether the procedure is to be performed percutaneously, laparoscopically or at open surgery.

1.3.2. Complication rate

In the clinical setting microwave ablation has principally been used in the far-east to treat hepatocellular carcinomas (HCC). The majority of these series involve percutaneous treatment of these tumours as the presence of background cirrhosis often means that these patients are unsuitable for a major surgical resection. Early reported series of microwave ablation suggested that the complication rates were encouragingly low ^{124, 125}, but results from later series reported high complication rates of 14.2 % in patients treated for HCC and 20.6% in those with metastases. The authors suggested a number of approaches to avoid bleeding, biloma formation and dissemination ¹²⁶. Other less common complications including portal vein thrombosis and post ablation pneumothorax ^{127, 128}. Overall however, the complication rates reported in large case series have been steadily reducing and consistently appear to be lower than those reported with RF and cryotherapy.

1.3.3. Local recurrence

Several series have compared microwave and RF ablation of hepatocellular carcinoma and found microwave to have a lower recurrence rate of 7% compared to 12.8% with RF ¹²⁹. Another study comparing microwave and RF recurrence, survival and complication

rates reported a lower recurrence rate of 11.8% with microwave compared to 20.9% for RF. In addition overall survival at one, two, three and four years for microwave (81%, 61%, 50% and 36% respectively) was better than for RF (71%, 47%, 37% and 24% respectively). However the overall major complication rate was higher with microwave (8.2% versus 5.7%)³⁶. While generally results were superior for microwave treatment some series found little difference and concluded that both modalities had equivalent therapeutic effects, complication rates and rates of residual foci of untreated disease¹³⁰. One large series of 288 patients with no microwave treatment related complications reported a local recurrence rate of 8% and 1, 2, 3, 4 and 5 year survival rates of 93%, 82%, 72%, 63% and 51% respectively. Survival was worst in patients with the largest tumours, those with the greatest number and also where there was a higher Child-Pugh classification¹³¹. Another large series with no major complications reported equally encouraging results in 234 patients undergoing ablation of 339 nodules. Survival at 1, 2, 3, 4 and 5-years was 92%, 81%, 72%, 66%, 56% respectively and a 90% of patients analysed post-ablation, either by biopsy or cross sectional imaging, showed no evidence of residual tumour¹³². In respect of 1, 2, 3 and 4-year survival rates of 94%, 78%, 78% and 62% respectively this is comparable with other series¹³³.

1.3.4. Survival

A 3 year survival rate of 40%, a local recurrence rate of 2% and an extremely low microwave related complication rate have been reported¹³⁴ and these results are supported by other groups, who report a low morbidity and mortality, a 2% local recurrence rate and similar survival rates¹³⁵. One randomised study suggested that treatment of patients with microwave therapy had comparable results to standard hepatic

resection for colorectal liver metastases. The authors concluded that the main advantages with percutaneous microwave ablation were the shorter treatment times, reduced blood loss and the option of repeated treatments. Results suggest that survival in patients undergoing resection and ablation is similar to those patients undergoing hepatic resection only ¹³⁶. The major studies are summarised in Table 1-3. Microwave ablation studies with at least 30 patients and 3 years follow up).

Table 1-3. Microwave ablation studies with at least 30 patients and 3 years follow up

Study	Type	Recurrence	1 year survival	2year	3year	4 year	5 year
Shibata 1999 ¹³⁷	CLM	n/a	71%	57%	14%		
Itamoto 1999 ¹³³	HCC	50%	Primary HCC 94%	78%	78%	62%	
			Recurrent HCC 100%	79%	62%	41%	
Liang 2005 ¹³¹	HCC	8%	93%	82%	72%	63%	51%
Xu 2005 ¹²⁹	HCC	RF 12%	75% *	58% *	50% *		
		MW 7%					
Lu 2005 ³⁶	HCC	RF 20%	71%	47%	37%	24%	
		MW 11%	81%	61%	50%	36%	
Dong 2006 ¹³⁸	HCC	52% #	84%	88%	80%	74%	68%
Tanaka 2006 ¹³⁶	CLM	22%	56%		39%	39%	
Wang 2007 ¹³⁹	HCC	n/a	72%		54%		33%
Bhardwaj 2008 ¹³⁴	Mixed	2%	71%	62%	40%		

*Combined survival of RF and MW

overall recurrence at 5 years

HCC -Hepatocellular carcinoma. CLM -colorectal metastases

1.3.5. Limitations and effect of surrounding vasculature

In addition to the larger volumes that are now possible, microwave coagulation is an extremely efficient way of heating tissue and has been shown to have a better convection profile, higher intra-tumoural temperatures, faster ablation times and larger ablation zones when compared to RF. This theoretical advantage is probably due to the broader field of power density surrounding the applicator, thus creating a larger and more uniform zone. In comparison, as described earlier, active RF heating is limited to a few mm around the applicator with reliance on conduction of cytotoxic temperatures through the tissues in order to create an ablation zone^{121, 140, 141}. As a consequence the final delivered current at the periphery of tissues and subsequent thermal energy with RF is inversely proportional to the square of the distance from the electrode¹⁴².

Limited experimental work has been performed on the safety and efficacy of microwave ablation near large vessels. Several experimental¹⁴³ and clinical studies^{144, 145} report that the ablation size increases on vascular clamping and is also associated with a lower local recurrence rate. Microwave ablation has expanded the indications for potentially curative resections particularly in those patients with bi-lobar liver tumours. However particularly with the early generation of machines one of the main limitations was the difficulty of creating consistent ablation zones larger than 3cm. This limited their use in larger tumours and considerable effort was expended in developing generators and probes that could overcome these limitations.

Recent work on porcine liver, preceding this research project has demonstrated the ability of these new generators to produce large volume (5 to 8cm) ablations reproducibly^{122, 146}.

The main disadvantage of microwave therapy is that its use as an ablative technology is still in its relative infancy in the West and indications and limitations for its use are still evolving. Nevertheless its increasing safety record and ability to produce larger lesions (similar in size to lesions produced by RF), in significantly less time than RF makes it an extremely attractive modality.

1.3.6. Histological studies and lesion evolution

There are only 10 studies which describe in detail the histological changes which occur following microwave ablation^{51, 122, 147-154} and only 5 described the lesion evolution at specific time points^{51, 122, 147, 149, 150}. The classical microwave lesion consists of a central area of 'fixed' cells in direct contact with the probe and tissue which has undergone coagulative necrosis. This is surrounded by a 'transition zone' of mixed marked inflammatory infiltrate, diffuse congestion and haemorrhage and an outer area of normal tissue or 'reference' zone. The 'fixative effect' on hepatocytes in direct contact with the applicator is unique to microwave ablation^{122 51, 122, 148, 149, 151-154}. Although these hepatocytes demonstrate intact morphology, vital oxidative stains prove that these cells are non-viable¹⁵¹⁻¹⁵⁵. Microwave irradiation has been used *in vitro* for many years to 'fix' cells in their morphological state^{156, 157} and this phenomenon probably explains the 'fixed effect' observed with microwave ablation *in vivo*. By week 1, the 3 distinct zones persist, consisting of shrunken necrotic central zone, neutrophil and necrotic hepatocyte infiltrated transition zone and fibroblast along with giant cell infiltrated outer zone. By week 2, there is shrinkage of central lesion and increased outer zone fibrosis and from month 1 onwards complete loss of zonal structure, central necrosis with foreign body

granulomas and fibrous capsule infiltrated by macrophages and giant cells is evident ^{51, 122, 147, 149, 150}.

At all time points, the edge of the ablated area is usually well demarcated and uniform, with very little disruption as a result of any surrounding vasculature ^{51, 122, 146, 148, 150}. It is therefore not surprising that there is an increasing body of evidence demonstrating that RF is more susceptible to the 'heat sink' effect than microwave ablation ⁵¹.

1.4. Ablation method limitations and unanswered questions

All ablative modalities suffer from a common Achilles heel; local recurrence and inadequate ablation particularly near blood vessels. Despite all the technological advances of the last decade, the perfect ablative modality still remains elusive. An ideal ablation should cause complete tumour destruction with negligible normal parenchyma disruption, be minimally invasive, reproducible, systemically safe, rapid and easily visualised intra-operatively. None of the above technologies fulfil all these criteria. Several areas of controversy still remain, particularly, the treatment of large tumours, and the effect of blood vessels on ablation morphology.

1.4.1. Previous research projects

Previous research conducted at the University of Leicester has addressed feasibility of large ablation sizes with microwave ablation (Strickland MD 2005). This was followed by a study which compared microwave, radiofrequency and cryotherapy and the systemic effects of large volume ablation in the rat liver (Ahmad MD 2009). This chapter has paid

particular attention to studies that describe the effect of any surrounding vasculature on ablation morphology and although there are experimental and research studies described there is a paucity of research in this area, in particular no comparison work describing peri-vascular lesion evolution in all three ablative modalities is available.

1.4.2. Aims of study

The aim of this study therefore will be to compare all 3 modalities and investigate the effect of ablating a set volume of liver in-vivo at various distances from major vascular structures on ablation morphology and surrounding parenchyma along with describing lesion evolution at various time points.

1. Ferlay J. Cancer incidence, mortality and prevalence worldwide. *IARC PRESS LYON*. 2004;IARC Cancer base 5(Version 2).
2. Office for National Statistics, 2009. Cancer statistics registrations: registrations of cancer diagnosed in 2006, England. <http://info.cancerresearchuk.org/cancerstats/types/liver/incidence/index.htm>.
3. Taylor-Robinson SD, Foster GR, Arora S, Hargreaves S, Thomas HC. Increase in primary liver cancer in the UK, 1979-94. *Lancet*. Oct 18 1997;350(9085):1142-1143.
4. Garden OJ, Rees M, Poston GJ, et al. Guidelines for resection of colorectal cancer liver metastases. *Gut*. Aug 2006;55 Suppl 3:iii1-8.
5. Lahr CJ, Soong SJ, Cloud G, Smith JW, Urist MM, Balch CM. A multifactorial analysis of prognostic factors in patients with liver metastases from colorectal carcinoma. *J Clin Oncol*. Nov 1983;1(11):720-726.
6. Cady B, Stone MD. The role of surgical resection of liver metastases in colorectal carcinoma. *Semin Oncol*. Aug 1991;18(4):399-406.
7. Choti MA, Bulkley GB. Management of hepatic metastases. *Liver Transpl Surg*. Jan 1999;5(1):65-80.
8. Fong Y, Fortner J, Sun RL, Brennan MF, Blumgart LH. Clinical score for predicting recurrence after hepatic resection for metastatic colorectal cancer: analysis of 1001 consecutive cases. *Ann Surg*. Sep 1999;230(3):309-318; discussion 318-321.
9. Scheele J, Stang R, Altendorf-Hofmann A, Paul M. Resection of colorectal liver metastases. *World J Surg*. Jan-Feb 1995;19(1):59-71.
10. Stangl R, Altendorf-Hofmann A, Charnley RM, Scheele J. Factors influencing the natural history of colorectal liver metastases. *Lancet*. Jun 4 1994;343(8910):1405-1410.
11. Balsells J, Charco R, Lazaro JL, et al. Resection of hepatocellular carcinoma in patients with cirrhosis. *Br J Surg*. Jun 1996;83(6):758-761.
12. Gillams AR. Liver ablation therapy. *Br J Radiol*. Sep 2004;77(921):713-723.
13. Goldberg SN, Charboneau JW, Dodd GD, 3rd, et al. Image-guided tumor ablation: proposal for standardization of terms and reporting criteria. *Radiology*. Aug 2003;228(2):335-345.
14. Rhim H, Yoon KH, Lee JM, et al. Major complications after radio-frequency thermal ablation of hepatic tumors: spectrum of imaging findings. *Radiographics*. Jan-Feb 2003;23(1):123-134; discussion 134-126.
15. Mulier S, Mulier P, Ni Y, et al. Complications of radiofrequency coagulation of liver tumours. *Br J Surg*. Oct 2002;89(10):1206-1222.
16. Livraghi T, Solbiati L, Meloni MF, Gazelle GS, Halpern EF, Goldberg SN. Treatment of focal liver tumors with percutaneous radio-frequency ablation: complications encountered in a multicenter study. *Radiology*. Feb 2003;226(2):441-451.

17. Jansen MC, van Duijnhoven FH, van Hillegersberg R, et al. Adverse effects of radiofrequency ablation of liver tumours in the Netherlands. *Br J Surg*. Oct 2005;92(10):1248-1254.
18. Dodd GD, 3rd, Napier D, Schoolfield JD, Hubbard L. Percutaneous radiofrequency ablation of hepatic tumors: postablation syndrome. *AJR Am J Roentgenol*. Jul 2005;185(1):51-57.
19. Curley SA, Izzo F, Delrio P, et al. Radiofrequency ablation of unresectable primary and metastatic hepatic malignancies: results in 123 patients. *Ann Surg*. Jul 1999;230(1):1-8.
20. Pearson AS, Izzo F, Fleming RY, et al. Intraoperative radiofrequency ablation or cryoablation for hepatic malignancies. *Am J Surg*. Dec 1999;178(6):592-599.
21. Solbiati L, Livraghi T, Goldberg SN, et al. Percutaneous radio-frequency ablation of hepatic metastases from colorectal cancer: long-term results in 117 patients. *Radiology*. Oct 2001;221(1):159-166.
22. Wong SL, Edwards MJ, Chao C, Simpson D, McMasters KM. Radiofrequency ablation for unresectable hepatic tumors. *Am J Surg*. Dec 2001;182(6):552-557.
23. Zhai, B. Xu A-M, Chen Y, Li X, -Y et al. . Radiofrequency ablation for larger Hepatocellular carcinomas. *Academic Journal of Second Military Medical University*. 2007;28(6):651-655.
24. Lu DS, Raman SS, Limanond P, et al. Influence of large peritumoral vessels on outcome of radiofrequency ablation of liver tumors. *J Vasc Interv Radiol*. Oct 2003;14(10):1267-1274.
25. Livraghi T, Goldberg SN, Lazzaroni S, et al. Hepatocellular carcinoma: radio-frequency ablation of medium and large lesions. *Radiology*. Mar 2000;214(3):761-768.
26. Mulier S, Ni Y, Jamart J, Ruers T, Marchal G, Michel L. Local recurrence after hepatic radiofrequency coagulation: multivariate meta-analysis and review of contributing factors. *Ann Surg*. Aug 2005;242(2):158-171.
27. Wood TF, Rose DM, Chung M, Allegra DP, Foshag LJ, Bilchik AJ. Radiofrequency ablation of 231 unresectable hepatic tumors: indications, limitations, and complications. *Ann Surg Oncol*. Sep 2000;7(8):593-600.
28. Llovet JM, Vilana R, Bru C, et al. Increased risk of tumor seeding after percutaneous radiofrequency ablation for single hepatocellular carcinoma. *Hepatology*. May 2001;33(5):1124-1129.
29. de Baere T, Risse O, Kuoch V, et al. Adverse events during radiofrequency treatment of 582 hepatic tumors. *AJR Am J Roentgenol*. Sep 2003;181(3):695-700.
30. Jaskolka JD, Asch MR, Kachura JR, et al. Needle tract seeding after radiofrequency ablation of hepatic tumors. *J Vasc Interv Radiol*. Apr 2005;16(4):485-491.
31. Buscarini L, Buscarini E, Di Stasi M, Vallisa D, Quaretti P, Rocca A. Percutaneous radiofrequency ablation of small hepatocellular carcinoma: long-term results. *Eur Radiol*. 2001;11(6):914-921.
32. Iannitti DA, Dupuy DE, Mayo-Smith WW, Murphy B. Hepatic radiofrequency ablation. *Arch Surg*. Apr 2002;137(4):422-426; discussion 427.

33. Guglielmi A, Ruzzenente A, Battocchia A, Tonon A, Fracastoro G, Cordiano C. Radiofrequency ablation of hepatocellular carcinoma in cirrhotic patients. *Hepatogastroenterology*. Mar-Apr 2003;50(50):480-484.
34. Abdalla EK, Vauthey JN, Ellis LM, et al. Recurrence and outcomes following hepatic resection, radiofrequency ablation, and combined resection/ablation for colorectal liver metastases. *Ann Surg*. Jun 2004;239(6):818-825; discussion 825-817.
35. Gillams AR, Lees WR. Radiofrequency ablation of colorectal liver metastases. *Abdom Imaging*. Jul-Aug 2005;30(4):419-426.
36. Lu MD, Xu HX, Xie XY, et al. Percutaneous microwave and radiofrequency ablation for hepatocellular carcinoma: a retrospective comparative study. *J Gastroenterol*. Nov 2005;40(11):1054-1060.
37. Tateishi R, Shiina S, Teratani T, et al. Percutaneous radiofrequency ablation for hepatocellular carcinoma. An analysis of 1000 cases. *Cancer*. Mar 15 2005;103(6):1201-1209.
38. Lin SM, Lin CJ, Lin CC, Hsu CW, Chen YC. Randomised controlled trial comparing percutaneous radiofrequency thermal ablation, percutaneous ethanol injection, and percutaneous acetic acid injection to treat hepatocellular carcinoma of 3 cm or less. *Gut*. Aug 2005;54(8):1151-1156.
39. Chen MH, Yang W, Yan K, et al. [Standard treatment of liver malignancies with radiofrequency ablation]. *Zhonghua Yi Xue Za Zhi*. Jul 6 2005;85(25):1741-1746.
40. Raut CP, Izzo F, Marra P, et al. Significant long-term survival after radiofrequency ablation of unresectable hepatocellular carcinoma in patients with cirrhosis. *Ann Surg Oncol*. Aug 2005;12(8):616-628.
41. Machi J, Bueno RS, Wong LL. Long-term follow-up outcome of patients undergoing radiofrequency ablation for unresectable hepatocellular carcinoma. *World J Surg*. Nov 2005;29(11):1364-1373.
42. Navarra G, Ayav A, Weber JC, et al. Short- and-long term results of intraoperative radiofrequency ablation of liver metastases. *Int J Colorectal Dis*. Nov 2005;20(6):521-528.
43. Lencioni R, Cioni D, Crocetti L, et al. Early-stage hepatocellular carcinoma in patients with cirrhosis: long-term results of percutaneous image-guided radiofrequency ablation. *Radiology*. Mar 2005;234(3):961-967.
44. Lermite E, Lebigot J, Oberti F, et al. Radiofrequency thermal ablation of liver carcinoma. Prospective study of 82 lesions. *Gastroenterol Clin Biol*. Jan 2006;30(1):130-135.
45. Choi D, Lim HK, Rhim H, et al. Percutaneous radiofrequency ablation for recurrent hepatocellular carcinoma after hepatectomy: long-term results and prognostic factors. *Ann Surg Oncol*. Aug 2007;14(8):2319-2329.
46. Choi D, Lim HK, Joh JW, et al. Combined hepatectomy and radiofrequency ablation for multifocal hepatocellular carcinomas: long-term follow-up results and prognostic factors. *Ann Surg Oncol*. Dec 2007;14(12):3510-3518.
47. Abitabile P, Hartl U, Lange J, Maurer CA. Radiofrequency ablation permits an effective treatment for colorectal liver metastasis. *Eur J Surg Oncol*. Feb 2007;33(1):67-71.

48. Lupo L, Panzera P, Giannelli G, Memeo M, Gentile A, Memeo V. Single hepatocellular carcinoma ranging from 3 to 5 cm: radiofrequency ablation or resection? *HPB (Oxford)*. 2007;9(6):429-434.
49. Livraghi T, Goldberg SN, Monti F, et al. Saline-enhanced radio-frequency tissue ablation in the treatment of liver metastases. *Radiology*. Jan 1997;202(1):205-210.
50. McGahan JP, Brock JM, Tesluk H, Gu WZ, Schneider P, Browning PD. Hepatic ablation with use of radio-frequency electrocautery in the animal model. *J Vasc Interv Radiol*. May 1992;3(2):291-297.
51. Wright AS, Sampson LA, Warner TF, Mahvi DM, Lee FT, Jr. Radiofrequency versus microwave ablation in a hepatic porcine model. *Radiology*. Jul 2005;236(1):132-139.
52. Tungjitkusolmun S, Staelin ST, Haemmerich D, et al. Three-Dimensional finite-element analyses for radio-frequency hepatic tumor ablation. *IEEE Trans Biomed Eng*. Jan 2002;49(1):3-9.
53. Nikfarjam M, Muralidharan V, Christophi C. Mechanisms of focal heat destruction of liver tumors. *J Surg Res*. Aug 2005;127(2):208-223.
54. Ritz JP, Lehmann KS, Isbert C, et al. In-vivo evaluation of a novel bipolar radiofrequency device for interstitial thermotherapy of liver tumors during normal and interrupted hepatic perfusion. *J Surg Res*. Jun 15 2006;133(2):176-184.
55. Yoshimoto T, Kotoh K, Horikawa Y, et al. Decreased portal flow volume increases the area of necrosis caused by radio frequency ablation in pigs. *Liver Int*. Apr 2007;27(3):368-372.
56. Frich L, Mala T, Gladhaug IP. Hepatic radiofrequency ablation using perfusion electrodes in a pig model: effect of the Pringle manoeuvre. *Eur J Surg Oncol*. Jun 2006;32(5):527-532.
57. Wiersinga WJ, Jansen MC, Straatsburg IH, et al. Lesion progression with time and the effect of vascular occlusion following radiofrequency ablation of the liver. *Br J Surg*. Mar 2003;90(3):306-312.
58. Kim SK, Lim HK, Ryu JA, et al. Radiofrequency ablation of rabbit liver in vivo: effect of the pringle maneuver on pathologic changes in liver surrounding the ablation zone. *Korean J Radiol*. Oct-Dec 2004;5(4):240-249.
59. Patterson EJ, Scudamore CH, Owen DA, Nagy AG, Buczkowski AK. Radiofrequency ablation of porcine liver in vivo: effects of blood flow and treatment time on lesion size. *Ann Surg*. Apr 1998;227(4):559-565.
60. Marchal F, Elias D, Rauch P, et al. Biliary lesions during radiofrequency ablation in liver. Study on the pig. *Eur Surg Res*. Mar-Apr 2004;36(2):88-94.
61. Ng KK, Lam CM, Poon RT, Shek TW, Fan ST, Wong J. Delayed portal vein thrombosis after experimental radiofrequency ablation near the main portal vein. *Br J Surg*. May 2004;91(5):632-639.
62. Stippel DL, Bangard C, Kasper HU, Fischer JH, Holscher AH, Gossmann A. Experimental bile duct protection by intraductal cooling during radiofrequency ablation. *Br J Surg*. Jul 2005;92(7):849-855.
63. Raman SS, Aziz D, Chang X, et al. Minimizing central bile duct injury during radiofrequency ablation: use of intraductal chilled saline perfusion--initial observations from a study in pigs. *Radiology*. Jul 2004;232(1):154-159.

64. Marchal F, Elias D, Rauch P, et al. Prevention of biliary lesions that may occur during radiofrequency ablation of the liver: study on the pig. *Ann Surg.* Jan 2006;243(1):82-88.
65. Elias D, Sideris L, Pocard M, Dromain C, De Baere T. Intraductal cooling of the main bile ducts during radiofrequency ablation prevents biliary stenosis. *J Am Coll Surg.* May 2004;198(5):717-721.
66. Coad JE, Kosari K, Humar A, Sielaff TD. Radiofrequency ablation causes 'thermal fixation' of hepatocellular carcinoma: a post-liver transplant histopathologic study. *Clin Transplant.* Aug 2003;17(4):377-384.
67. Hinz S, Egberts JH, Pauser U, Schafmayer C, Fandrich F, Tepel J. Electrolytic ablation is as effective as radiofrequency ablation in the treatment of artificial liver metastases in a pig model. *J Surg Oncol.* Aug 1 2008;98(2):135-138.
68. Raman SS, Lu DS, Vodopich DJ, Sayre J, Lassman C. Creation of radiofrequency lesions in a porcine model: correlation with sonography, CT, and histopathology. *AJR Am J Roentgenol.* Nov 2000;175(5):1253-1258.
69. Lee JD, Lee JM, Kim SW, Kim CS, Mun WS. MR imaging-histopathologic correlation of radiofrequency thermal ablation lesion in a rabbit liver model: observation during acute and chronic stages. *Korean J Radiol.* Jul-Sep 2001;2(3):151-158.
70. Scudamore CH, Buczkowski A, Nagy A et al. . Possible injuries to intrahepatic and perihepatic structures with radiofrequency probe. *Surgical Endoscopy.* 1997;11:193.
71. Lu DS, Raman SS, Vodopich DJ, Wang M, Sayre J, Lassman C. Effect of vessel size on creation of hepatic radiofrequency lesions in pigs: assessment of the "heat sink" effect. *AJR Am J Roentgenol.* Jan 2002;178(1):47-51.
72. Scudamore CH, Lee SI, Patterson EJ, et al. Radiofrequency ablation followed by resection of malignant liver tumors. *Am J Surg.* May 1999;177(5):411-417.
73. Morimoto M, Sugimori K, Shirato K, et al. Treatment of hepatocellular carcinoma with radiofrequency ablation: radiologic-histologic correlation during follow-up periods. *Hepatology.* Jun 2002;35(6):1467-1475.
74. Tamaki K, Shimizu I, Oshio A, et al. Influence of large intrahepatic blood vessels on the gross and histological characteristics of lesions produced by radiofrequency ablation in a pig liver model. *Liver Int.* Dec 2004;24(6):696-701.
75. Hansen PD, Rogers S, Corless CL, Swanstrom LL, Siperstien AE. Radiofrequency ablation lesions in a pig liver model. *J Surg Res.* Nov 1999;87(1):114-121.
76. Sato K, Nakamura K, Hamuro M, et al. The influence of radiofrequency ablation on hepatic vessels in porcine liver. *Hepatogastroenterology.* Mar-Apr 2005;52(62):571-574.
77. Khatri VP, McGahan J. Non-resection approaches for colorectal liver metastases. *Surg Clin North Am.* Apr 2004;84(2):587-606.
78. Gage AA, Baust J. Mechanisms of tissue injury in cryosurgery. *Cryobiology.* Nov 1998;37(3):171-186.
79. Gage AA, Guest K, Montes M, Caruana JA, Whalen DA, Jr. Effect of varying freezing and thawing rates in experimental cryosurgery. *Cryobiology.* Apr 1985;22(2):175-182.

80. Seifert JK, Gerharz CD, Mattes F, et al. A pig model of hepatic cryotherapy. In vivo temperature distribution during freezing and histopathological changes. *Cryobiology*. Dec 2003;47(3):214-226.
81. Lee FT, Jr., Chosy SG, Littrup PJ, Warner TF, Kuhlman JE, Mahvi DM. CT-monitored percutaneous cryoablation in a pig liver model: pilot study. *Radiology*. Jun 1999;211(3):687-692.
82. Seifert JK, Morris DL. World survey on the complications of hepatic and prostate cryotherapy. *World J Surg*. Feb 1999;23(2):109-113; discussion 113-104.
83. Seifert JK, Morris DL. Prognostic factors after cryotherapy for hepatic metastases from colorectal cancer. *Ann Surg*. Aug 1998;228(2):201-208.
84. Sarantou T, Bilchik A, Ramming KP. Complications of hepatic cryosurgery. *Semin Surg Oncol*. Mar 1998;14(2):156-162.
85. Sohn RL, Carlin AM, Steffes C, et al. The extent of cryosurgery increases the complication rate after hepatic cryoablation. *Am Surg*. Apr 2003;69(4):317-322; discussion 322-313.
86. Adam R, Akpinar E, Johann M, Kunstlinger F, Majno P, Bismuth H. Place of cryosurgery in the treatment of malignant liver tumors. *Ann Surg*. Jan 1997;225(1):39-38; discussion 48-50.
87. Mala T, Edwin B, Mathisen O, et al. Cryoablation of colorectal liver metastases: minimally invasive tumour control. *Scand J Gastroenterol*. Jun 2004;39(6):571-578.
88. Onik G, Rubinsky B, Zemel R, et al. Ultrasound-guided hepatic cryosurgery in the treatment of metastatic colon carcinoma. Preliminary results. *Cancer*. Feb 15 1991;67(4):901-907.
89. Seifert JK, Morris DL. Indicators of recurrence following cryotherapy for hepatic metastases from colorectal cancer. *Br J Surg*. Feb 1999;86(2):234-240.
90. Kornprat P, Jarnagin WR, DeMatteo RP, Fong Y, Blumgart LH, D'Angelica M. Role of intraoperative thermoablation combined with resection in the treatment of hepatic metastasis from colorectal cancer. *Arch Surg*. Nov 2007;142(11):1087-1092.
91. Zhou XD, Tang ZY. Cryotherapy for primary liver cancer. *Semin Surg Oncol*. Mar 1998;14(2):171-174.
92. Kerkar S, Carlin AM, Sohn RL, et al. Long-term follow up and prognostic factors for cryotherapy of malignant liver tumors. *Surgery*. Oct 2004;136(4):770-779.
93. Seifert JK, Springer A, Baier P, Junginger T. Liver resection or cryotherapy for colorectal liver metastases: a prospective case control study. *Int J Colorectal Dis*. Nov 2005;20(6):507-520.
94. Paganini AM, Rotundo A, Barchetti L, Lezoche E. Cryosurgical ablation of hepatic colorectal metastases. *Surg Oncol*. Dec 2007;16 Suppl 1:S137-140.
95. Weaver ML, Ashton JG, Zemel R. Treatment of colorectal liver metastases by cryotherapy. *Semin Surg Oncol*. Mar 1998;14(2):163-170.
96. Sheen AJ, Poston GJ, Sherlock DJ. Cryotherapeutic ablation of liver tumours. *Br J Surg*. Nov 2002;89(11):1396-1401.
97. Yan DB, Clingan P, Morris DL. Hepatic cryotherapy and regional chemotherapy with or without resection for liver metastases from colorectal carcinoma: how many are too many? *Cancer*. Jul 15 2003;98(2):320-330.

98. Joosten J, Jager G, Oyen W, Wobbes T, Ruers T. Cryosurgery and radiofrequency ablation for unresectable colorectal liver metastases. *Eur J Surg Oncol*. Dec 2005;31(10):1152-1159.
99. Brooks AJ, Wang F, Alfredson M, Yan TD, Morris DL. Synchronous liver resection and cryotherapy for colorectal metastases: survival analysis. *Surgeon*. Aug 2005;3(4):265-268.
100. Yan TD, Padang R, Morris DL. Longterm results and prognostic indicators after cryotherapy and hepatic arterial chemotherapy with or without resection for colorectal liver metastases in 224 patients: longterm survival can be achieved in patients with multiple bilateral liver metastases. *J Am Coll Surg*. Jan 2006;202(1):100-111.
101. Niu R, Yan TD, Zhu JC, Black D, Chu F, Morris DL. Recurrence and survival outcomes after hepatic resection with or without cryotherapy for liver metastases from colorectal carcinoma. *Ann Surg Oncol*. Jul 2007;14(7):2078-2087.
102. Mala T, Samset E, Aurdal L, Gladhaug I, Edwin B, Soreide O. Magnetic resonance imaging-estimated three-dimensional temperature distribution in liver cryolesions: a study of cryolesion characteristics assumed necessary for tumor ablation. *Cryobiology*. Nov 2001;43(3):268-275.
103. Gage AA, Baust JG. Cryosurgery for tumors. *J Am Coll Surg*. Aug 2007;205(2):342-356.
104. Mala T, Frich L, Aurdal L, et al. Hepatic vascular inflow occlusion enhances tissue destruction during cryoablation of porcine liver. *J Surg Res*. Dec 2003;115(2):265-271.
105. Neel HB, 3rd, Ketcham AS, Hammond WG. Cryonecrosis of normal and tumor-bearing rat liver potentiated by inflow occlusion. *Cancer*. Nov 1971;28(5):1211-1218.
106. Jungraithmayr W, Szarzynski M, Neeff H, et al. Significance of total vascular exclusion for hepatic cryotherapy: an experimental study. *J Surg Res*. Jan 2004;116(1):32-41.
107. Seifert JK, Dutkowski P, Junginger T, Morris DL. Bile duct warmer in hepatic cryosurgery--a pig liver model. *Cryobiology*. Nov 1997;35(3):299-302.
108. Gage AA, Fazekas G, Riley EE, Jr. Freezing injury to large blood vessels in dogs. With comments on the effect of experimental freezing of bile ducts. *Surgery*. May 1967;61(5):748-754.
109. Eggstein S, Neeff H, Szarzynski M, et al. Hepatic cryotherapy involving the vena cava. Experimental study in a pig liver model. *Eur Surg Res*. Mar-Apr 2003;35(2):67-74.
110. Weber SM, Lee FT, Jr., Warner TF, Chosy SG, Mahvi DM. Hepatic cryoablation: US monitoring of extent of necrosis in normal pig liver. *Radiology*. Apr 1998;207(1):73-77.
111. Neel HB, Ketcham AS, Hammond WG. Ischemia potentiating cryosurgery of primate liver. *Ann Surg*. Aug 1971;174(2):309-318.
112. Heard BE. The histological appearances of some normal tissues at low temperatures. *Br J Surg*. Jan 1955;42(174):430-437.

113. Weber SM, Lee FT, Jr., Chinn DO, Warner T, Chosy SG, Mahvi DM. Perivascular and intralesional tissue necrosis after hepatic cryoablation: results in a porcine model. *Surgery*. Oct 1997;122(4):742-747.
114. Schuder G, Pistorius G, Fehringer M, Feifel G, Menger MD, Vollmar B. Complete shutdown of microvascular perfusion upon hepatic cryothermia is critically dependent on local tissue temperature. *Br J Cancer*. Feb 2000;82(4):794-799.
115. Ravikumar TS, Steele GD, Jr. Hepatic cryosurgery. *Surg Clin North Am*. Apr 1989;69(2):433-440.
116. Rivoire ML, Voiglio EJ, Kaemmerlen P, et al. Hepatic cryosurgery precision: evaluation of ultrasonography, thermometry, and impedancemetry in a pig model. *J Surg Oncol*. Apr 1996;61(4):242-248.
117. Onik G, Gilbert J, Hoddick W, et al. Sonographic monitoring of hepatic cryosurgery in an experimental animal model. *AJR Am J Roentgenol*. May 1985;144(5):1043-1047.
118. Matsumoto R, Selig AM, Colucci VM, Jolesz FA. MR monitoring during cryotherapy in the liver: predictability of histologic outcome. *J Magn Reson Imaging*. Sep-Oct 1993;3(5):770-776.
119. Kahlenberg MS, Volpe C, Klippenstein DL, Penetrante RB, Petrelli NJ, Rodriguez-Bigas MA. Clinicopathologic effects of cryotherapy on hepatic vessels and bile ducts in a porcine model. *Ann Surg Oncol*. Dec 1998;5(8):713-718.
120. Jacob G, Li AK, Hobbs KE. A comparison of cryodestruction with excision or infarction of an implanted tumor in rat liver. *Cryobiology*. Apr 1984;21(2):148-156.
121. Simon CJ, Dupuy DE, Mayo-Smith WW. Microwave ablation: principles and applications. *Radiographics*. Oct 2005;25 Suppl 1:S69-83.
122. Swift B, Strickland A, West K, Clegg P, Cronin N, Lloyd D. The histological features of microwave coagulation therapy: an assessment of a new applicator design. *Int J Exp Pathol*. Feb 2003;84(1):17-30.
123. Tabuse K. A new operative procedure of hepatic surgery using a microwave tissue coagulator. *Nippon Geka Hokan*. Mar 1 1979;48(2):160-172.
124. Saitsu H, Mada Y, Taniwaki S, et al. [Investigation of microwave coagulation necrotic therapy for 21 patients with small hepatocellular carcinoma less than 5 cm in diameter]. *Nippon Geka Gakkai Zasshi*. Apr 1993;94(4):359-365.
125. Sato M, Watanabe Y, Ueda S, et al. Microwave coagulation therapy for hepatocellular carcinoma. *Gastroenterology*. May 1996;110(5):1507-1514.
126. Shimada S, Hirota M, Beppu T, et al. Complications and management of microwave coagulation therapy for primary and metastatic liver tumors. *Surg Today*. 1998;28(11):1130-1137.
127. Kojima Y, Suzuki S, Sakaguchi T, et al. Portal vein thrombosis caused by microwave coagulation therapy for hepatocellular carcinoma: report of a case. *Surg Today*. 2000;30(9):844-848.
128. Garcea G, Lloyd TD, Aylott C, Maddern G, Berry DP. The emergent role of focal liver ablation techniques in the treatment of primary and secondary liver tumours. *Eur J Cancer*. Oct 2003;39(15):2150-2164.

129. Xu HX, Xie XY, Lu MD, et al. Ultrasound-guided percutaneous thermal ablation of hepatocellular carcinoma using microwave and radiofrequency ablation. *Clin Radiol*. Jan 2004;59(1):53-61.
130. Shibata T, Iimuro Y, Yamamoto Y, et al. Small hepatocellular carcinoma: comparison of radio-frequency ablation and percutaneous microwave coagulation therapy. *Radiology*. May 2002;223(2):331-337.
131. Liang P, Dong B, Yu X, et al. Prognostic factors for survival in patients with hepatocellular carcinoma after percutaneous microwave ablation. *Radiology*. Apr 2005;235(1):299-307.
132. Dong B, Liang P, Yu X, et al. Percutaneous sonographically guided microwave coagulation therapy for hepatocellular carcinoma: results in 234 patients. *AJR Am J Roentgenol*. Jun 2003;180(6):1547-1555.
133. Itamoto T, Asahara T, Kohashi T, et al. [Percutaneous microwave coagulation therapy for hepatocellular carcinoma]. *Gan To Kagaku Ryoho*. Oct 1999;26(12):1841-1844.
134. Bhardwaj N, Strickland AD, Ahmad F, et al. Microwave ablation for unresectable hepatic tumours: Clinical results using a novel microwave probe and generator. *Eur J Surg Oncol*. Oct 30 2009.
135. Iannitti DA, Martin RC, Simon CJ, et al. Hepatic tumor ablation with clustered microwave antennae: the US Phase II Trial. *HPB (Oxford)*. 2007;9(2):120-124.
136. Tanaka K, Shimada H, Nagano Y, Endo I, Sekido H, Togo S. Outcome after hepatic resection versus combined resection and microwave ablation for multiple bilobar colorectal metastases to the liver. *Surgery*. Feb 2006;139(2):263-273.
137. Shibata T, Niinobu T, Ogata N, Takami M. Microwave coagulation therapy for multiple hepatic metastases from colorectal carcinoma. *Cancer*. Jul 15 2000;89(2):276-284.
138. Dong BW, Liang P, Yu XL, et al. [Long-term results of percutaneous sonographically-guided microwave ablation therapy of early-stage hepatocellular carcinoma]. *Zhonghua Yi Xue Za Zhi*. Mar 28 2006;86(12):797-800.
139. Wang ZL, Liang P, Dong BW, Yu XL, Yu de J. Prognostic factors and recurrence of small hepatocellular carcinoma after hepatic resection or microwave ablation: a retrospective study. *J Gastrointest Surg*. Feb 2008;12(2):327-337.
140. Organ LW. Electrophysiologic principles of radiofrequency lesion making. *Appl Neurophysiol*. 1976;39(2):69-76.
141. Skinner MG, Iizuka MN, Kolios MC, Sherar MD. A theoretical comparison of energy sources--microwave, ultrasound and laser--for interstitial thermal therapy. *Phys Med Biol*. Dec 1998;43(12):3535-3547.
142. McKay A, Dixon E, Taylor M. Current role of radiofrequency ablation for the treatment of colorectal liver metastases. *Br J Surg*. Oct 2006;93(10):1192-1201.
143. Takamura M, Murakami T, Shibata T, et al. Microwave coagulation therapy with interruption of hepatic blood in- or outflow: an experimental study. *J Vasc Interv Radiol*. May 2001;12(5):619-622.
144. Ishida T, Murakami T, Shibata T, et al. Percutaneous microwave tumor coagulation for hepatocellular carcinomas with interruption of segmental hepatic blood flow. *J Vasc Interv Radiol*. Feb 2002;13(2 Pt 1):185-191.

145. Shibata T, Murakami T, Ogata N. Percutaneous microwave coagulation therapy for patients with primary and metastatic hepatic tumors during interruption of hepatic blood flow. *Cancer*. Jan 15 2000;88(2):302-311.
146. Strickland AD, Clegg PJ, Cronin NJ, et al. Experimental study of large-volume microwave ablation in the liver. *Br J Surg*. Aug 2002;89(8):1003-1007.
147. Denisov-Nikol'skii YI, Shafranov VV, Mazokhin VN, et al. Morphological changes in the liver after microwave destruction. *Bull Exp Biol Med*. Apr 2001;131(4):377-381.
148. Garrean S, Hering J, Saied A, et al. Ultrasound monitoring of a novel microwave ablation (MWA) device in porcine liver: lessons learned and phenomena observed on ablative effects near major intrahepatic vessels. *J Gastrointest Surg*. Feb 2009;13(2):334-340.
149. Kato T, Suto Y, Hamazoe R. Effects of microwave tissue coagulation on the livers of normal rabbits: a comparison of findings of image analysis and histopathological examination. *Br J Radiol*. Jun 1996;69(822):515-521.
150. Ohno T, Kawano K, Sasaki A, Aramaki M, Yoshida T, Kitano S. Expansion of an ablated site and induction of apoptosis after microwave coagulation therapy in rat liver. *J Hepatobiliary Pancreat Surg*. 2001;8(4):360-366.
151. Simon CJ, Dupuy DE, Iannitti DA, et al. Intraoperative triple antenna hepatic microwave ablation. *AJR Am J Roentgenol*. Oct 2006;187(4):W333-340.
152. Yamaguchi T, Mukaisho K, Yamamoto H, et al. Disruption of erythrocytes distinguishes fixed cells/tissues from viable cells/tissues following microwave coagulation therapy. *Dig Dis Sci*. Jul 2005;50(7):1347-1355.
153. Yamashiki N, Kato T, Bejarano PA, et al. Histopathological changes after microwave coagulation therapy for patients with hepatocellular carcinoma: review of 15 explanted livers. *Am J Gastroenterol*. Sep 2003;98(9):2052-2059.
154. Mukaisho K, Sugihara H, Tani T, et al. Effects of microwave irradiation on rat hepatic tissue evaluated by enzyme histochemistry for acid phosphatase. *Dig Dis Sci*. Feb 2002;47(2):376-379.
155. Mukaisho K, Kurumi Y, Sugihara H, et al. Enzyme histochemistry is useful to assess viability of tumor tissue after microwave coagulation therapy (MCT): metastatic adenocarcinoma treated by lateral segmentectomy after MCT. *Dig Dis Sci*. Nov 2002;47(11):2441-2445.
156. Login GR. Microwave fixation versus formalin fixation of surgical and autopsy tissue. *Am J Med Technol*. May 1978;44(5):435-437.
157. Leong AS, Daymon ME, Milios J. Microwave irradiation as a form of fixation for light and electron microscopy. *J Pathol*. Aug 1985;146(4):313-321.

CHAPTER 2: METHODS

2. Chapter 2: Methods.....	46
2.1. Rat liver anatomy	46
2.2. Surgical procedure.....	49
2.2.1. Radiofrequency ablation	51
2.2.2. Microwave ablation	52
2.2.1. Cryoablation.....	52
2.3. Histology & Immunocytochemistry.....	53
2.3.1. Haematoxylin and Eosin	53
2.3.2. Immunocytochemistry: HSP 70.....	54
2.3.3. Immunocytochemistry: Caspase 3	55
Figure 2-1. Rat liver anatomy	47
Figure 2-2. Corrosion cast of hepatic veins	48
Figure 2-3. Mean ablation distances	51
Figure 2-4. RF set up	57
Figure 2-5. Radiofrequency ablation	58
Figure 2-6. Microwave probe	59
Figure 2-7. Microwave ablation.....	60
Figure 2-8. Cryotherapy set up	61
Figure 2-10. Cryotherapy ablation.....	62
Figure 2-11. Cryotherapy ablation-immediate.....	63
Figure 2-12. Ablation sectioned.....	64

2. Chapter 2: Methods

The methods are divided into surgical procedures (rat ablation) and histological and immunocytochemical analyses.

2.1. Rat liver anatomy

The human liver is comprised of 8 lobes, the segmentation based on the principal divisions of the hepatic artery, portal vein and hepatic ducts. All lobes drain via hepatic veins to the inferior vena cava. The rat's liver is topographically different to the human liver, as it has 4 lobes; 3 equally divided large lobes and a small caudate lobe. Anatomically, however the rat liver shares the same fundamental characteristics to the human liver^{1,2} (Figure 2-1. Rat liver anatomy).

Figure 2-1 illustrates the arrangement of each of the main lobes. The rat liver like in humans is dependent upon its attachment to the Inferior Vena Cava by a narrow vascular pedicle to maintain its position. The rest of the lobe is free and is only held in place by avascular ligamentous attachments to the anterior abdominal wall and diaphragm. Each of the main lobes is drained by segmental hepatic veins, increasing in diameter as they approach the inferior vena cava (Figure 2-2. Corrosion cast of hepatic veins).

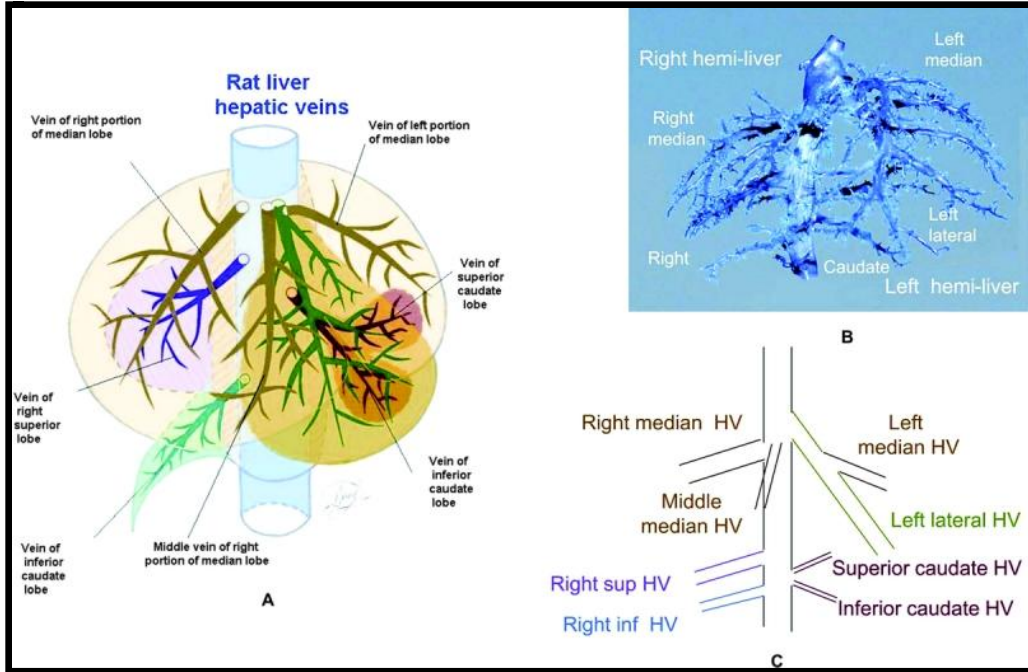


Figure 2-1. Rat liver anatomy

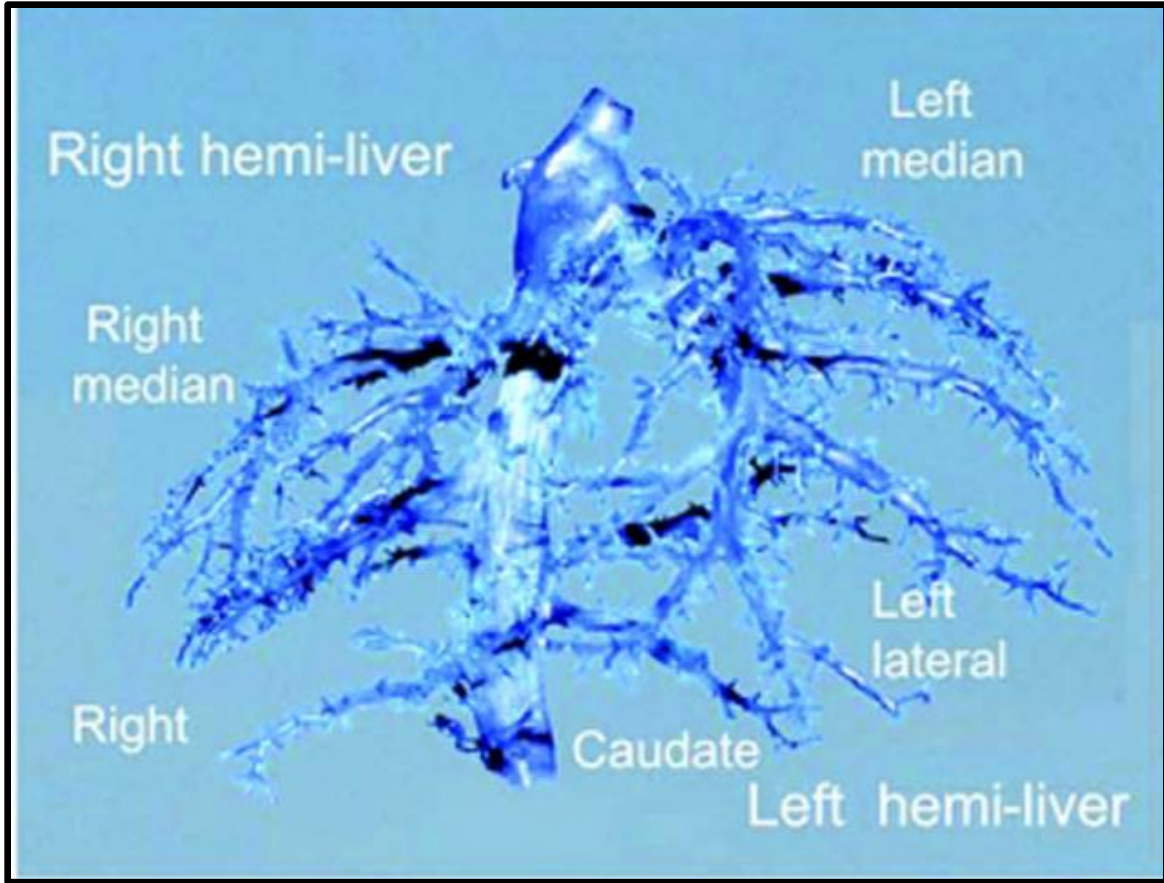


Figure 2-2. Corrosion cast of hepatic veins

The rat liver therefore is extremely well suited to the investigation of the heat sink effect; it has lobes that can be distinguished easily and exteriorised, each lobe is thin and the anatomy constant thus allowing accurate placement and monitoring of the ablation diameter. Each lobe has a major vascular pedicle draining to the hilum.

2.2. Surgical procedure

All animal experimentation was conducted in accordance with the Operation of Animals (Scientific Procedures) Act 1986 after authorisation from the University of Leicester Ethical Committee and the Home office. A total of 90 male Sprague-Dawley rats were randomly assigned to either receive cryotherapy, microwave ablation or radiofrequency.

All rats were anaesthetised by using inhalation anaesthetic and subcutaneous injections of (0.9%) normal saline and opiate analgesia were administered. The weight of each rat was recorded and blood was withdrawn from the tail vein for pre-operative liver function tests and a full blood count. These blood tests were repeated at regular intervals post-operatively, but the animal licence restricted the volume and frequency of blood that could be withdrawn. A midline laparotomy was performed; the liver mobilised and the 3 major lobes of the liver were exposed.

The maximum lobe width and length were recorded with the use of callipers and each lobe was randomly assigned to receive a 1cm ablation placed either proximally, intermediately or distally in relation to the liver outflow. Callipers were used to determine

the exact distances from the hilum to the ablation zone prior to the ablation being carried out. All proximal ablation were 1-2 cm from the hilum, intermediate ablations were 2-3 cm and distal ablations were at least 3cm away (Figure 2-3. Mean ablation distances & Figure 2-5. Radiofrequency ablation). Pilot studies performed prior to the main study determined the time and power requirement of each of the ablation modalities in order to produce a 1cm ablation diameter. This method was easily reproducible as all rats were between 350-400 grams and therefore had similar sized lobes. In addition, the power settings on the ablation modalities were easily adjusted to consistently produce a 1cm ablation.

A moist pack was placed under the lobes undergoing ablation in order to protect the intra-abdominal organs. After the ablation all animals undergoing recovery had their laparotomy wound closed and local anaesthetic injected into the wound. They were given a further bolus of subcutaneous normal saline and monitored closely during the post-operative period with free access to food and water. Five rats were culled at each time point; immediate, 4 hours, 24 hours, 48 hours, 2 weeks and 1 month (Table 4. Time points). All rats were culled by a schedule one method, the laparotomy wound opened, the lobes sizes measured again and the ablation sites inspected and the diameter recorded. The livers were then harvested and preserved in 10% formalin. The livers were sliced down the middle of the ablation zone (Figure 2-11. Ablation sectioned) and the cut surface fixed in wax blocks, sliced and mounted on slides for histological analysis.

Time Points	0	4hrs	24hrs	48hrs	2 wks	4wks
RF	5	5	5	5	5	5
Cryotherapy	5	5	5	5	5	5
Microwave	5	5	5	5	5	5

Table 4. Time points

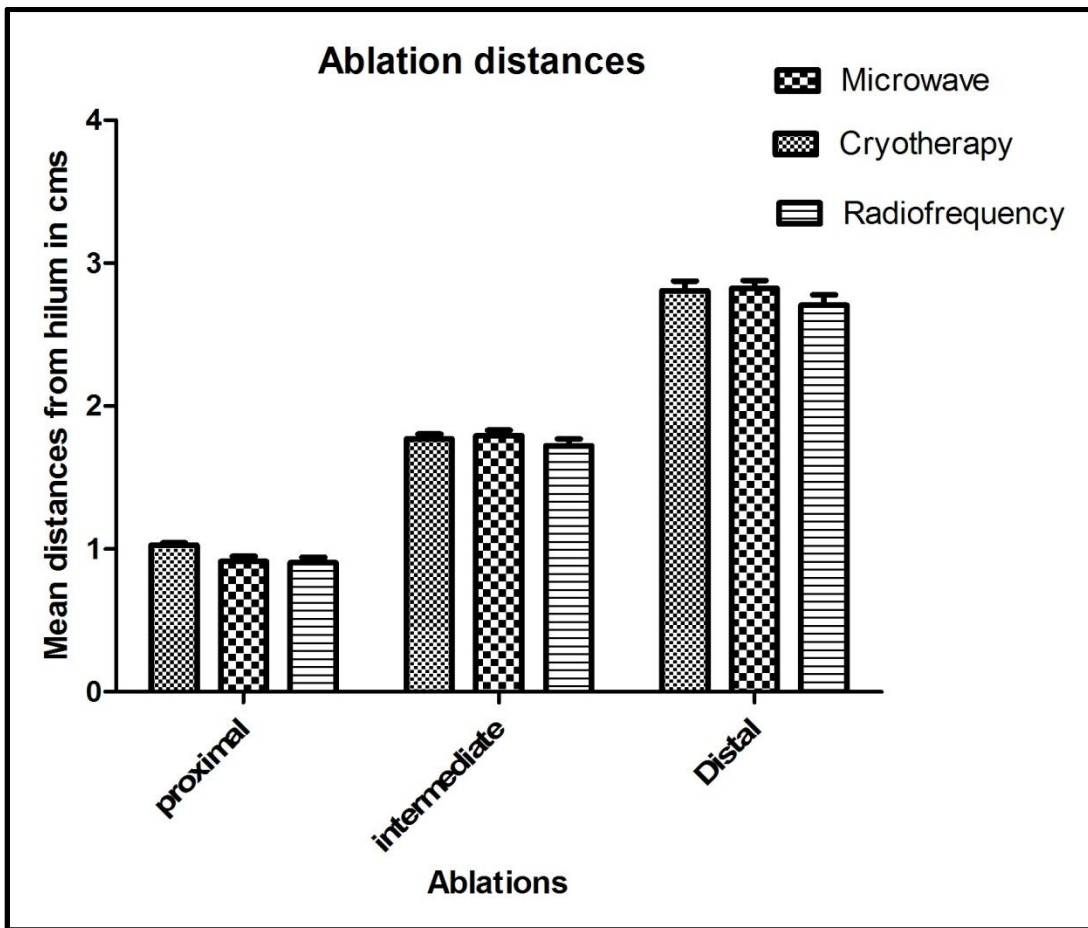


Figure 2-3. Mean ablation distances

2.2.1. Radiofrequency ablation

Thirty rats underwent radiofrequency ablation as described above. The ablations were performed using an internally cooled probe powered by an RF generator (Tyco healthcare, USA). The rat was part of a closed loop consisting of the RF generator, a diathermy pad placed on the shaved back of the rat and the internally cooled RF probe (Figure 2-4. RF set up). The power was varied manually adjusted to tissue impedance and the ablation continued till a 1cm burn was macroscopically visible (Figure 2-5. Radiofrequency ablation). The ablation time, approximately 2-3 minutes was slightly longer compared to microwave.

2.2.2. Microwave ablation

Thirty rats underwent microwave ablation as described above; using a microwave machine (Wessex 2654-SA) and a special bench model probe was used to perform the ablation (Figure 2-6. Microwave probe). The probe was inserted perpendicular to the lobe and the power turned on at a constant 20watts. A 1cm burn usually took between 20-30 seconds. On withdrawal of the probe, no bleeding occurred and the ablation site was clearly demarcated macroscopically (Figure 2-7. Microwave ablation).

Cryoablation

The Cryoablation machine (Spembly Medical, UK) was used to create ablation zones in 30 rats as described above (Figure 2-8. Cryotherapy set up). The machine was filled with liquid nitrogen and a single freeze-thaw cycle was sufficient to create the necessary macroscopic ablations. The intra-operative appearance (Figure 2-9. Cryotherapy

ablation), looked very different to the final result compared to the other two modalities (Figure 2-10. Cryotherapy ablation-immediate)

2.3. Histology & Immunocytochemistry

2.3.1. Haematoxylin and Eosin

The livers were sectioned (Figure 2-11. Ablation sectioned) fixed in 10% formalin for 24-48 hours, processed and embedded in paraffin wax. The wax blocks were sectioned and mounted on slides. The staining then took place as follows:

- Deparaffinised in an oven at 65°C for 5 minutes
- Immersed in xylene then hydrated through graded alcohols to running water
- Immersed in Mayer's Haematoxylin for 5 minutes
- Washed in running tap water for 5 minutes
- Counterstained with 1% eosin for 3 minutes
- Rinsed in tap water
- Dehydrated in 95% & 99% absolute alcohols (two changes of 2 minutes each)
- Clear in xylene (two changes of 2 minutes each)
- Mount in DPX

2.3.2. Immunocytochemistry: HSP 70

- Slides were deparaffinised in an oven at 65°C for 5 minutes
- Immersed in Xylene for 3 minutes followed by rehydration through graded alcohols
- Tap water wash for 10 minutes
- Slides were then immersed in 10 mM Citrate Buffer (pH 6) and placed in 750 W microwave for 20 minutes on full power and allowed to cool for 40 minutes in room temperature
- Slides were then placed in a Hellendahl slide container and soaked in TBS
- Followed by 10 minute immersion in Avidin, followed by 3 minute immersion in TBS, followed by 10 minute immersion in Biotin and a further 3 minutes in TBS
- Normal Rabbit serum (1:5) was pipetted onto each slide for 10 minutes and then drained
- Primary Mouse Anti-HSP 70 (1:50) Monoclonal antibody (*stressgen, USA*) was added and the slides incubated overnight at 4°C
- Followed by 2 X 5 minute TBS washes
- Biotinylated rabbit anti mouse serum was added (1:400) for 30 minutes followed by 2 X 5 minute TBS washes
- Followed by incubation for 30 minutes in Streptavidin Biotin Complex/AP (*DakoCytomation, Denmark*)
- After 2 further 5 minute TBS washes the slides were washed in ultra pure water for 5 minutes.

- The slides were stained with NBT/BCIP (Roche, 1 697 471); 1 tablet in 10 mls of ultra pure water-filtered twice and covered in the dark for 10 minutes.
- Slides were then washed in running tap water for 10 minutes and mounted with aqueous mounting media.
- A positive control and a negative control (primary antibody replaced by TBS) were part of each run
- Normal liver tissue from the hilum and the untreated caudate lobe formed internal controls

2.3.3. Immunocytochemistry: Caspase 3

- Slides were deparaffinised in an oven at 65°C for 5 minutes
- Immersed in Xylene for 3 minutes followed by rehydration through graded alcohols
- Tap water wash for 10 minutes
- Slides were then immersed in 10 mM Citrate Buffer (pH 6) and placed in 750 W microwave for 20 minutes on full power and allowed to cool for 40 minutes in room temperature
- Slides were then placed in a Hellendahl slide container and soaked in TBS
- Followed by 10 minute immersion in Avidin, followed by 3 minute immersion in TBS, followed by 10 minute immersion in Biotin and a further 3 minutes in TBS

- Normal swine serum (1:5) was pipetted onto each slide for 10 minutes and then drained
- Primary polyclonal affinity-purified Rabbit Anti-human/mouse Caspase-3 Active (1:1000) antibody (*R&D systems, Minneapolis, MN, USA*) was added and the slides incubated overnight at 4°C
- Followed by 2 X 5 minute TBS washes
- Biotinylated swine anti rabbit serum was added (1:400) for 30 minutes followed by 2 X 5 minute TBS washes
- Followed by incubation for 30 minutes in Streptavidin Biotin Complex/AP (*DakoCytomation, Denmark*)
- After 2 further 5 minute TBS washes the slides were washed in ultra pure water for 5 minutes.
- The slides were stained with NBT/BCIP (*Roche, 1 697 471*); 1 tablet in 10 mls of ultra pure water-filtered twice), covered in the dark for 10 minutes.
- Slides were then washed in running tap water for 10 minutes and mounted with aqueous mounting media.
- A positive control and a negative control (primary antibody replaced by TBS) were part of each run
- Normal liver tissue from the hilum and the untreated caudate lobe formed internal controls

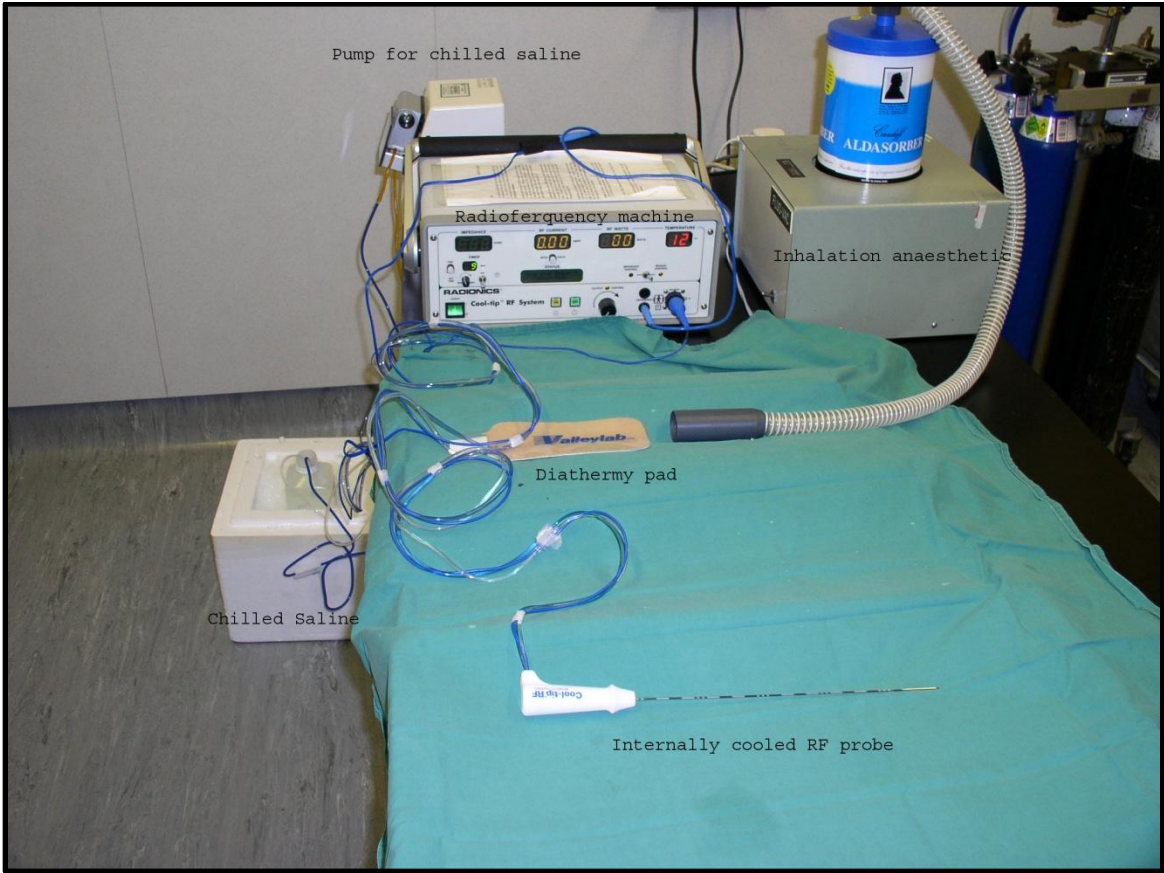


Figure 2-4. RF set up

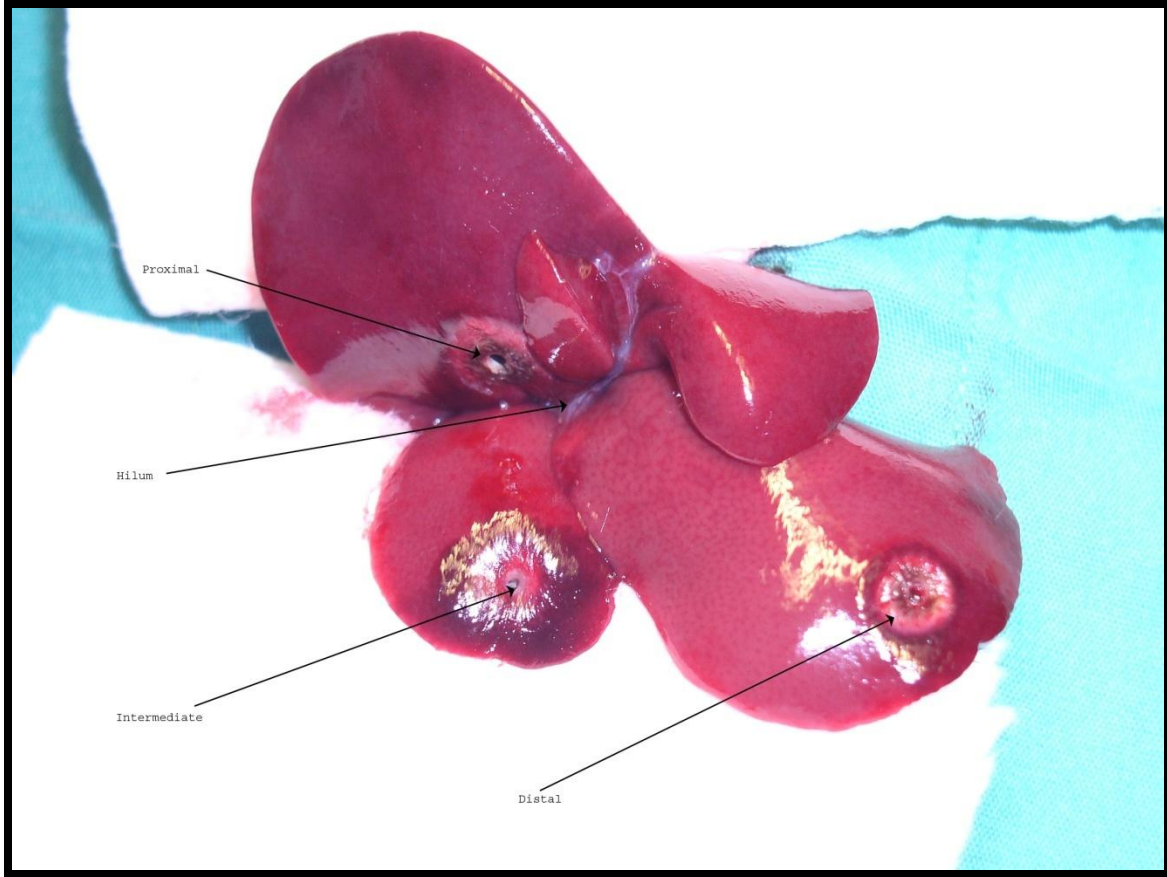


Figure 2-5. Radiofrequency ablation

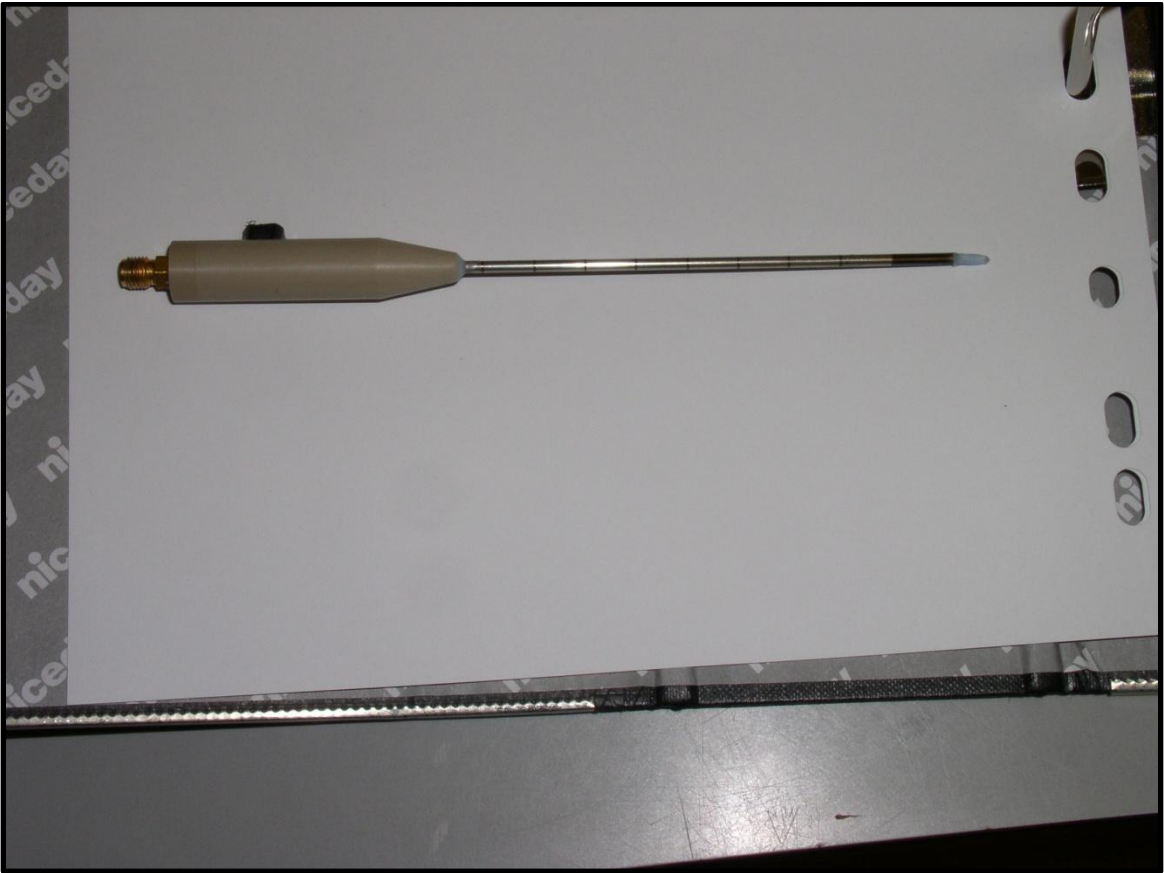


Figure 2-6. Microwave probe

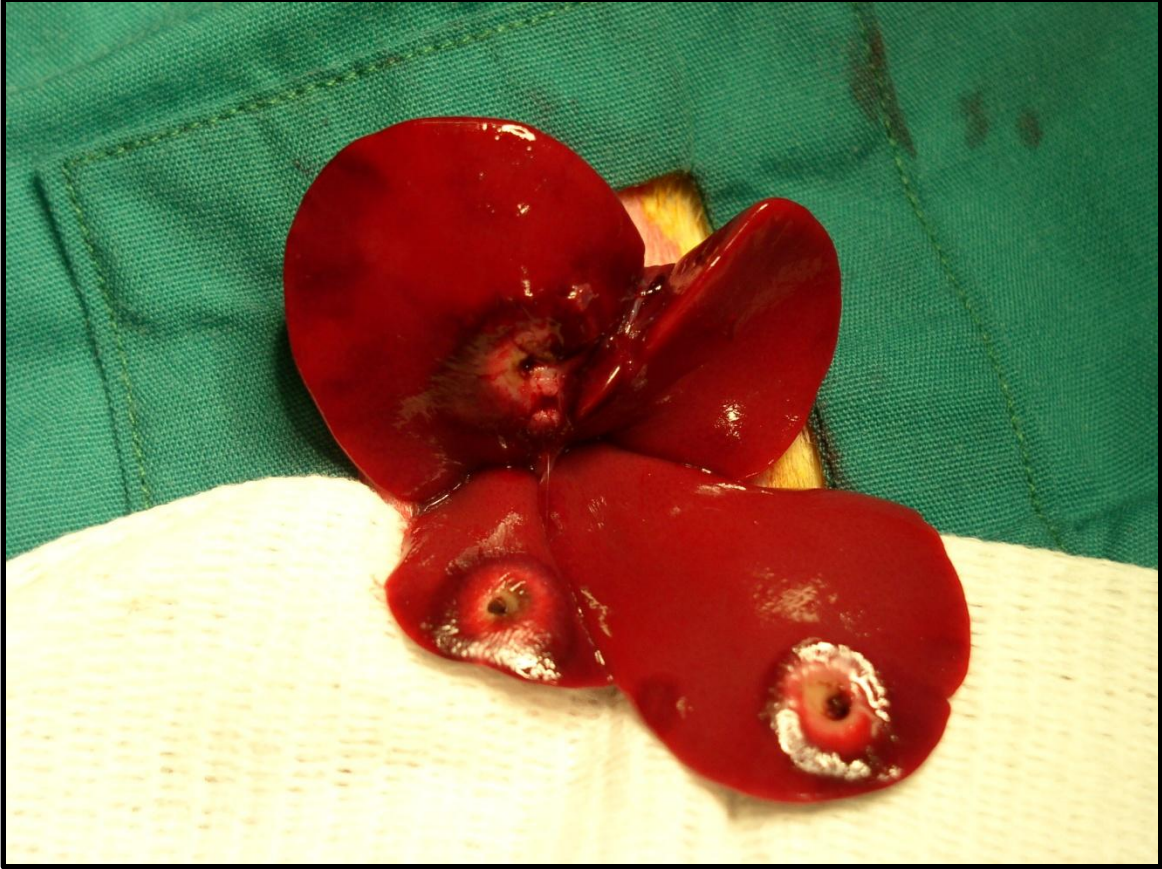


Figure 2-7. Microwave ablation

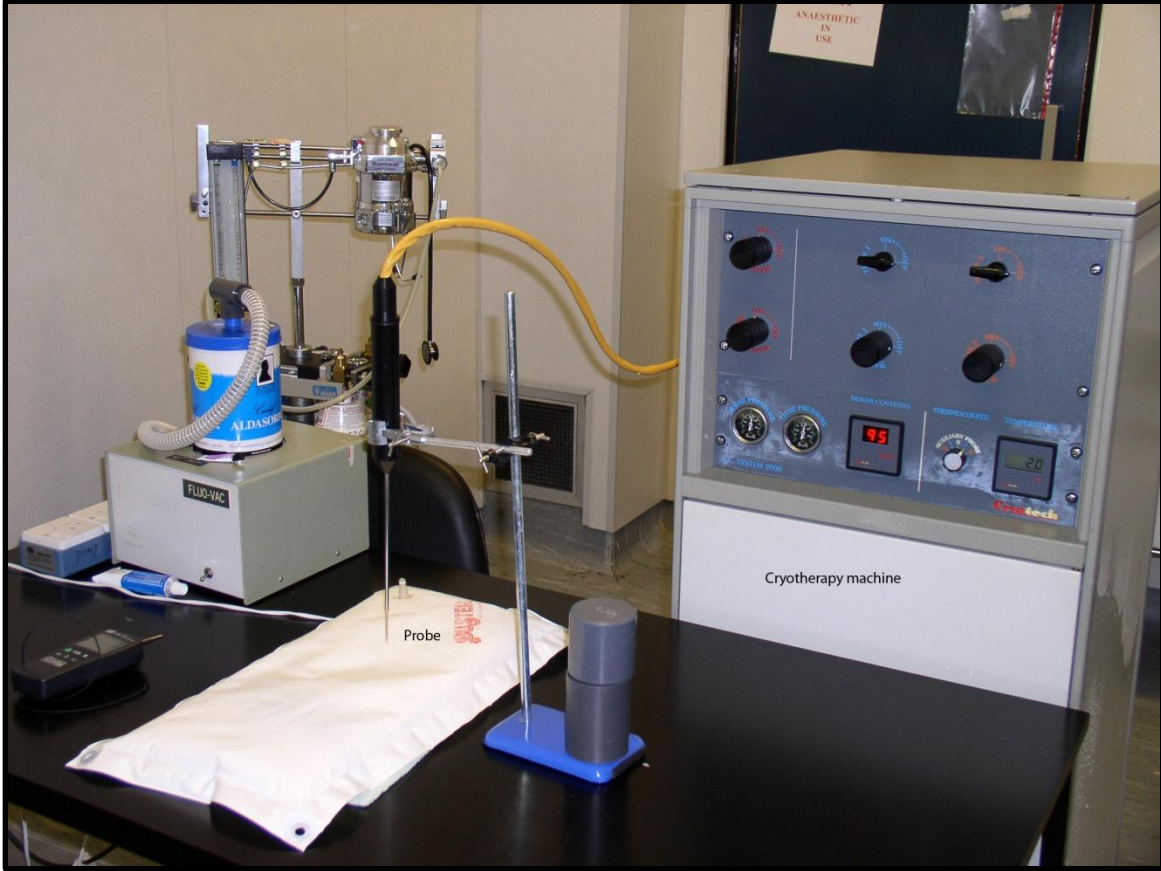


Figure 2-8. Cryotherapy set up

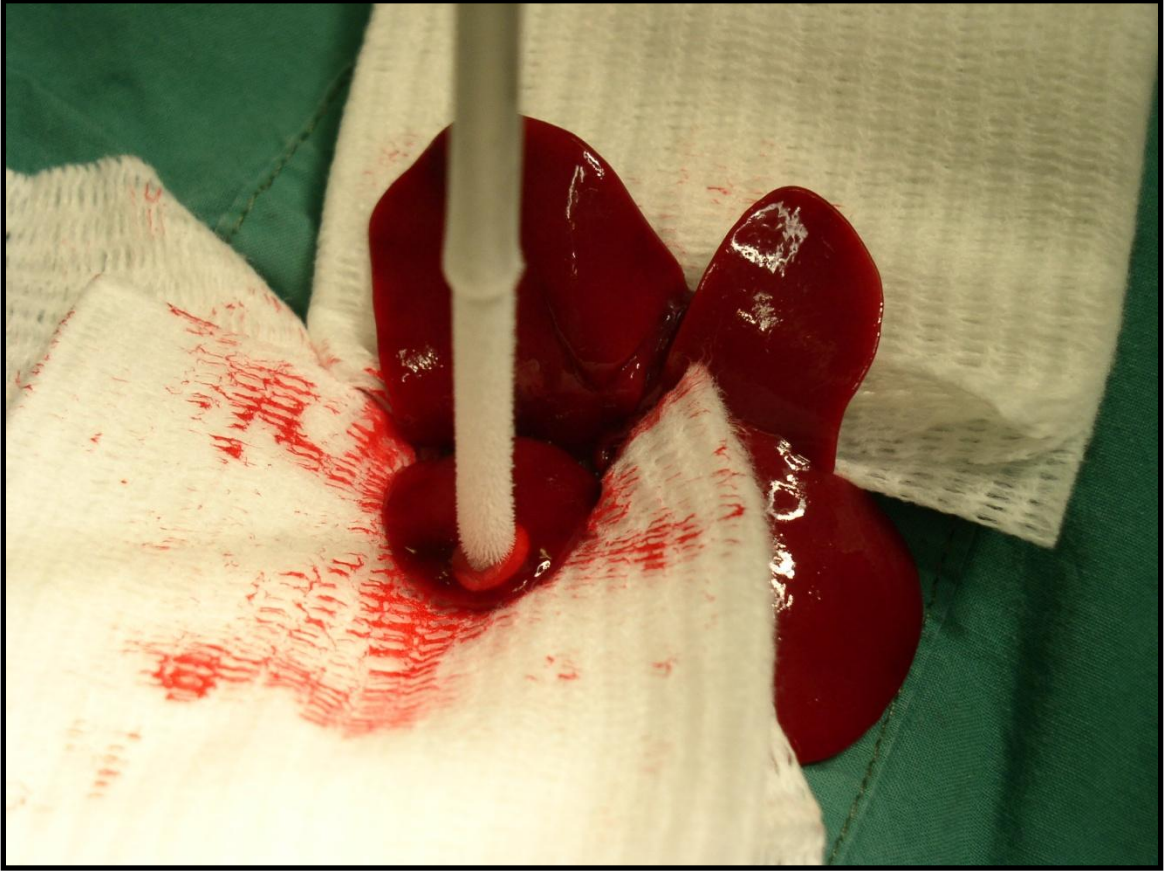


Figure 2-9. Cryotherapy ablation

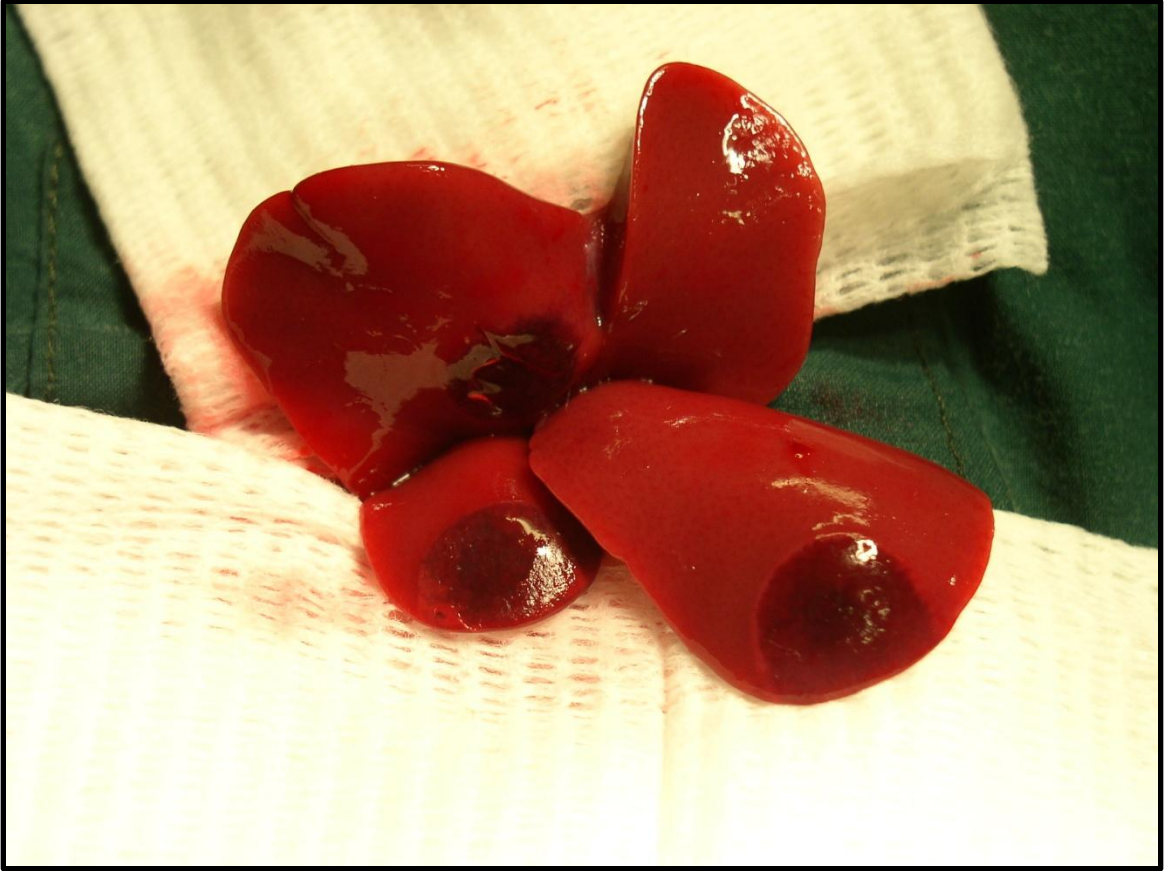


Figure 2-10. Cryotherapy ablation-immediate

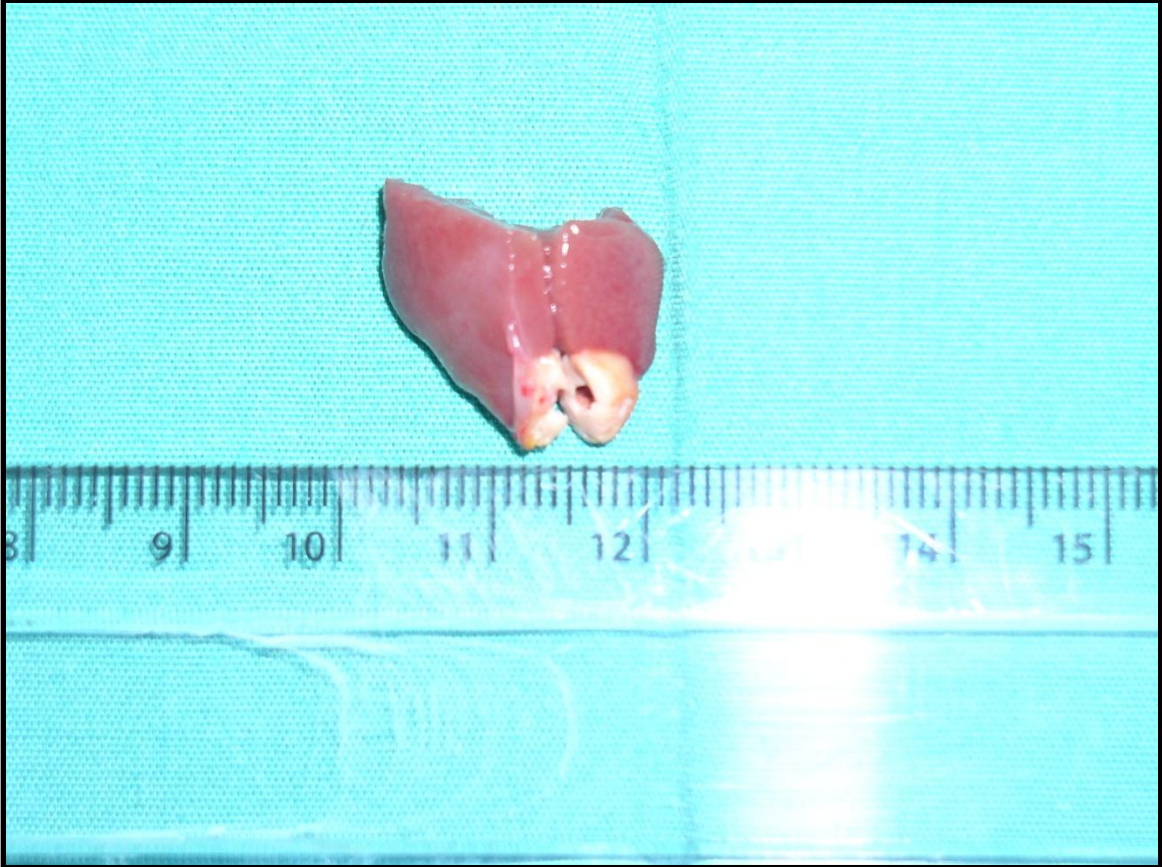


Figure 2-11. Ablation sectioned

1. Martins PN, Neuhaus P. Surgical anatomy of the liver, hepatic vasculature and bile ducts in the rat. *Liver Int* 2007;**27**(3): 384-392.
2. Madrahimov N, Dirsch O, Broelsch C, Dahmen U. Marginal hepatectomy in the rat: from anatomy to surgery. *Ann Surg* 2006;**244**(1): 89-98.

CHAPTER 3: SURVIVAL, WEIGHT AND BLOODS

3. Results: survival, weight and bloods.	67
3.1. Statistical analyses.....	67
3.2. Survival	67
3.3. Weight	67
3.4. Bloods.....	71
3.4.1. Alanine Transaminase (ALT)	71
3.4.2. Haemoglobin.....	74
3.4.3. Platelets.....	75
3.5. Discussion	77
Figure. 3-1. Microwave rat weight n=5 at each time point.....	68
Figure 3-2. Radiofrequency rat weight n=5 at each time point	69
Figure 3-3. Cryotherapy rat weights n=5 at each time point	70
Figure 3-5. ALT rise	73
Figure 3-4. ALT rise compared a 24 hours.....	73
Figure 3-6. Haemoglobin analyses (mean \pm sem)	75
Figure 3-7. Platelet analyses (mean \pm sem)	76

3. Chapter 3. Survival, weight and bloods.

3.1. Statistical analyses

Results were analysed by a statistician using SAS version 9.1 and were examined graphically using histograms, stem-and-leaf plots, box-plots and normal probability plots. These were found to be non-parametrically distributed, therefore group comparisons were made using non-parametric methods (Wilcoxon Exact Test for 2 groups, and the Kruskal-Wallis Test for >2 groups). A $p < 0.05$ was taken as significant.

3.2. Survival

All rats recovered from the anaesthetic within 2-3 hours and survived.

3.3. Weight

All rats were weighed pre-operatively and at the time of sacrifice. The mean weight was calculated for each group and graphically presented as mean \pm sem. There was no meaningful change in weight over the experimental period across all three modalities. (Figure 3-1. Microwave rat weight), (Figure 3-2. Radiofrequency rat weight) and (Figure 3-3. Cryotherapy rat weights).

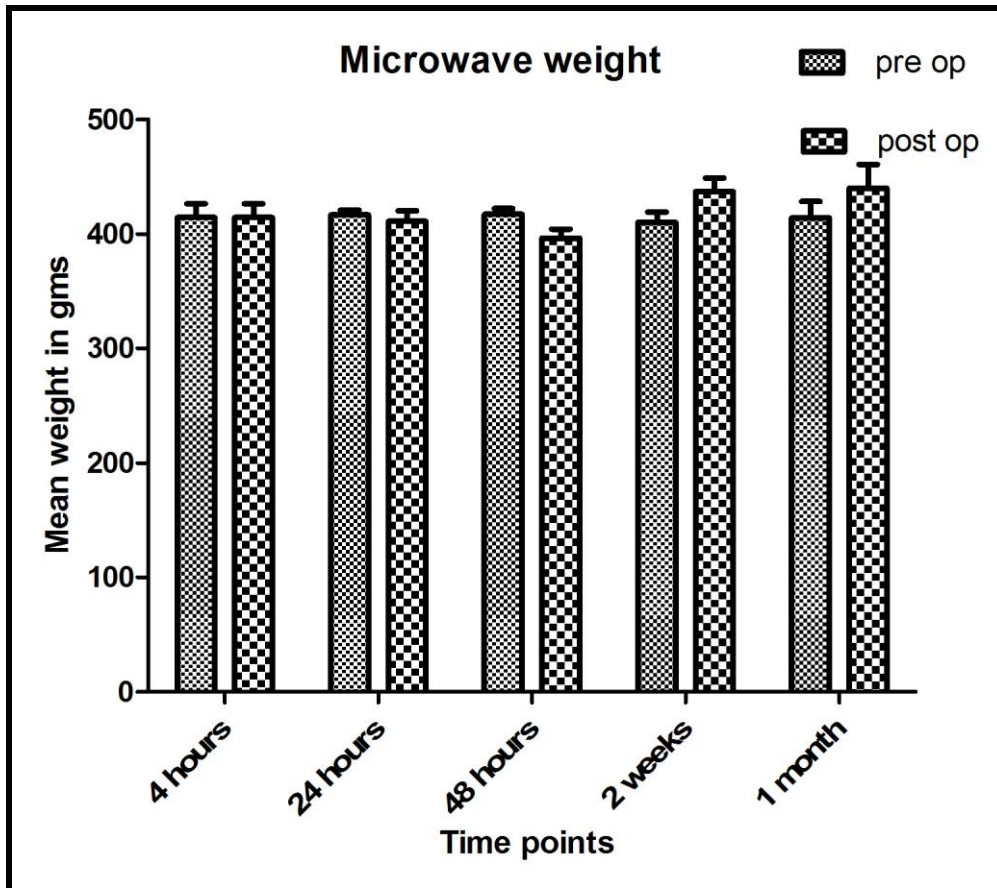


Figure. 3-1. Microwave rat weight n=5 at each time point

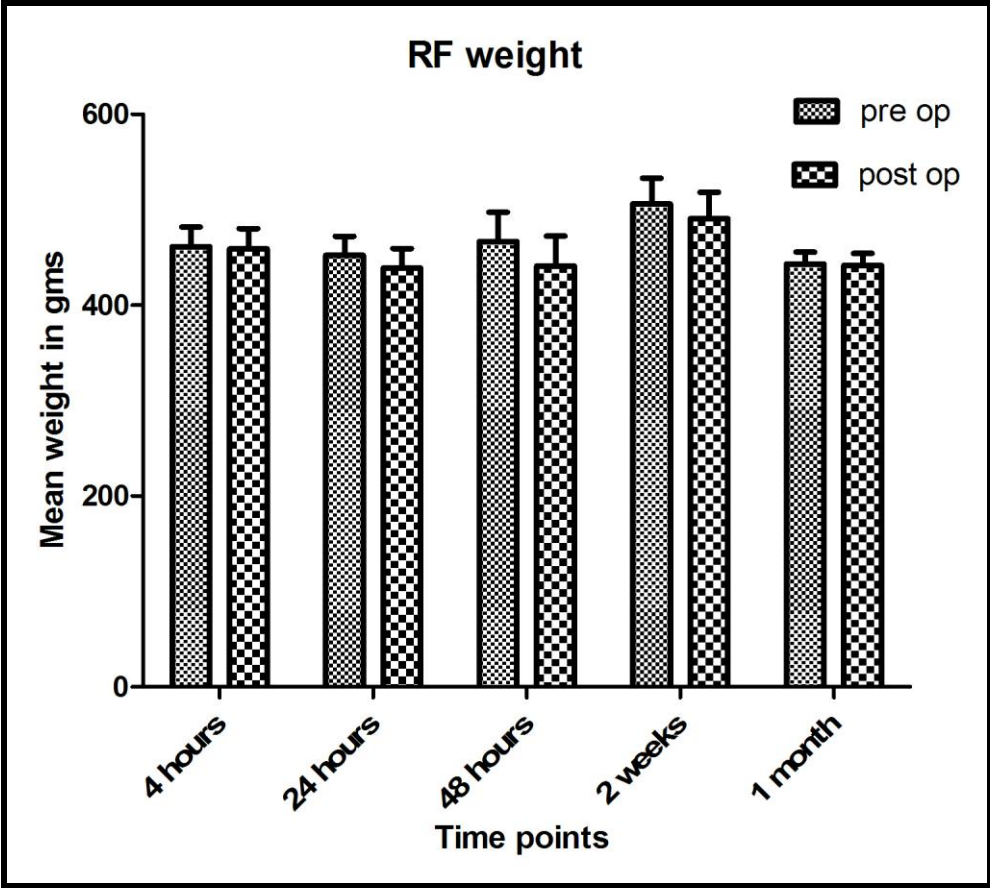


Figure 3-2. Radiofrequency rat weight n=5 at each time point

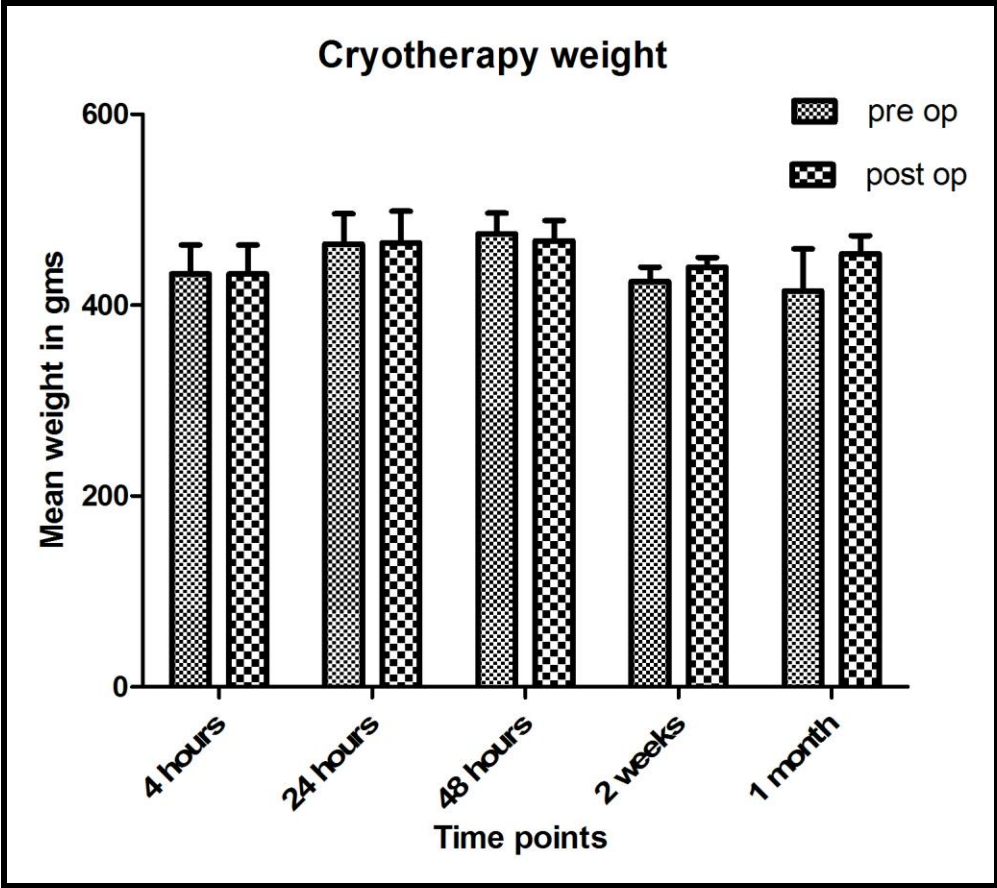


Figure 3-3. Cryotherapy rat weights n=5 at each time point

3.4. Bloods

All rats underwent pre-operative and regular post operative blood analyses. The animal licence restricted the volume of blood that could be withdrawn at each time point (no greater than 10% of total blood volume) and the frequency of venepuncture (no greater than 15% of total circulating volume withdrawn in any 28 day period). Blood was therefore taken pre-operatively from all animals and the main parameters measured were; full blood count, (including white cell count, platelets and haemoglobin) and liver function tests (including alanine transaminase, bilirubin, alkaline phosphatase and albumin). In rats, as in humans, alkaline phosphatase and bilirubin are associated with biliary obstruction or intra-hepatic cholestasis ^{1, 2}. Despite some ablations in close proximity to the liver hilum, none of the rats exhibited biochemical evidence of biliary obstruction. The white cell count was also normal post-operatively indicating that there was no evidence of infection. Similarly a normal albumin level post-operatively was observed and this, like in humans, is an indication of a healthy states in rats ³. Alanine Transaminase (ALT) on the other hand showed the greatest change in the post operative phase. Cryoablation is associated with liver cracking, haemorrhage and thrombocytopenia ⁴. Bleeding is also a well recognised side effect of microwave ablation and RF ⁵⁻⁷. Therefore, haemoglobin and platelets in addition to alanine transaminase levels are reported in detail.

3.4.1. Alanine Transaminase (ALT)

Alanine transaminase is an abundant hepatic enzyme that catalyses the transfer of amino groups to form the hepatic metabolite pyruvate. As in humans, it is found in the hepatocyte cytoplasm of

many animals including rats and released from damaged hepatocytes into the blood after hepatocellular injury or death. It is found in relatively low concentrations in tissues other than liver and the degree of increase in ALT activity correlates with the number of hepatocytes damaged. The half life of ALT is between 24-72 hours and usually peaks 24 hours post insult and returns to normal within a week ⁸.

In humans, there is a direct correlation between the volume of liver ablated, the rise in ALT levels and the incidence of post-ablation syndrome ⁹. Very few studies regularly report liver transaminase levels, however those that do, report a two- to four-fold increase in transaminases post ablation which normalise between 1-4 weeks ⁹⁻¹¹.

An increase in ALT was observed in all treatments, it started to rise by 4 hours, peaked at 24 hours and normalized by 2 weeks. The preoperative ALT is a median of all rats pre-operatively and the ALT value at 4 and 24 hours were grouped together (n=10) as this emphasises the trend (Figure 3-4. Mean ALT rise). Radiofrequency had the greatest ALT rise followed by cryotherapy and microwave and this may be a reflection of the degree of hepatocyte damage caused. The rise 24 hours post ablation also suggests that more hepatocytes are damaged as the ablated lesion continues to evolve. The ALT rise at 24 hours (n=5 for each modality) was statistically significant (p<0.001). The sample size for weight and blood analyses were similar, however statistical analyses of ALT is possible as there is a significant change in value.

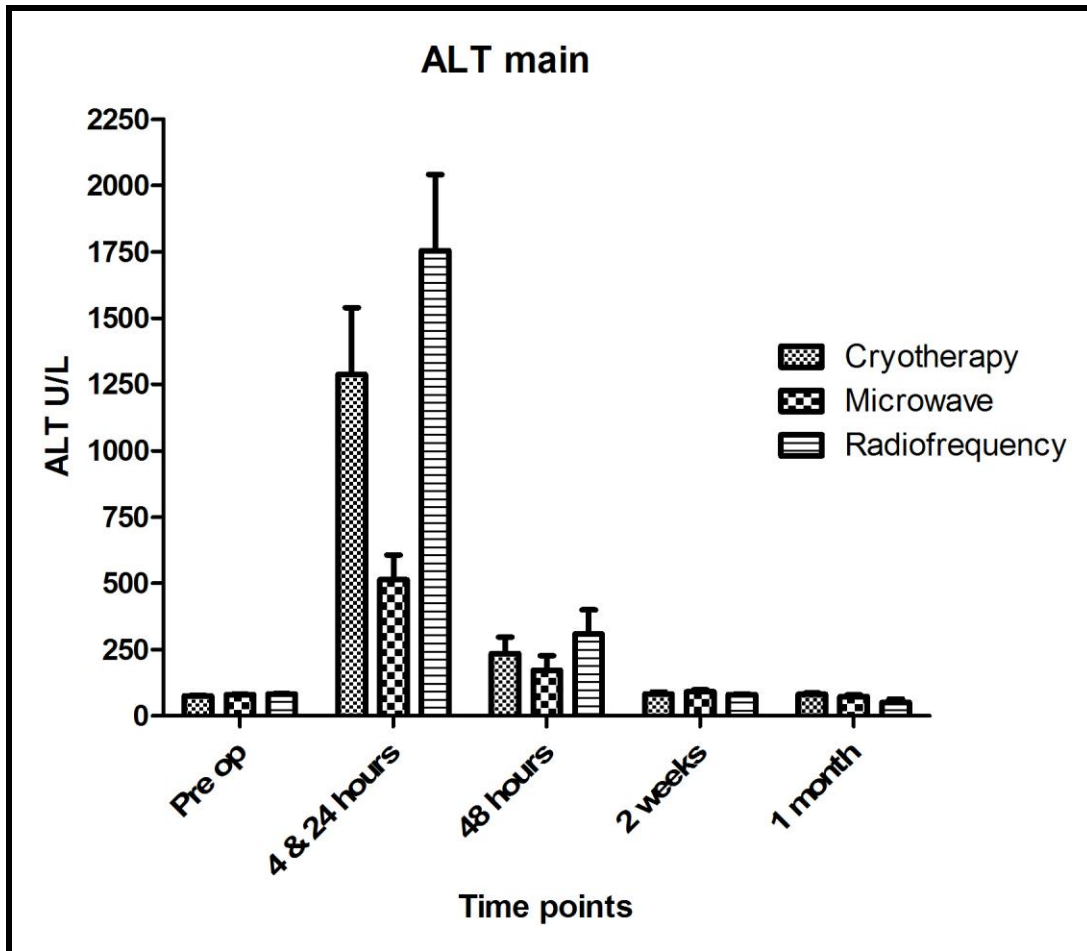


Figure 3-4. Mean ALT rise. n=5 for each modality at each time point except at 4&24 hours where n=10

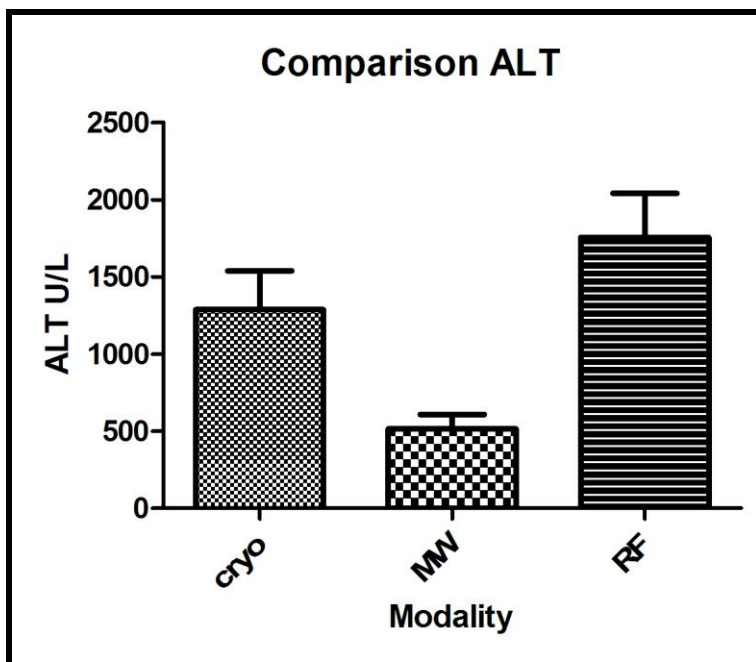


Figure 3-5. ALT rise compared a 24 hours n=5 in each modality.

3.4.2. Haemoglobin

There was a drop in haemoglobin in all modalities and this downward trend continued for microwave and cryotherapy up to two weeks post ablation however, the level began to normalise 1 month post ablation. Radiofrequency on the other hand continued to fall up to 1 month post ablation (Figure 3-6. Haemoglobin analyses (mean \pm sem)).

Although the results were not statistically significant, it highlights the fact that even small volume ablations can cause a drop in haemoglobin. It is unlikely that this is a dilutional effect as all rats had the same amount of post-operative subcutaneous fluids. As no bleeding was visible macroscopically, intra or peri-lesional haemorrhage may account for the drop in haemoglobin. The continued drop in haemoglobin up to 2 weeks post-operatively suggests that there must be some degree of on going reactionary haemorrhage either in the ablated tissue or in liver parenchyma adjacent to it even after the initial insult has ceased. It may be apparent once histological analyses are undertaken as to whether there is any evidence that red blood cells are sequestered in the ablated tissue to account for the drop in haemoglobin.

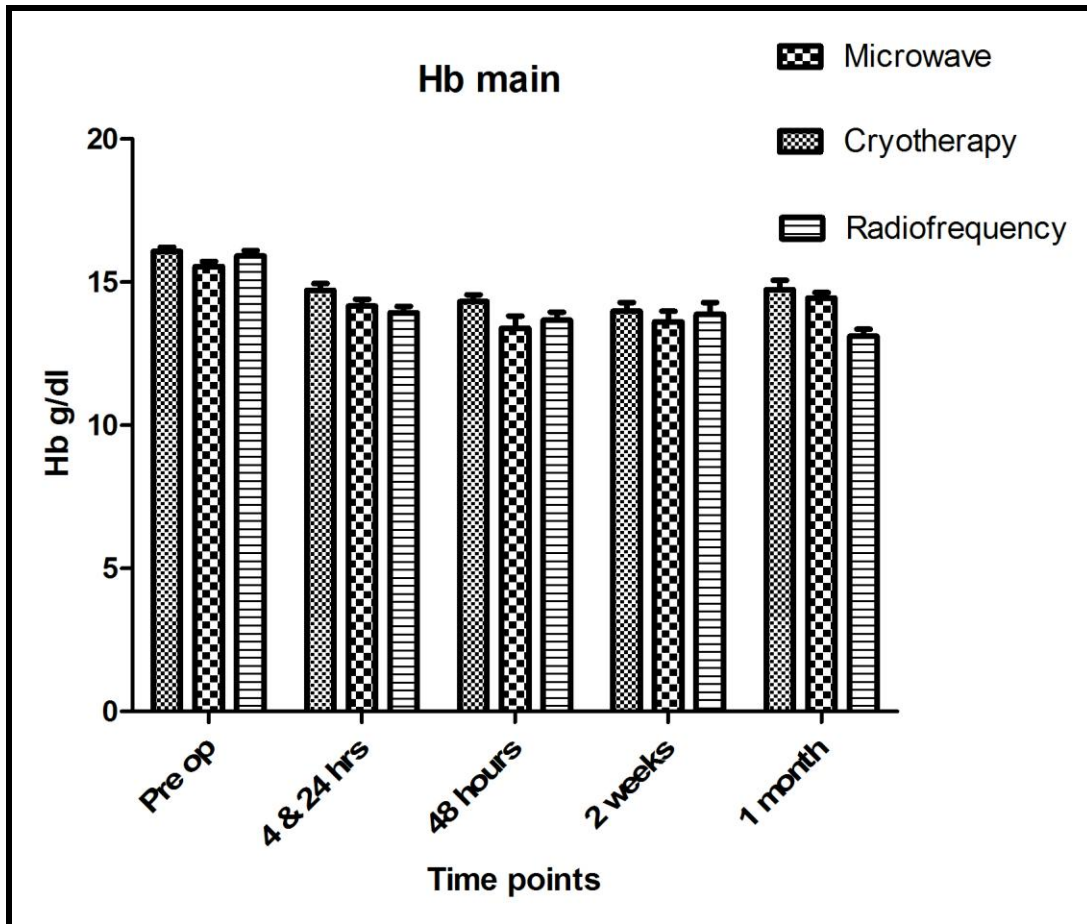


Figure 3-6. Haemoglobin analyses (mean \pm sem). N=5 at each time point except at 4&24 hrs where n=10

3.4.3. Platelets

Cryotherapy has been reported to cause a thrombocytopenia post ablation, thought to be secondary to repeated free-thaw cycles¹². This was not the case in this study and may be due to small volume ablations and single freeze-thaw cycles used. A statistically significant increase from baseline was observed at 2 weeks post ablation. Reactive or secondary thrombocytosis often occurs post surgery as part of the ‘stress’ response and is usually self-limiting¹³, however is usually only detectable in the early post-operative period. So although the increase at week 2 may be related to lesion evolution, it is difficult to justify and perhaps histological analyses may explain this phenomenon. All modalities showed an increase in baseline platelets at 2 weeks, this

was statistically significant in cryotherapy and radiofrequency but not microwave ($p < 0.01$)

Figure 3-7. Platelet analyses (mean \pm sem).

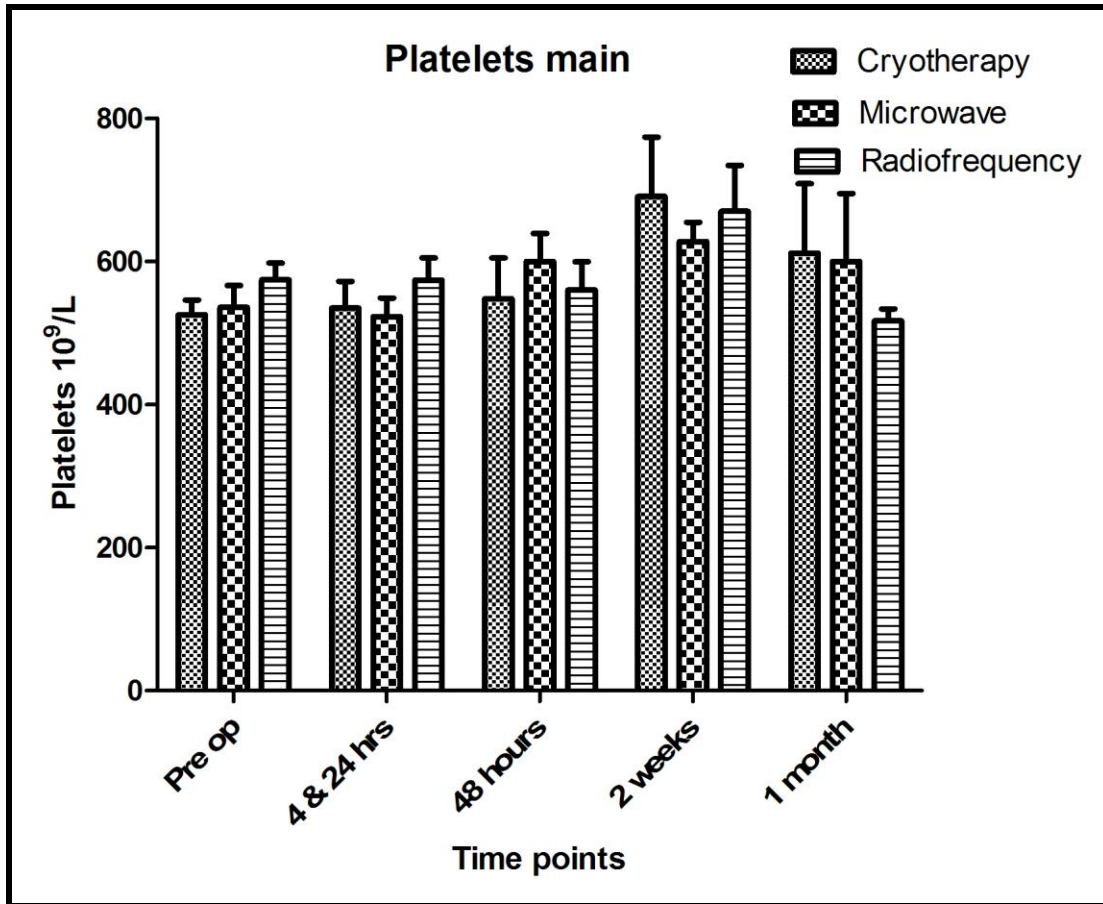


Figure 3-7. Platelet analyses (mean \pm sem). N=5 at each time point except at 4&24 hrs where n=10

3.5. Discussion

All rats survived the procedure and recovered well post-operatively. Weight gain is usually a good indicator of return to normal function and it was encouraging to find that most rats gained weight post-operatively. A rise in ALT is a reflection of the degree of hepatocyte damage that occurs. Macroscopically, the same volume is ablated in each modality as described in chapter 2, methods. However, varying levels of ALT rise post ablation indicate that varying degrees of hepatocyte damage occurs. The cause for this may be clearer once ablated and surrounding tissue are examined histologically, as either the ablated volume increases in size or peripheral damage occurs distal to the ablated site. Histological analyses may also explain the drop in haemoglobin as no intraperitoneal bleeding was visible either intra-operatively or when the abdomen was re-examined once the animals were culled. Platelet rise as described is usually secondary to the body's stress response to surgery and as the half life of platelets is around 7-10 days, perhaps a rise in circulating platelets is to be expected day 14 post-operatively.

1. Hoffman WE, Solter, P.E. Wilson, B.W. . Clinical enzymology. In: Loeb WF, Quimby, F.W., ed. *The Clinical Chemistry of Laboratory Animals*. 2nd ed. Philadelphia: Taylor and Francis; 1999:399-444.
2. Travlos GS, Morris RW, Elwell MR, Duke A, Rosenblum S, Thompson MB. Frequency and relationships of clinical chemistry and liver and kidney histopathology findings in 13-week toxicity studies in rats. *Toxicology*. Jan 22 1996;107(1):17-29.
3. O'Leary MJ, Koll M, Ferguson CN, et al. Liver albumin synthesis in sepsis in the rat: influence of parenteral nutrition, glutamine and growth hormone. *Clin Sci (Lond)*. Dec 2003;105(6):691-698.
4. Bhardwaj N, Strickland AD, Ahmad F, Dennison AR, Lloyd DM. Liver ablation techniques: a review. *Surg Endosc*. Feb 2010;24(2):254-265.
5. Shimada S, Hirota M, Beppu T, et al. Complications and management of microwave coagulation therapy for primary and metastatic liver tumors. *Surg Today*. 1998;28(11):1130-1137.
6. Mulier S, Mulier P, Ni Y, et al. Complications of radiofrequency coagulation of liver tumours. *Br J Surg*. Oct 2002;89(10):1206-1222.
7. Rhim H, Yoon KH, Lee JM, et al. Major complications after radio-frequency thermal ablation of hepatic tumors: spectrum of imaging findings. *Radiographics*. Jan-Feb 2003;23(1):123-134; discussion 134-126.
8. Bain PJ. Liver. In: Latimer KSM, E. A. Prasse, K. W. , ed. *Duncan and Prasse's Veterinary Laboratory Medicine: Clinical Pathology*. 4th ed. Iowa State Press: Ames; 2003:193-214.
9. Dodd GD, 3rd, Napier D, Schoolfield JD, Hubbard L. Percutaneous radiofrequency ablation of hepatic tumors: postablation syndrome. *AJR Am J Roentgenol*. Jul 2005;185(1):51-57.
10. Livraghi T, Goldberg SN, Solbiati L, Meloni F, Ierace T, Gazelle GS. Percutaneous radio-frequency ablation of liver metastases from breast cancer: initial experience in 24 patients. *Radiology*. Jul 2001;220(1):145-149.
11. Curley SA, Izzo F, Delrio P, et al. Radiofrequency ablation of unresectable primary and metastatic hepatic malignancies: results in 123 patients. *Ann Surg*. Jul 1999;230(1):1-8.
12. Seifert JK, Morris DL. World survey on the complications of hepatic and prostate cryotherapy. *World J Surg*. Feb 1999;23(2):109-113; discussion 113-104.
13. Schafer AI. Thrombocytosis and thrombocythemia. *Blood Rev*. Dec 2001;15(4):159-166.
14. Sarantou T, Bilchik A, Ramming KP. Complications of hepatic cryosurgery. *Semin Surg Oncol*. Mar 1998;14(2):156-162.
15. Sohn RL, Carlin AM, Steffes C, et al. The extent of cryosurgery increases the complication rate after hepatic cryoablation. *Am Surg*. Apr 2003;69(4):317-322; discussion 322-313.
16. Saitsu H, Mada Y, Taniwaki S, et al. [Investigation of microwave coagulo-necrotic therapy for 21 patients with small hepatocellular carcinoma less than 5 cm in diameter]. *Nippon Geka Gakkai Zasshi*. Apr 1993;94(4):359-365.
17. Sato M, Watanabe Y, Ueda S, et al. Microwave coagulation therapy for hepatocellular carcinoma. *Gastroenterology*. May 1996;110(5):1507-1514.

- 18.** Kojima Y, Suzuki S, Sakaguchi T, et al. Portal vein thrombosis caused by microwave coagulation therapy for hepatocellular carcinoma: report of a case. *Surg Today*. 2000;30(9):844-848.
- 19.** Garcea G, Lloyd TD, Aylott C, Maddern G, Berry DP. The emergent role of focal liver ablation techniques in the treatment of primary and secondary liver tumours. *Eur J Cancer*. Oct 2003;39(15):2150-2164.

CHAPTER 4: HAEMATOXYLIN AND EOSIN

4. Results: Macroscopic lesion size and Haematoxylin & Eosin.....	82
4.1. Macroscopic lesion size	82
4.2. Microscopic analyses	84
4.3. Microwave ablation.....	84
4.3.1. Macroscopic Findings	84
4.3.2. Microscopic Findings.....	84
4.3.3. Discussion	94
4.4. Cryotherapy	96
4.4.1. Macroscopic Findings	96
4.4.2. Microscopic Findings.....	96
4.4.3. Discussion	102
4.5. Radiofrequency	107
4.5.1. Macroscopic Findings	107
4.5.2. Microscopic Findings.....	107
4.5.3. Discussion	114
4.6. Conclusion.....	116
Figure 4-1 Mean macroscopic ablation sizes \pm SEM	83
Figure 4-2. Microwave: Edge of burn at time zero x20.....	86
Figure 4-3. Microwave: Intralesional portal tract at time zero x40	86
Figure 4-4. Microwave: Adjacent portal tract time zero x40.....	87
Figure 4-5. Microwave: Edge apoptosis at four hours x40.....	88
Figure 4-6. Microwave: Edge apoptosis, neutrophils, necrosis & reactive fibroblasts at time four hours x100.....	89
Figure 4-7. Microwave: Adjacent portal triad with apoptosis and neutrophils at time four hours x100.....	89
Figure 4-8. Microwave: Well demarcated burn edge with edge apoptosis.....	90
Figure 4-9. Microwave: less apoptosis at edge at 48 hours x 40	91
Figure 4-10. Microwave: Fibroblast proliferation at 48 hours x 200	92
Figure 4-11. Microwave: Fibrous capsule with bile duct reduplication at 2 weeks x40	93
Figure 4-12. Cryotherapy: marked areas of haemorrhage at time 0 x 20	97
Figure 4-13. Cryotherapy: scalloped edge at edge at 4 hours x20.....	98
Figure 4-14. Cryotherapy: apoptosis at the edge at 4 hoursx 40	98
Figure 4-15. Cryotherapy: Scalloped edge with perivascular/periportal cell survival at 24 hours x 40.....	99
Figure 4-16. Cryotherapy: edge apoptosis at 24 hours x 40	100
Figure 4-17. Cryotherapy: Burn edge at 48 hours x 40	101
Figure 4-18. Cryotherapy: lesion at 2 weeks x20	102
Figure 4-19. RF: Haemorrhagic burn at time 0 x20.....	108
Figure 4-20. RF: poorly demarcated burn edge with white arrows showing marginal apoptosis and black arrows showing scattered deep apoptosis in normal parenchyma at 4 hours x 40.....	109
Figure 4-21. RF: Edge showing neutrophil infiltration at 24 hours x 40.....	110
Figure 4-22. RF: Edge at 48 hours x20.....	111

Figure 4-23. RF: edge x 40	112
Figure 4-24. RF: Burn edge at 2 weeks x40	113
Figure 4-25. RF: Edge and fibroblastic islands at 1 month x20	114

4. Chapter 4. Macroscopic lesion size and Haematoxylin & Eosin.

4.1. Macroscopic lesion size

As described in chapter 2, each rat underwent 3 ablations of 1 cm each at various distances from the hilum. At each time point a total of 5 rats were culled, therefore 15 ablation sizes were recorded. The following graph represents the evolution of ablation sizes at each time point (Figure 4-1 Mean macroscopic ablation sizes \pm SEM).

The mean ablation size peaked at 24 hours for microwave and cryotherapy and 48 hours for RF ($p < 0.001$). This was statistically significant at 24 and 48 hours when compared between modalities. No obvious correlation was evident between distance from the hilum and lesion size.

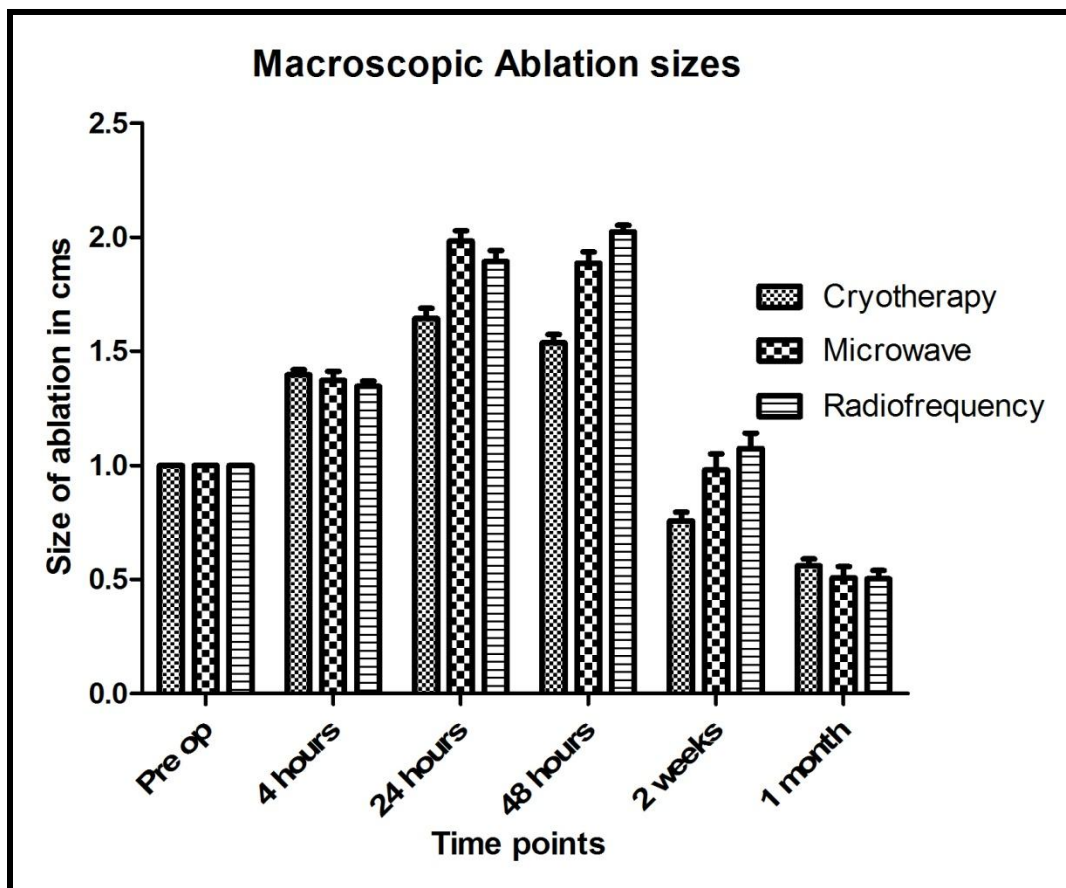


Figure 4-1 Mean macroscopic ablation sizes \pm SEM

4.2. Microscopic analyses

The method for H&E analyses has been described in Chapter 2: methods. All analyses were conducted by two pathologists who were blinded to the slides. The morphological descriptions were observed in the majority of specimens. No correlation was evident between H&E descriptions and distance from the hilum.

4.3. Microwave ablation

4.3.1. Macroscopic Findings

At time zero and 4 hours a well demarcated circular lesion with a central cavity representing the applicator site was visible. The central area was surrounded by a blanched area and a darker hyperaemia rim. Between twenty four and forty eight hours this burn zone expanded in size and was well demarcated with a sharp edge. At two weeks the lesion size had shrunk and at four weeks a much smaller white scar was visible.

4.3.2. Microscopic Findings

Time zero:

Immediately following treatment a central area consisting of a mixture of thermally damaged hepatocytes with eosinophilic cytoplasm or hyperchromatic wrinkled nuclei and homogenous cytoplasm was visible. There were no sign of haemorrhage with the burn extended to the liver capsule in most cases and apparently bounded by portal tracts up to acinar zone 1. Adjacent to the central area a second zone was visible which consisted of liver plate collapse, sinusoidal dilatation and haemorrhage (Figure 4-2. Microwave: Edge of burn at time zero x20.) Intralesional portal tracts also showed thermal damage to the bile duct epithelium and vascular endothelium with abnormal portal tract collagen (Figure 4-3. Microwave: Intralesional portal tract at time zero x40). Similar changes were seen adjacent to the burn in portal tracts not directly involved in the lesion although this decreased with distance from the burn, with the collagen abnormalities being more marked (Figure 4-4. Microwave: Adjacent portal tract time zero x40). No inflammation, apoptosis or fibrosis was observed outside the burn area and apart from the described portal changes and occasional central vein thrombi the adjacent liver parenchyma appeared unremarkable.

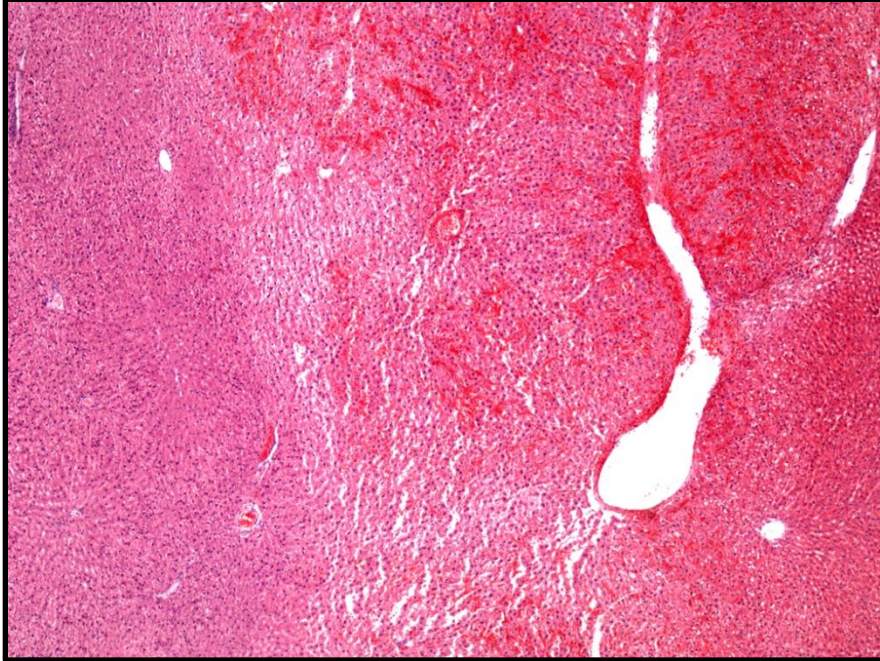


Figure 4-2. Microwave: Edge of burn at time zero x20.



Figure 4-3. Microwave: Intralesional portal tract at time zero x40



Figure 4-4. Microwave: Adjacent portal tract time zero x40

Four hours:

By four hours the burn had become sharply demarcated and extended to the outer edge of the previously noted haemorrhagic zone. A zone of hepatocytes within the lesion demonstrated complete karyorrhexis leaving eosinophilic ghosts, while others closer to the probe retained their nuclei. At the edge of the burn a mild infiltrate of neutrophils was present with neutrophil margination in adjacent vessels and focal haemorrhage. In addition, shrunken hepatocytes with retraction away from the stroma with typically apoptotic appearances (condensed densely eosinophilic cytoplasm, shrunken homogenous hyperchromatic nuclei but intact nuclear and plasma membranes) were marked along the edge of the burn and extended into the adjacent parenchyma. They were seen to be grouped around the damaged portal tracts and central veins (vide supra) and there were sporadic foci of spindled cells (Figure 4-5. Microwave: Edge

apoptosis at four hours x40 and Figure 4-6. Microwave: Edge apoptosis, neutrophils, necrosis & reactive fibroblasts at time four hours x100). A focal neutrophil infiltrate and apoptosis was also seen around some portal tracts outside the lesion (Figure 4-7. Microwave: Adjacent portal triad with apoptosis and neutrophils at time four hours x100).

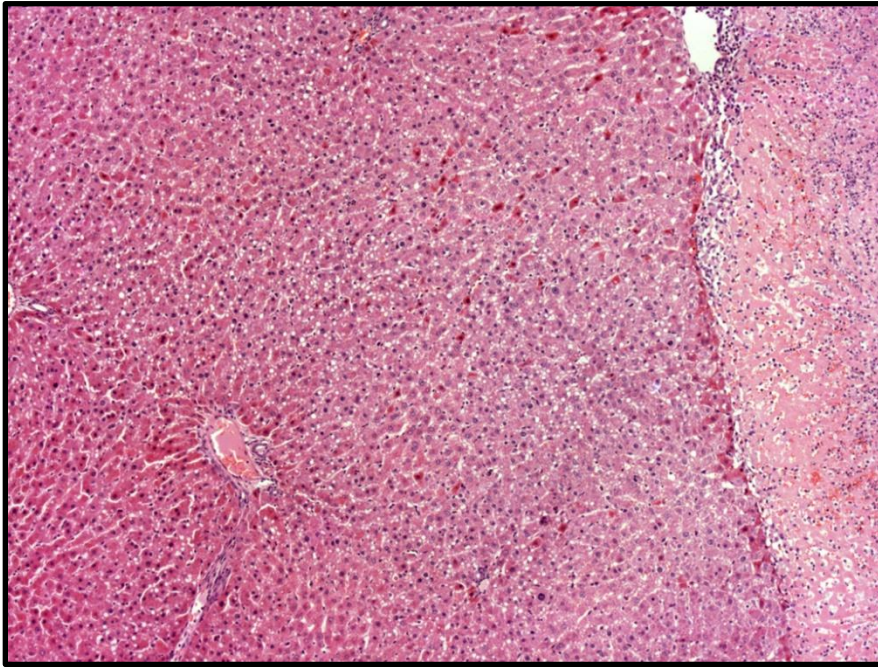


Figure 4-5. Microwave: Edge apoptosis at four hours x40

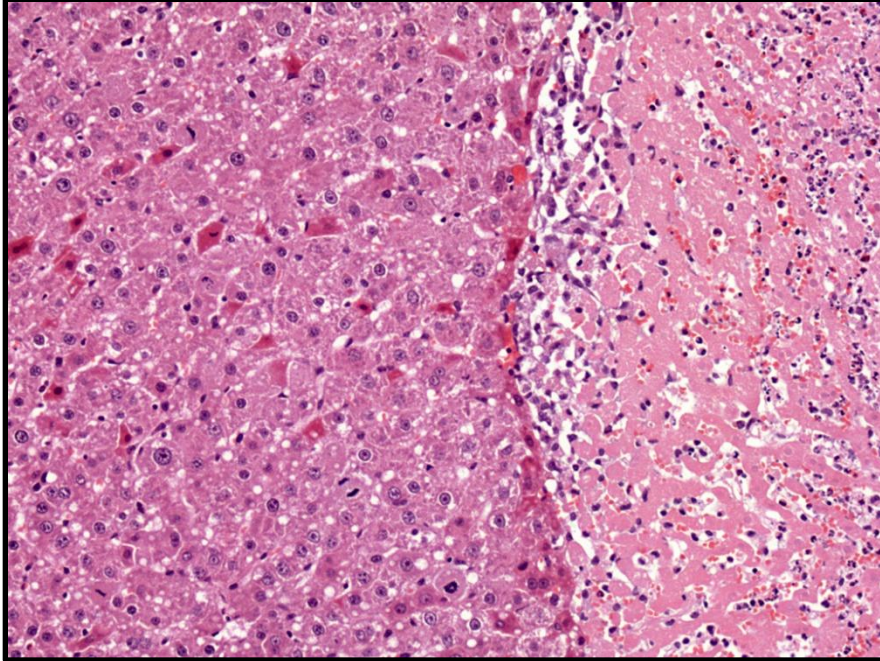


Figure 4-6. Microwave: Edge apoptosis, neutrophils, necrosis & reactive fibroblasts at time four hours x100

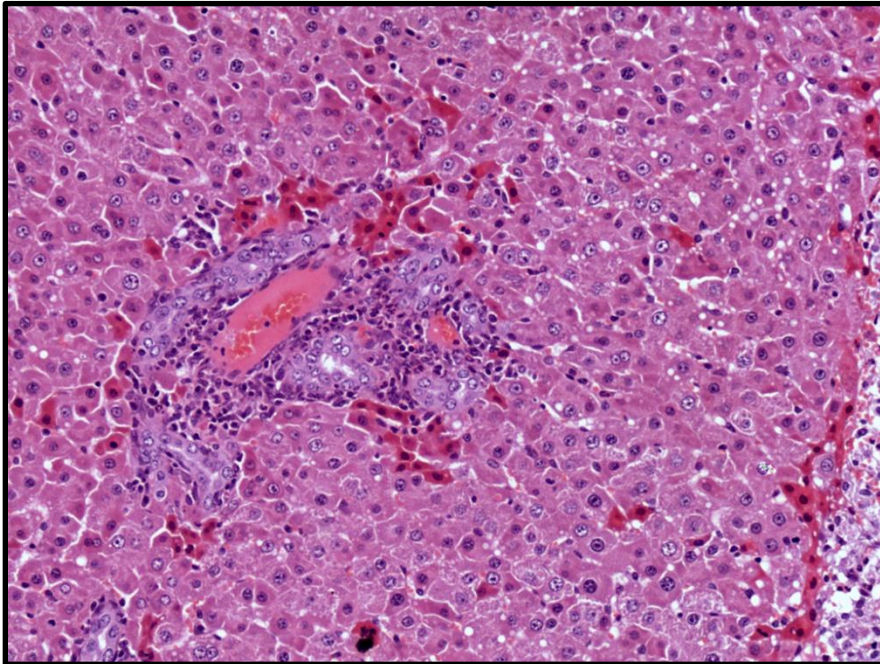


Figure 4-7. Microwave: Adjacent portal triad with apoptosis and neutrophils at time four hours x100

Twenty four hours:

At twenty four hours the appearance of the burn remained essentially unchanged (retention of nuclei adjacent to the probe position is now marked). There was complete necrosis of hepatocytes up to the edge of the burn with no viable cells within the burn limits, including up to portal tracts and vessels. The burn edge remained very well demarcated with neutrophil infiltration extending into the lesion. Focal areas of inflammation were apparent within the liver parenchyma, associated with damaged portal tracts and hepatocytes. Apoptotic hepatocytes persisted along the burn edge and extend into the adjacent parenchyma but do not appear as concentrated around portal tracts as at earlier time points (Figure 4-8. Microwave: Well demarcated burn edge with edge apoptosis). An occasional area of fibroblastic proliferation was seen adjacent to involved portal tracts along the burn edge.

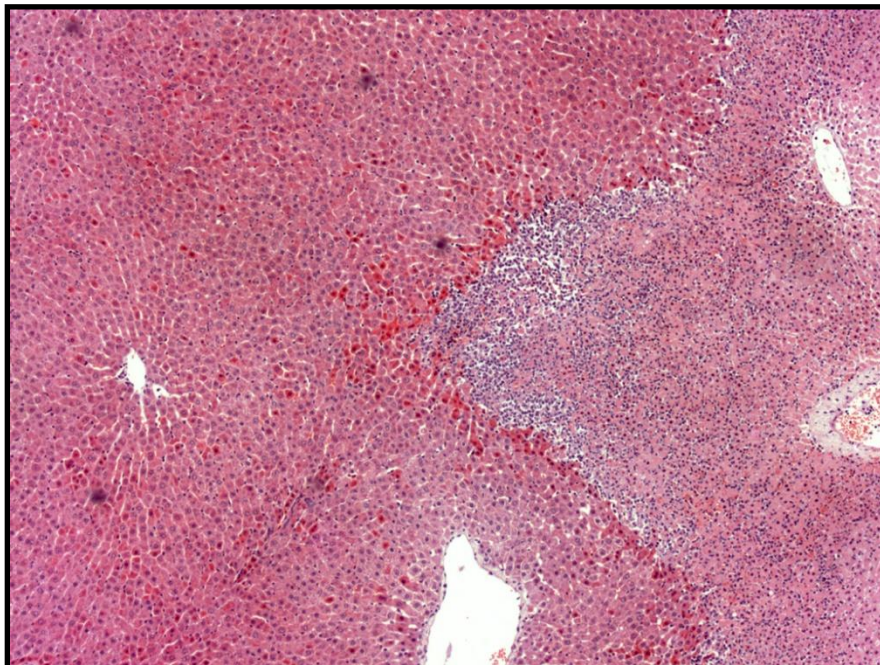


Figure 4-8. Microwave: Well demarcated burn edge with edge apoptosis

Forty eight hours:

By forty eight hours the area within the burn remained unchanged with preserved nuclei and no haemorrhage into the burn, possibly due to coagulation of vessels. Neutrophil infiltration into the burn from the edge has progressed with larger foci of inflammation around damaged portal tracts. This was associated with frank necrosis of adjacent liver parenchyma which was most marked around the central veins. Apoptotic bodies are now less prominent at the burn edge though some were still scattered in the adjacent liver parenchyma (Figure 4-9. Microwave: less apoptosis at edge at 48 hours x 40). Fibroblast proliferation was now prominent along the burn edge and also surrounding some damaged adjacent portal tracts (Figure 4-10. Microwave: Fibroblast proliferation at 48 hours x 200).

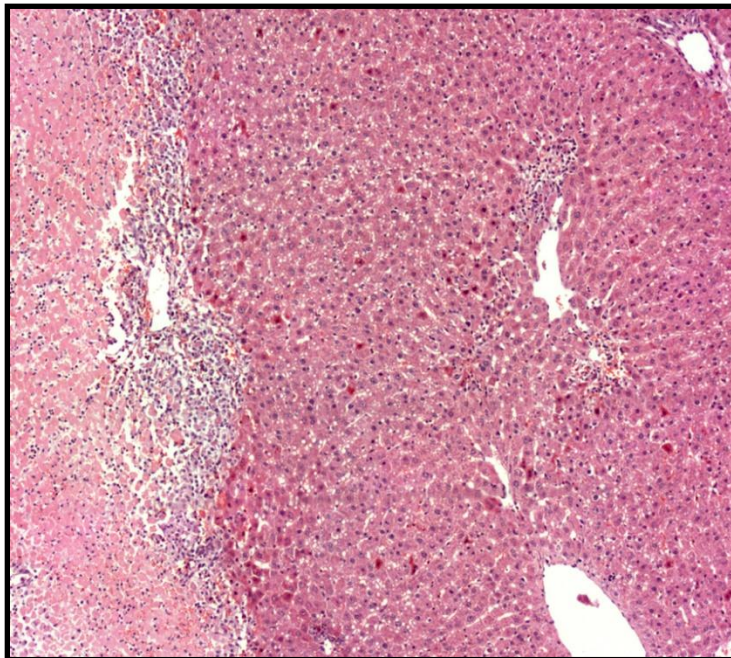


Figure 4-9. Microwave: less apoptosis at edge at 48 hours x 40

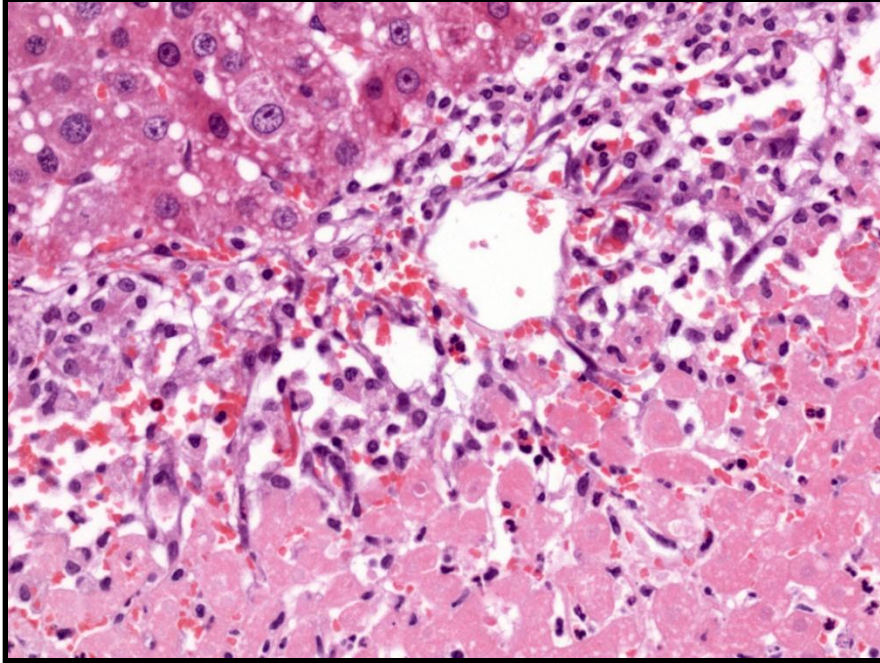


Figure 4-10. Microwave: Fibroblast proliferation at 48 hours x 200

Two weeks

By two weeks there had been significant evolution of the lesion with a shrunken burn area, hepatocytes with nuclear preservation with focal calcification of ablated hepatocytes and cystic change. The burn was now encapsulated by a fibrotic capsule containing prominent bile duct reduplication, foci of macrophages, giant cells and a sparse infiltrate of lymphocytes (Figure 4-11. Microwave: Fibrous capsule with bile duct reduplication at 2 weeks x40). Although mild fibrosis around some adjacent portal tracts was visible there were no neutrophils or apoptotic bodies.

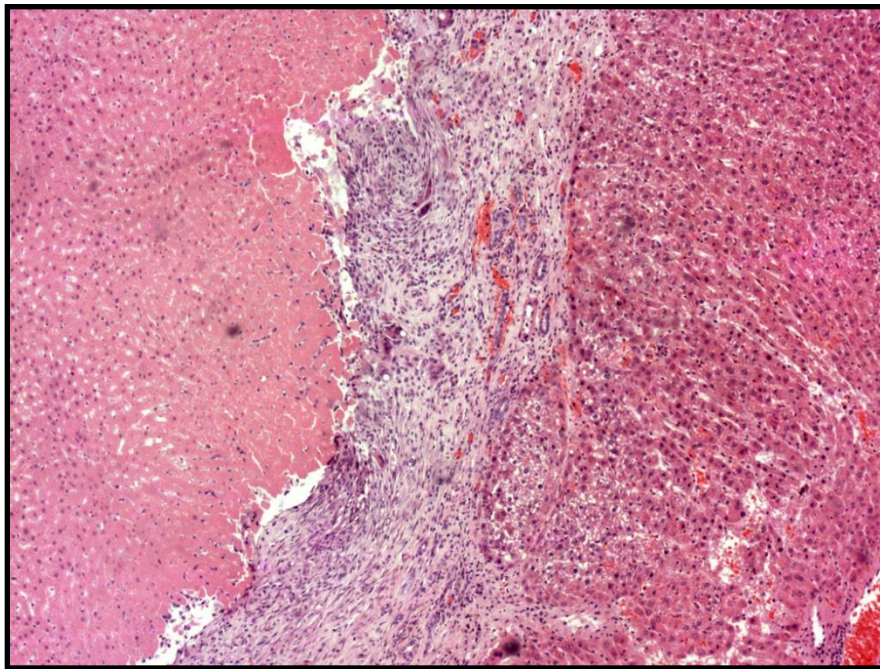


Figure 4-11. Microwave: Fibrous capsule with bile duct reduplication at 2 weeks x40

Four weeks:

Finally by four weeks there had been a significant reduction in the size of the burn which was encapsulated with a thicker fibrous capsule being visible. Lymphocytes were more prominent in the fibrous capsule although they were limited to this area.

4.3.3. Discussion

As reported in Chapter 1, only 10 studies describe in detail the histological changes which occur following microwave ablation ¹⁻¹⁰ and only 5 described the lesion evolution at specific time points ^{1, 3, 4, 6, 7}. The macroscopic and microscopic changes described immediately post ablation in this study are in keeping with previously reported studies ^{6, 2, 3, 5, 7}, particularly the ‘fixative effect’ microwave has on hepatocytes in direct contact with the applicator in the central area ⁵⁻¹⁰.

Few studies describe the evolution of the lesions with time ^{1, 3, 4, 6, 7} and although the present study is generally in agreement with previous findings, apoptosis at the margin of the treated area and in normal adjacent parenchyma (particularly grouped around portal tracts) has not been reported previously. This phenomenon was present immediately post ablation and was markedly reduced by 48 hours. Previous research project on the pig liver (Strickland MD 2005) described subtle collagen destruction in the portal triad which was present in pathologically normal parenchyma distal to the ablation and which was only demonstrable by its loss of birefringence under polarised light ⁶. The degree of apoptosis in this present study seems to reduce at increasing distances from the ablation edge and coincided with vascular structures, in and

immediately adjacent to the lesion, becoming completely thrombosed. It is possible be that the two observation are connected and there may be a degree of transference or conduction of heat which produces cytotoxic temperatures away from the ablated zone.

The edge of the ablated area was well demarcated and uniform, with very little disruption as a result of any surrounding vasculature and this has been described previously in several studies ^{2, 4, 6, 7, 11} . There is evidence that microwave is less affected by the heat sink effect compared to radiofrequency ^{2, 7} , but there will inevitably be some conductive loss of heat down blood vessels and this may account for the distal vascular and biliary tree damage. The Pringle manoeuvre, which involves compression of the hepatoduodenal ligament, does reduce the heat sink effect and has shown to increase lesion size ^{7, 12} but is also associated with increase bile duct and portal vein damage ^{13, 14} and of course is difficult to perform percutaneously. The other potential cause for distal damage may be necrotic debris eluting from ablated tissue and causing an inflammatory reaction. This ability to coagulate vessels within the lesion not only prevents the disruption of the ablation morphology, but may also account for the relatively low systemic pro-inflammatory and inflammatory response observed with microwave ablation compared to radiofrequency and cryotherapy ¹⁵ .

From the above observations it appears that the transition zone, the interface between the ablated, dead tissue and normal liver parenchyma, plays a vital role in determining whether an ablation will be successful. This is particularly important when treating large tumours or those located adjacent to or directly in contact with vascular structures. The ratio between the volume of ablated, dead tissue and the transition zone has previously been investigated ²⁶ and may account

for the expansion of the ablation site noted in this study and previously ⁶. Accumulation of apoptotic cell at the ablation edge during the early phase following microwave ablation suggests that cells at the periphery undergo thermal damage but perhaps not as swiftly as those in the centre, and hence do not undergo the fixative effect.

4.4. Cryotherapy

4.4.1. Macroscopic Findings

Immediately following the ablation a hyperaemic lesion was visible which gradually, over the course of 24-48 hours became a greyish-white, well demarcated lesion. This reduced to approximately 50% of the initial size by week 4.

4.4.2. Microscopic Findings

Time zero:

Immediately following the treatment the initial ablation zone was largely well demarcated with variable penetration into the parenchyma. Examination demonstrated thermally damaged hepatocytes with eosinophilic cytoplasm and hyperchromatic nuclei. Marked haemorrhage was localised around the portal tracts compared to microwave (acinar zone 1) with no adjacent areas of sinusoidal dilatation (Figure 4-12. Cryotherapy: marked areas of haemorrhage at time 0 x 20). Intra-lesional portal tracts showed marked thermal damage with loss of and damage to the biliary epithelium and vascular endothelium. The non-lesional portal areas appeared essentially normal with only minimal thermal damage to the tracts closest to the periphery of the treated area.

Interestingly the endothelium of the portal veins appears particularly sensitive and was damaged preferentially. No inflammation, fibrosis or apoptosis was seen and the adjacent parenchyma appeared normal.



Figure 4-12. Cryotherapy: marked areas of haemorrhage at time 0 x 20

Four hours:

At 4 hours the treated area became more clearly demarcated, although the edge was scalloped (Figure 4-13. Cryotherapy: scalloped edge at edge at 4 hours x20). Intra-lesional hepatocytes retained their nuclei at this stage but the features of thermal damage were now more severe and homogenous involving the whole of the treated area and coalescent zones of haemorrhage were also evident. Intralesional and subcapsular infiltration by neutrophils and apoptotic hepatocytes appeared focally along the periphery of the treated area and extended some way into the adjacent

parenchyma. Adjacent portal tracts again demonstrated preferential endothelial damage with surrounding inflammation. At this stage there was no proliferation of fibroblasts.

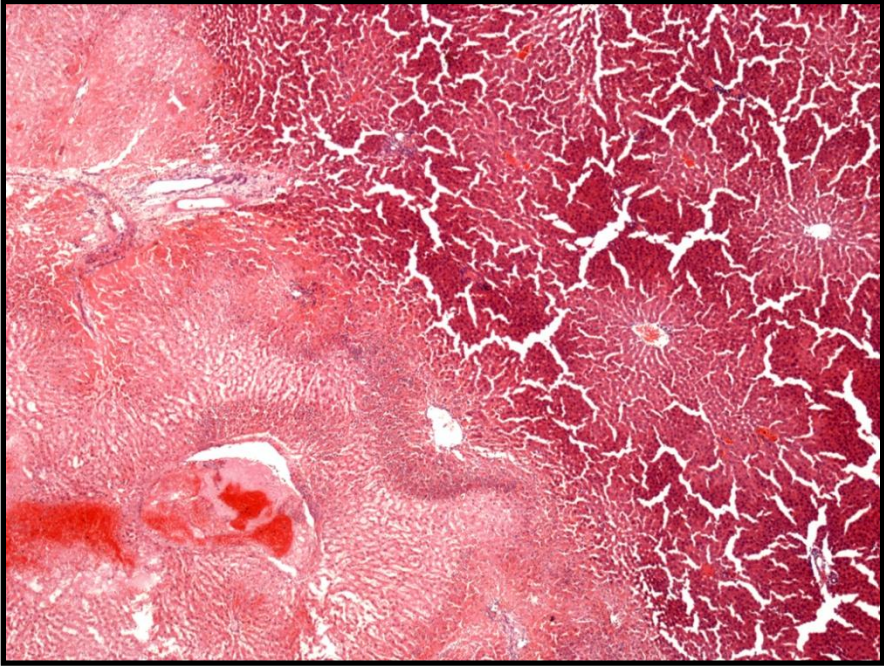


Figure 4-13. Cryotherapy: scalloped edge at edge at 4 hours x20

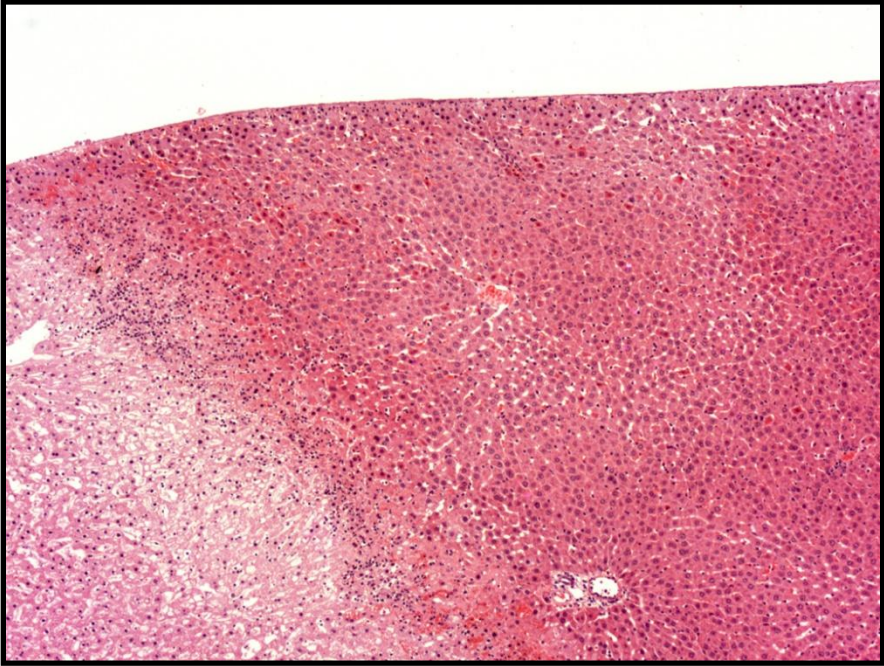


Figure 4-14. Cryotherapy: apoptosis at the edge at 4 hours x 40

Twenty four hours:

At 24 hours after treatment the ablated liver tissue demonstrated less haemorrhage and complete coagulative necrosis, leaving eosinophilic ghosts with no remaining nuclei. The peripheral zone was again well demarcated but scalloped with some perivascular and periportal survival of hepatocytes and portal tract elements at the periphery (Figure 4-15. Cryotherapy: Scalloped edge with perivascular/periportal cell survival at 24 hours x 40). The neutrophil infiltrate extended deeply into the ablated tissue and apoptotic bodies, now slightly more numerous, only appeared focally along burn edge and scattered into the adjacent parenchyma (Figure 4-16. Cryotherapy: edge apoptosis at 24 hours x 40). Portal tracts were unchanged from 0 and 4 hours with no evidence of fibroblast proliferation.

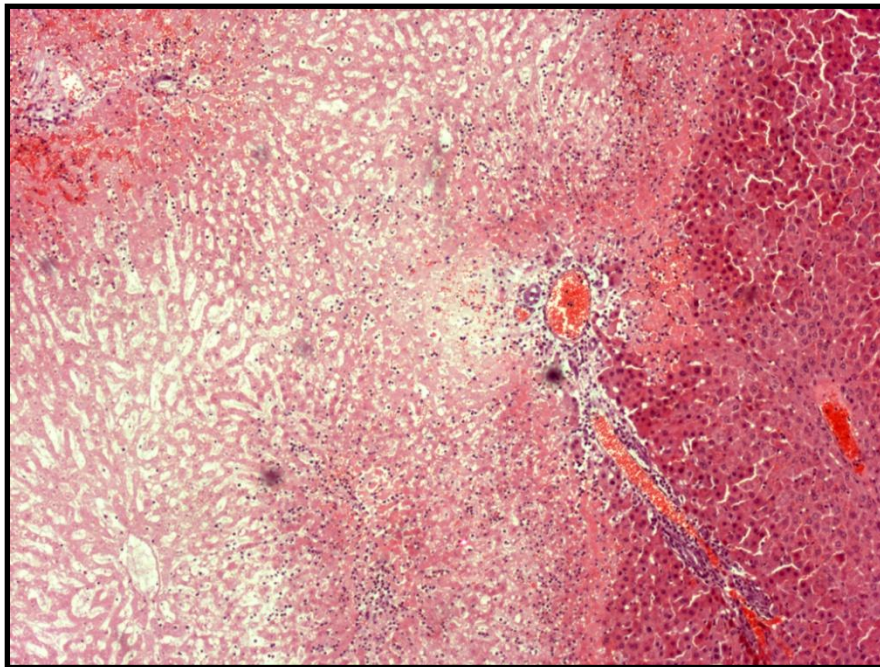


Figure 4-15. Cryotherapy: Scalloped edge with perivascular/periportal cell survival at 24 hours x 40

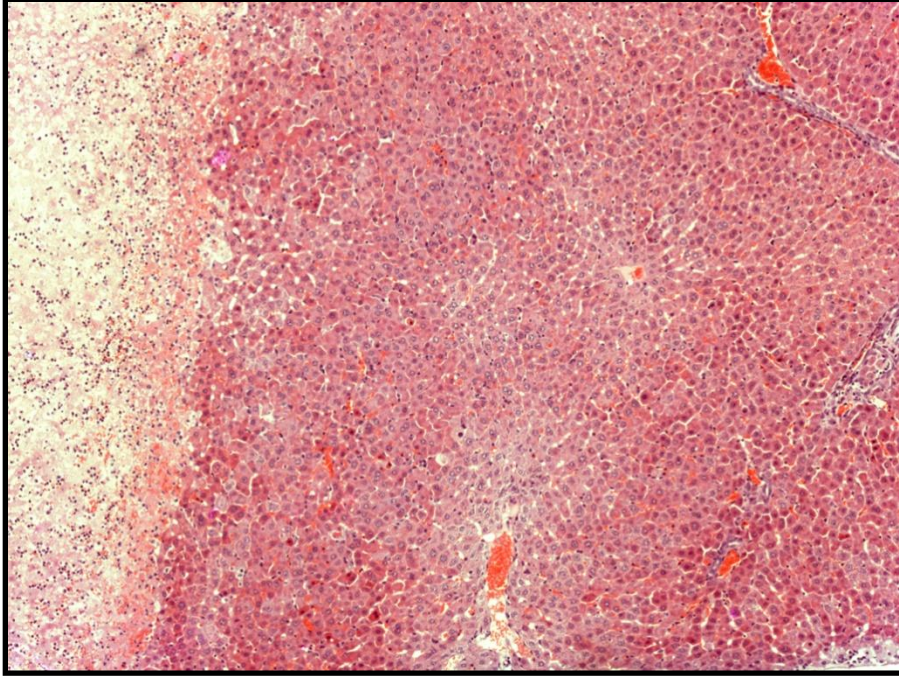


Figure 4-16. Cryotherapy: edge apoptosis at 24 hours x 40

Forty eight hours:

After 48 hours the appearance of the treated area was largely unchanged. Neutrophils were present in focal collections and much less prominent than at previous time points. The peripheral zone appeared slightly more irregular with survival of perivascular and periportal hepatocytes and surrounding haemorrhage. Some focal areas of periportal inflammation and oedema were still observed around the most peripheral portal tracts. Endothelial damage was still prominent and the biliary epithelium was now slightly irregular with some surrounding apoptosis. Occasional apoptosis was also seen in the adjacent parenchyma with the development of early surrounding fibroblast proliferation.

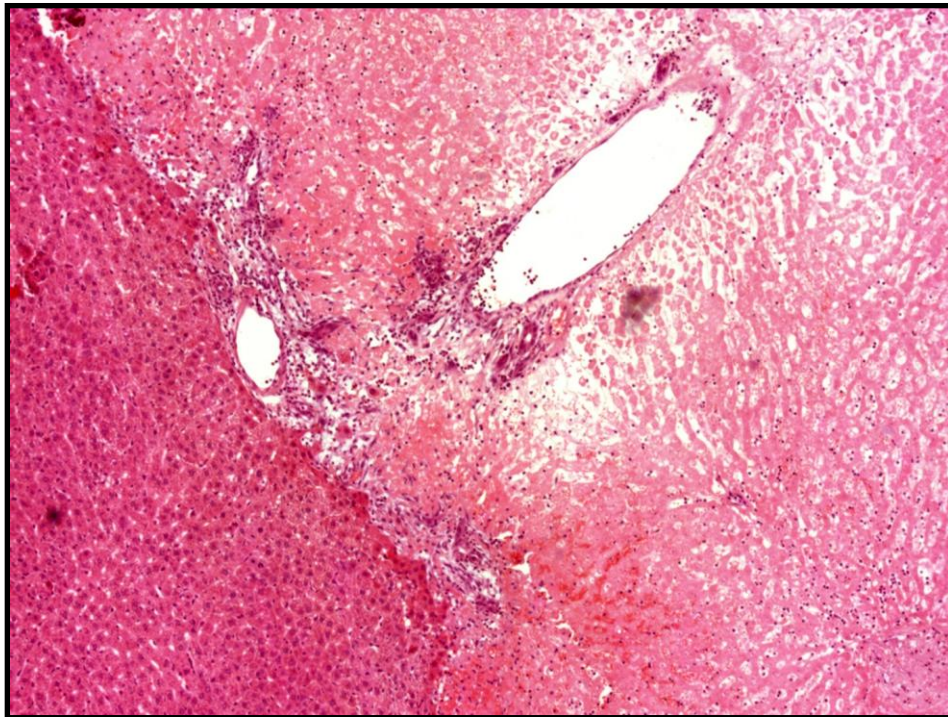


Figure 4-17. Cryotherapy: Burn edge at 48 hours x 40

Two weeks:

At two weeks, a mature, well demarcated fibrous capsule surrounded the ablated area which contained foci of ductular proliferation and focal infiltration by macrophages and lymphocytes. Haemosiderin deposition and some entrapped, surviving hepatocytes were present within the fibrous capsule. The ablated area was reduced in size and fibrosis extended down immediately adjacent portal tracts indicating some damage to these structures that had not previously been evident. No neutrophils or apoptotic cells remained at this stage.

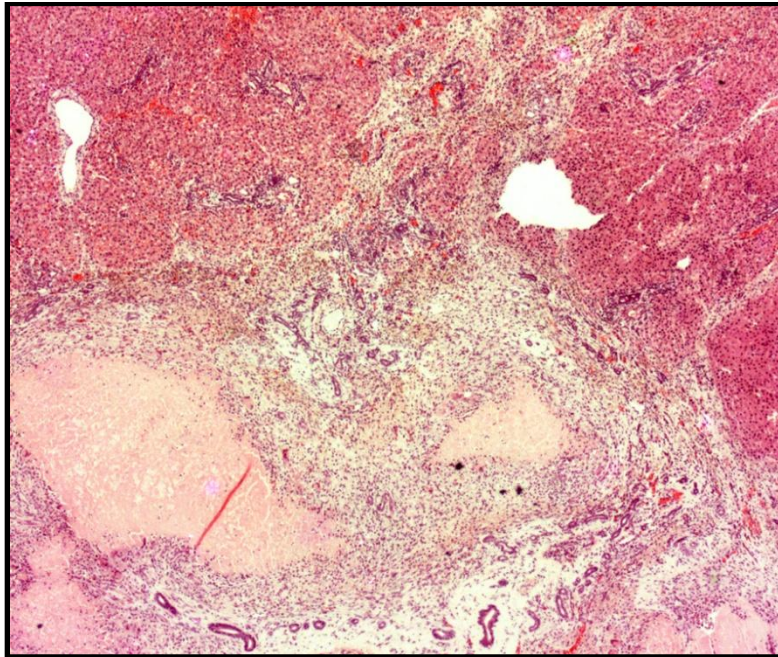


Figure 4-18. Cryotherapy: lesion at 2 weeks x20

Four weeks:

After 4 weeks the treated area was further reduced in size and there had been some increase in the thickness of the thicker fibrous capsule and marked haemosiderin deposition.

4.4.3. Discussion

The macroscopic appearance of the cryoablated lesion described in this study is in agreement with the published literature. The lesion is described as initially yellowish-white during freezing and hyperaemic during thawing but evolves over time to become a uniform grey by the 3rd day. Subsequently there is a gradual reduction of the necrotic area which is completely replaced by fibrous tissue by the fourth week ¹⁶.

Cell death within the ablated zone is due to a combination of factors; intracellular and extracellular ice formation leads to ice crystal formation and cellular dehydration with consequent rupture. Electrolyte disturbance and small vessel stasis causes destruction and thrombosis leading to hypoxia and reduced tissue perfusion. Mechanical damage to cellular integrity by expansion of large ice crystals from the interstitial space, denaturation of membrane lipid protein complexes and osmotic changes during thawing all contribute to cellular destruction ^{17, 18}. Close to the probe the main mechanisms of cell death consist of ice crystals which form within and around cells. During the thaw phase these crystals rupture cell membranes leading to tissue death ¹⁹. The temperature drops more rapidly and to lower temperatures with decreasing distance from the cryoprobe ²⁰, making cells in the periphery more susceptible to sub lethal freezing and subsequent survival.

Several studies have since described the “cryotherapy lesion” in detail. Immediately following treatment, examination of the ablated area always finds an area of central necrosis ^{21, 22}. The initial necrosis is heterogenous with leukocyte infiltration ¹⁷ or complete loss of nuclear and cytoplasmic detail ²³. This is surrounded by sinusoidal congestion and haemorrhage, principally observed in the portal zone connective tissue and central veins ^{24, 25}. In addition, our study

revealed apoptotic cells deep in the non-ablated parenchyma with relative sparing of non-lesional biliary epithelium. This is similar to the findings with microwave above. There is however marked damage to remote vascular endothelium draining the ablation zone. Intra-lesional peripheral cell damage is mainly mediated by vascular damage as ice crystals form only within arterioles and venules but not within cells, contrasting with the situation next to the probe. In this way the extracellular fluid becomes hypertonic and unfrozen cells dehydrate. Furthermore, the extracellular fluid accumulates within vessels which consequently rupture during thawing and haemorrhage produces tissue hypoxia and reduced tissue nutrition ¹⁹. This suggests that the distal extra-lesional vascular damage may be due to conductance of the cytotoxic effects of freezing down the vascular tree. These effects may also be exacerbated by necrotic debris from the ablation zone causing local endothelial damage.

Several investigators have examined the hepatic cryolesion at 24 hours following ablation in a number of different animal models ^{19-21, 26-29}. One study sub-divided the lesion into 3 zones; a central zone of pan-coagulative necrosis, an intermediate zone of infiltrating polymorphonuclear leukocytes and a thin outer zone of reactive hyperaemia ²⁸. This description identifies separate and distinct zones which are similar to those found in our study and in addition there is a consistent finding of intensively eosinophilic cytoplasm and nuclei with condensation of the nuclear stain along the disintegrated membrane ²⁰. The lesions at 24 and 48 hours in this study demonstrated a well demarcated but scalloped edge with survival of cells perivascularly and deep infiltration of inflammatory cells. We did however notice an increased number of apoptotic cells around the periphery of the treated area, with extension into the adjacent normal parenchyma. This provides further evidence that there must be transference or conduction of the

freezing cytotoxic temperatures beyond the ablated zone. At 48 hours, biliary damage is clearly evident with persistence of the previously noted vascular endothelial damage.

Although we did not analyse the lesion between days 4 and 7, published studies confirm that the demarcation of the 3 zones becomes increasingly obvious with the development of a central necrotic zone, an intermediate zone with patchy hepatocyte survival, viable and proliferating bile ducts, vessels, fibroblasts and inflammatory cells and a peripheral zone of infiltrating inflammatory cells²⁴. Interestingly, in proximity to large blood vessels there was an increase in the distance between the edge of the central zone of necrosis and the normal hepatic parenchyma³⁰ with a pronounced band of fibrosis at the deep margins of the lesion, capillary proliferation and mild inflammation extending from adjacent normal liver into the area of coagulation necrosis resulting in the scalloped appearance of the margin²⁶. By day 7 the outer zone (the hyperemic area noted on the second day) was largely replaced by granulation tissue and early changes associated with the formation of fibrosis (loose fibrous tissue with neo-vascularization, proliferating biliary ductules, hemosiderin-laden macrophages, foreign-body type giant cells and foci of calcification)²⁸. The finding of granulation tissue has also been confirmed by other studies²⁴, but importantly medium- to large-size bile ducts and arteries were preserved in both the zones of coagulative necrosis and granulation tissue whereas smaller adjacent veins showed endothelial damage²⁸.

Examination of lesions up to day 7 suggests that vascular structures in and around the ablated area play an important role. Clinically, tumours in close proximity to blood vessels have a higher incidence of local recurrence³¹⁻³³ and several studies have demonstrated distortion of the ablated

lesion as a consequence of surrounding blood vessels^{21, 30}. This phenomenon is also observed in other thermal ablative modalities such as radiofrequency and microwave and is due to the “heat sink effect” which results from, and is defined as the preservation of temperatures which allow cellular survival (tissue cooling) due to adjacent vessels of greater than one millimetre in diameter which deflect the ablation zone away from the vessel³⁴. A similar mechanism is proposed in cryotherapy although technically the inflowing warm blood causes a “cold sink” rather than a heat sink effect, causing inadequate tissue freezing and subsequent cell survival adjacent to these large vessels.

The regenerative process begins by week 2 and this has been previously described and is confirmed in our study. Ductal proliferation which is particularly evident in the intermediate zone occurs from normal liver tissue infiltrated with mononuclear cells^{26, 35} and in addition in our study the lesion was well demarcated with a clear fibrous capsule and evidence of adjacent resolving portal tract damage. In most studies by day 21 after cryoablation, two clear zones have developed with a central area of persistent necrosis and an outer area of granulation and fibrous tissue without an intervening inflammatory zone²⁴. There are a smaller number of reports where the persistence of the initial three zones is described up to a month post ablation³⁶. From the outer zone, fibrous septa extend into the area of coagulative necrosis which appears significantly reduced in size^{24, 28}. By week 4 the lesion consists principally of fibrous tissue, although with survival of large vessels and bile ducts^{24, 26-28}. After more than sixty days following cryoablation, a small area of fibrosis was the only evidence of previous cellular destruction^{26, 37}.

4.5. Radiofrequency

4.5.1. Macroscopic Findings

Immediately following treatment and at 4 hours, a hyperaemic lesion with an irregular burn edge was visible. Twenty-four hours later this burn zone was more clearly demarcated with a sharp edge visible at 48 hours. By two weeks the lesion had reduced in size and at four weeks a significantly smaller white scar was all that was visible.

4.5.2. Microscopic Findings

Time zero:

Immediately following ablation an irregular burn area with a central cystic zone was evident. This cystic area was surrounded by patchy thermal damage but the demarcation of the area which had suffered from burn damage from normal liver parenchyma was not clear and there was a zone of haemorrhage which surrounded the burn edge. The central cystic area was probably due to the trauma related to the insertion of the probe. Surprisingly, although there was obvious damage to surrounding endothelium, there was relative sparing of bile duct epithelium.

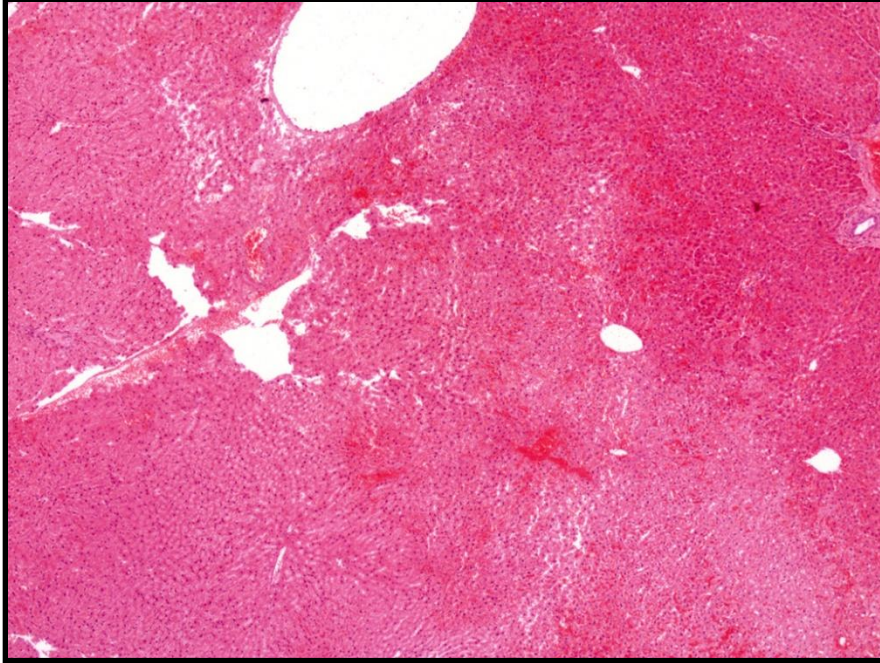


Figure 4-19. RF: Haemorrhagic burn at time 0 x20

Four hours:

By four hours eosinophilic 'ghost' cells were visible in the burn zone, though some cells showing nuclei preservation. Prominent haemorrhage was visible at the burn edge along with apoptotic hepatocytes which were also scattered deeply within adjacent normal liver parenchyma. Again persistent vascular endothelial damage in surrounding portal tracts was visible.

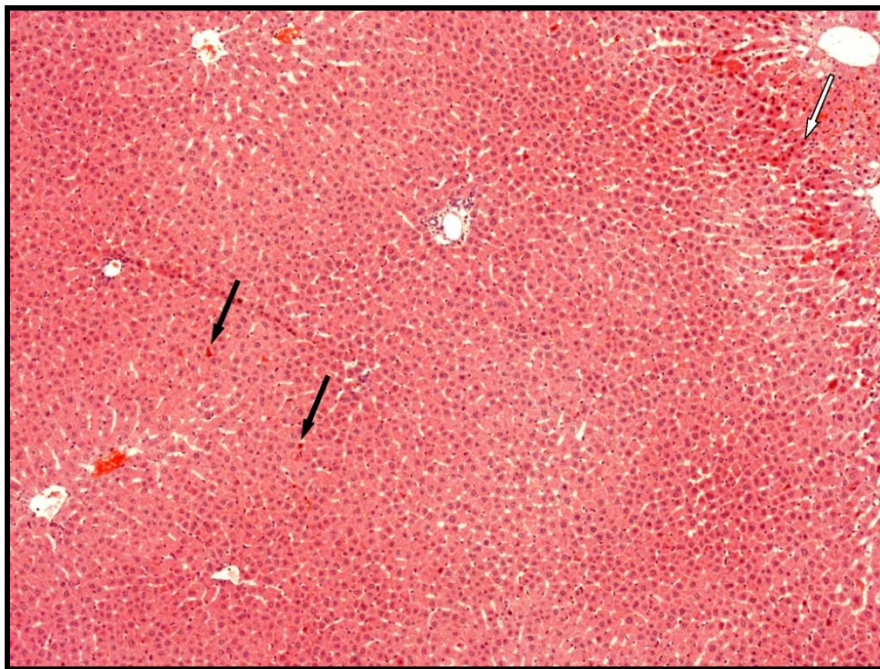


Figure 4-20. RF: poorly demarcated burn edge with white arrows showing marginal apoptosis and black arrows showing scattered deep apoptosis in normal parenchyma at 4 hours x 40

Twenty four hours:

At twenty four hours there was an increased number of 'ghost' like cells with eosinophilic cytoplasm, though some cells in the ablated tissue demonstrated nuclear preservation. There was no progression of the burn edge, however, islands of necrotic liver parenchyma were dotted

irregularly at the interface between ablated and normal liver parenchyma with neutrophil infiltration replacing the haemorrhagic zone (Figure 4-21. RF: Edge showing neutrophil infiltration at 24 hours x 40). An increased number of apoptotic cells were visible in the adjacent normal parenchyma and they were mainly concentrated around portal tracts.

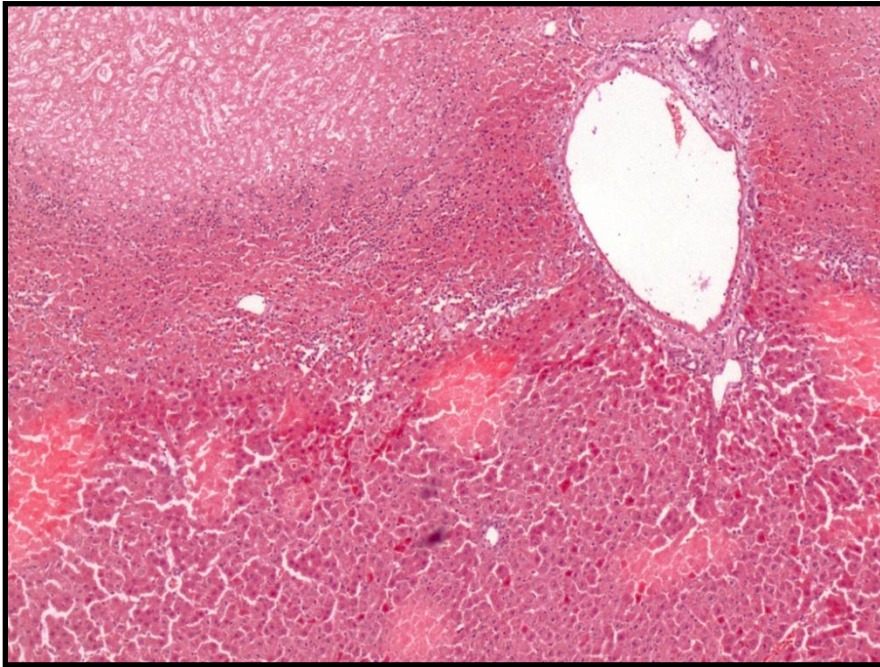


Figure 4-21. RF: Edge showing neutrophil infiltration at 24 hours x 40

Forty eight hours:

By forty eight hours 'fixed' looking hepatocytes which were eosinophilic and hyalinised but retained their nuclei were scattered widely in the ablated area and adjacent tissue, particularly around portal areas. A reduction in neutrophil infiltration was evident and islands of necrosis at the periphery of the burn now coalesced to form a scalloped irregular edge with preferential survival around portal areas. There was also scattered apoptosis in the adjacent normal parenchyma and the beginning of fibroblastic proliferation.



Figure 4-22. RF: Edge at 48 hours x20

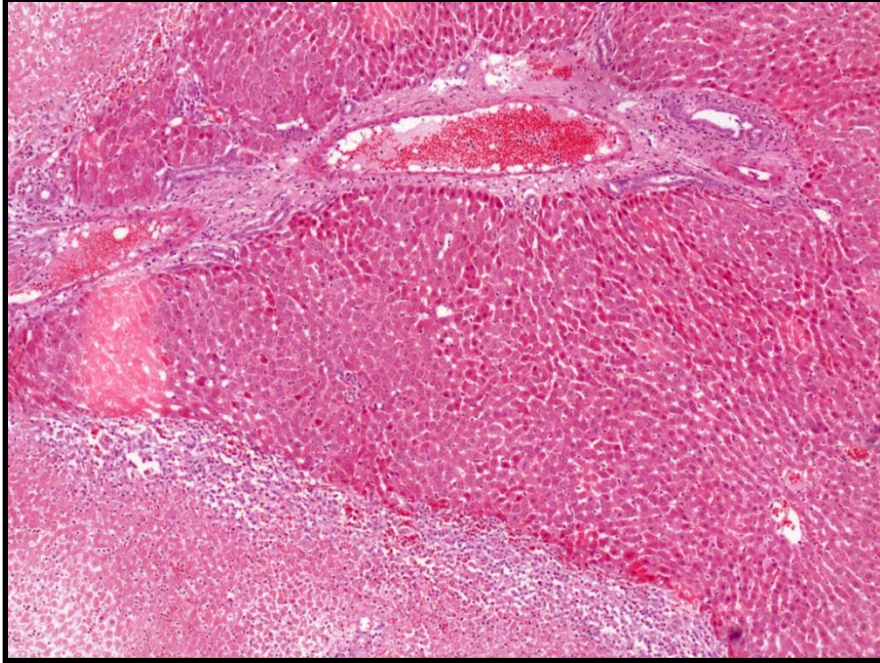


Figure 4-23. RF: edge x 40

Week two:

After two weeks there was again evidence of ‘fixed’ hepatocytes in the ablated tissue with foci of fibroblast proliferation around portal areas was visible. There was collapse of the burn size to around 50% of its original and the surrounding zone which had previously been haemorrhagic and infiltrated by inflammatory cells was replaced by a fibrous capsule. Occasional apoptotic cells were still present in adjacent tissue.

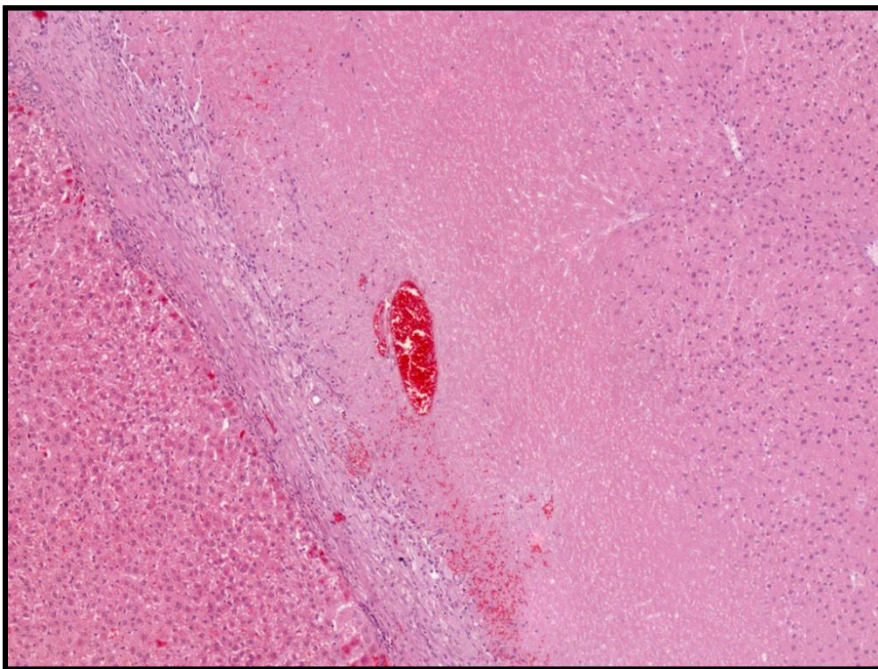


Figure 4-24. RF: Burn edge at 2 weeks x40

Week four:

At four weeks there was continuing evidence of fibroblastic proliferation in the ablated zone with haemosiderin deposition in the surrounding fibrous capsule, demonstrating previous haemorrhage.

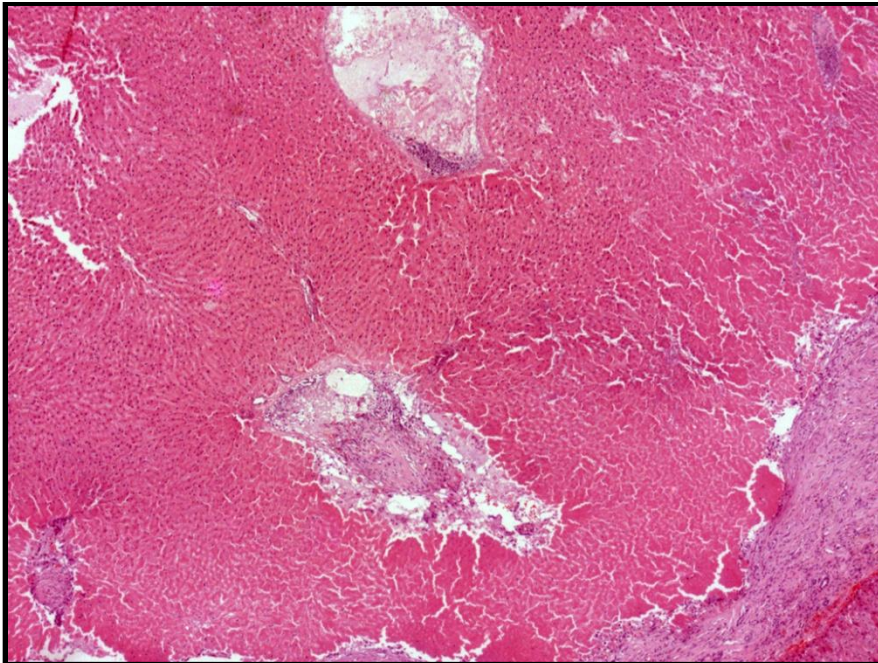


Figure 4-25. RF: Edge and fibroblastic islands at 1 month x20

4.5.3. Discussion

As described in Chapter 1, classically the ablated lesion is described as comprising of three distinct zones; the ablated zone consists of disrupted cells with cytoplasmic eosinophilia indicative of coagulative necrosis. This is usually surrounded by a zone of either haemorrhage or inflammatory infiltration, evolving to a fibroblastic reaction the extent of which depends upon the length of time after the ablation. The outer rim is generally essentially normal liver^{7, 38-46}.

Although these findings are reproduced in the present study there are some additional features which are potentially important clinically, such as relative sparing of biliary epithelium but with damage to the surrounding vascular endothelium. There was also evidence of apoptotic hepatocytes deep in the surrounding normal liver parenchyma which was clustered around the edge of the burn zone (and which itself was very irregular). All ablative modalities suffer from the ‘heat-sink’ and in this study both the preservation of the biliary epithelium and damage to the vascular epithelium were noticeable around portal tracts. As described in Chapter 1, the majority of tissue heating by RF is dependent upon conduction but blood vessels in and around the burn zone may provide “a path of least resistance” and thus have a particularly corrupting effect on the uniformity of the ablation. This transference of heat down the vessel may account for the peri-portal apoptotic hepatocytes which are visible at remote sites which are significant distances from the burn. Cells in the centre of the burn either develop a ‘fixed’ cellular appearance with preservation of nuclear structure or complete destruction with an eosinophilic cytoplasm and loss of cellular detail. Peripheral cells particularly around blood vessels however demonstrated features which suggested that they would survive the ablation producing the irregular ablation edge which we have previously described. The pattern of cell survival and vascular damage was random and therefore it was not possible to quantify the vessel size or location that conferred increased susceptibility to the cytotoxic effects of the ablation. Local recurrence is probably a multi-factorial phenomenon but this characteristic is likely to account for the high recurrence rates when treating large tumours ^{47 48}.

4.6. Conclusion

The H&E studies of all three ablative modalities are in general agreement with the published literature. In addition we have observed a number of new phenomena such as ablation edge apoptosis and extra-lesional distal apoptosis (particularly in close proximity to vascular structures) and regenerative changes in portal vessels. These additional findings provide further supporting evidence that blood flow through and around the ablated lesion has an important role to play in ablation success. This is particularly significant when one considers that tumours are extremely vascular in nature with abnormal blood vessels which do not respond normally to external stimuli.

Extra-lesional apoptosis is also a significant finding as these may be clinically significant particularly when large volume ablations are used to treat hepatocellular cancers, which often occur on the background of liver cirrhosis. It is imperative in these patients that the ablation volume is limited to the tumour and an oncologically safe margin as these patients have a (frequently extremely) limited reserve.

Importantly, there was no set pattern in relation to vessel size or relative location of the burn to the hilum to the distribution of cells which survived at the edge of the burn or to hepatocyte damage in the normal adjacent tissue. This may either due to there being no relationship or secondary to the fact that H&E was used. H&E is an excellent tool for examining gross pathological changes in the tissue; however may not be a sensitive enough marker for subtle changes.

The expansion of the macroscopic ablation zone in all three modalities is difficult to explain and this was mainly due to the relatively small size of the ablation. The central, transition and reference zone sizes are difficult to measure as the margins were not always clear and each area is evolving. Therefore the inter-observer variability prevents from providing exact dimensions and hence makes it difficult to explain the exact reason behind expansion of the lesion size at 24-48 hours post ablation.

It is clear that all modalities induce necrosis in liver tissue either in contact with or immediately surrounding the probe. The H&E result highlight the importance of the evolutionary changes that undergo in the transition zone. The final outcome of cells in the transition zone ultimately decides ablation success and further work involving measuring the stress response in ablated and surrounding hepatocytes along with quantifying apoptosis was undertaken and the following chapters describe these findings in detail.

1. Denisov-Nikol'skii YI, Shafranov VV, Mazokhin VN, Borkhunova EN, Doktorov AA, Mikhaleva LM, Mikhalev AP, Pligin VA, Taganov AV. Morphological changes in the liver after microwave destruction. *Bull Exp Biol Med* 2001;**131**(4): 377-381.
2. Garrean S, Hering J, Saied A, Hoopes PJ, Helton WS, Ryan TP, Espat NJ. Ultrasound monitoring of a novel microwave ablation (MWA) device in porcine liver: lessons learned and phenomena observed on ablative effects near major intrahepatic vessels. *J Gastrointest Surg* 2009;**13**(2): 334-340.
3. Kato T, Suto Y, Hamazoe R. Effects of microwave tissue coagulation on the livers of normal rabbits: a comparison of findings of image analysis and histopathological examination. *Br J Radiol* 1996;**69**(822): 515-521.
4. Ohno T, Kawano K, Sasaki A, Aramaki M, Yoshida T, Kitano S. Expansion of an ablated site and induction of apoptosis after microwave coagulation therapy in rat liver. *J Hepatobiliary Pancreat Surg* 2001;**8**(4): 360-366.
5. Simon CJ, Dupuy DE, Iannitti DA, Lu DS, Yu NC, Aswad BI, Busuttill RW, Lassman C. Intraoperative triple antenna hepatic microwave ablation. *AJR Am J Roentgenol* 2006;**187**(4): W333-340.
6. Swift B, Strickland A, West K, Clegg P, Cronin N, Lloyd D. The histological features of microwave coagulation therapy: an assessment of a new applicator design. *Int J Exp Pathol* 2003;**84**(1): 17-30.
7. Wright AS, Sampson LA, Warner TF, Mahvi DM, Lee FT, Jr. Radiofrequency versus microwave ablation in a hepatic porcine model. *Radiology* 2005;**236**(1): 132-139.
8. Yamaguchi T, Mukaisho K, Yamamoto H, Shiomi H, Kurumi Y, Sugihara H, Tani T. Disruption of erythrocytes distinguishes fixed cells/tissues from viable cells/tissues following microwave coagulation therapy. *Dig Dis Sci* 2005;**50**(7): 1347-1355.
9. Yamashiki N, Kato T, Bejarano PA, Berho M, Montalvo B, Shebert RT, Goodman ZD, Seki T, Schiff ER, Tzakis AG. Histopathological changes after microwave coagulation therapy for patients with hepatocellular carcinoma: review of 15 explanted livers. *Am J Gastroenterol* 2003;**98**(9): 2052-2059.
10. Mukaisho K, Sugihara H, Tani T, Kurumi Y, Kamitani S, Tokugawa T, Hattori T. Effects of microwave irradiation on rat hepatic tissue evaluated by enzyme histochemistry for acid phosphatase. *Dig Dis Sci* 2002;**47**(2): 376-379.
11. Strickland AD, Clegg PJ, Cronin NJ, Swift B, Festing M, West KP, Robertson GS, Lloyd DM. Experimental study of large-volume microwave ablation in the liver. *Br J Surg* 2002;**89**(8): 1003-1007.
12. Awad MM, Devgan L, Kamel IR, Torbensen M, Choti MA. Microwave ablation in a hepatic porcine model: correlation of CT and histopathologic findings. *HPB (Oxford)* 2007;**9**(5): 357-362.

13. Patterson EJ, Scudamore CH, Owen DA, Nagy AG, Buczkowski AK. Radiofrequency ablation of porcine liver in vivo: effects of blood flow and treatment time on lesion size. *Ann Surg* 1998;**227**(4): 559-565.
14. Mulier S, Mulier P, Ni Y, Miao Y, Dupas B, Marchal G, De Wever I, Michel L. Complications of radiofrequency coagulation of liver tumours. *Br J Surg* 2002;**89**(10): 1206-1222.
15. Ahmad F, Strickland AD, Bhardwaj N, Lloyd DM. Systemic inflammatory response following hepatic cryotherapy, radiofrequency ablation, microwave tissue ablation and standard hepatic resection. *BJS* 2006;**93**(S1): 191.
16. Fraser J, Gill W. Observations on ultra-frozen tissue. *The British journal of surgery* 1967;**54**(9): 770-776.
17. Healey WV, Priebe CJ, Jr., Farrer SM, Phillips LL. Hepatic cryosurgery. Acute and long-term effects. *Arch Surg* 1971;**103**(3): 384-392.
18. Rubinsky B, Lee CY, Bastacky J, Onik G. The process of freezing and the mechanism of damage during hepatic cryosurgery. *Cryobiology* 1990;**27**(1): 85-97.
19. Lee FT, Jr., Chosy SG, Littrup PJ, Warner TF, Kuhlman JE, Mahvi DM. CT-monitored percutaneous cryoablation in a pig liver model: pilot study. *Radiology* 1999;**211**(3): 687-692.
20. Seifert JK, Gerharz CD, Mattes F, Nassir F, Fachinger K, Beil C, Junginger T. A pig model of hepatic cryotherapy. In vivo temperature distribution during freezing and histopathological changes. *Cryobiology* 2003;**47**(3): 214-226.
21. Weber SM, Lee FT, Jr., Chinn DO, Warner T, Chosy SG, Mahvi DM. Perivascular and intralesional tissue necrosis after hepatic cryoablation: results in a porcine model. *Surgery* 1997;**122**(4): 742-747.
22. Schuder G, Pistorius G, Fehringer M, Feifel G, Menger MD, Vollmar B. Complete shutdown of microvascular perfusion upon hepatic cryothermia is critically dependent on local tissue temperature. *British journal of cancer* 2000;**82**(4): 794-799.
23. Ravikumar TS, Steele GD, Jr. Hepatic cryosurgery. *The Surgical clinics of North America* 1989;**69**(2): 433-440.
24. Rivoire ML, Voiglio EJ, Kaemmerlen P, Molina G, Treilleux I, Finzy J, Delay E, Gory F. Hepatic cryosurgery precision: evaluation of ultrasonography, thermometry, and impedancemetry in a pig model. *Journal of surgical oncology* 1996;**61**(4): 242-248.
25. Onik G, Gilbert J, Hoddick W, Filly R, Callen P, Rubinsky B, Farrel L. Sonographic monitoring of hepatic cryosurgery in an experimental animal model. *Ajr* 1985;**144**(5): 1043-1047.

26. Neel HB, Ketcham AS, Hammond WG. Ischemia potentiating cryosurgery of primate liver. *Annals of surgery* 1971;**174**(2): 309-318.
27. Neel HB, 3rd, Ketcham AS, Hammond WG. Cryonecrosis of normal and tumor-bearing rat liver potentiated by inflow occlusion. *Cancer* 1971;**28**(5): 1211-1218.
28. Matsumoto R, Selig AM, Colucci VM, Jolesz FA. MR monitoring during cryotherapy in the liver: predictability of histologic outcome. *J Magn Reson Imaging* 1993;**3**(5): 770-776.
29. Weber SM, Lee FT, Jr., Warner TF, Chosy SG, Mahvi DM. Hepatic cryoablation: US monitoring of extent of necrosis in normal pig liver. *Radiology* 1998;**207**(1): 73-77.
30. Mala T, Frich L, Aurdal L, Clausen OP, Edwin B, Soreide O, Gladhaug IP. Hepatic vascular inflow occlusion enhances tissue destruction during cryoablation of porcine liver. *The Journal of surgical research* 2003;**115**(2): 265-271.
31. Pearson AS, Izzo F, Fleming RY, Ellis LM, Delrio P, Roh MS, Granchi J, Curley SA. Intraoperative radiofrequency ablation or cryoablation for hepatic malignancies. *American journal of surgery* 1999;**178**(6): 592-599.
32. Seifert JK, Morris DL. Indicators of recurrence following cryotherapy for hepatic metastases from colorectal cancer. *The British journal of surgery* 1999;**86**(2): 234-240.
33. Seifert JK, Morris DL. Prognostic factors after cryotherapy for hepatic metastases from colorectal cancer. *Annals of surgery* 1998;**228**(2): 201-208.
34. Goldberg SN, Charboneau JW, Dodd GD, 3rd, Dupuy DE, Gervais DA, Gillams AR, Kane RA, Lee FT, Jr., Livraghi T, McGahan JP, Rhim H, Silverman SG, Solbiati L, Vogl TJ, Wood BJ. Image-guided tumor ablation: proposal for standardization of terms and reporting criteria. *Radiology* 2003;**228**(2): 335-345.
35. Tacke J, Adam G, Haage P, Sellhaus B, Grosskortenhaus S, Gunther RW. MR-guided percutaneous cryotherapy of the liver: in vivo evaluation with histologic correlation in an animal model. *J Magn Reson Imaging* 2001;**13**(1): 50-56.
36. Kahlenberg MS, Volpe C, Klippenstein DL, Penetrante RB, Petrelli NJ, Rodriguez-Bigas MA. Clinicopathologic effects of cryotherapy on hepatic vessels and bile ducts in a porcine model. *Annals of surgical oncology* 1998;**5**(8): 713-718.
37. Jacob G, Li AK, Hobbs KE. A comparison of cryodestruction with excision or infarction of an implanted tumor in rat liver. *Cryobiology* 1984;**21**(2): 148-156.
38. Coad JE, Kosari K, Humar A, Sielaff TD. Radiofrequency ablation causes 'thermal fixation' of hepatocellular carcinoma: a post-liver transplant histopathologic study. *Clin Transplant* 2003;**17**(4): 377-384.

39. Hinz S, Egberts JH, Pauser U, Schafmayer C, Fandrich F, Tepel J. Electrolytic ablation is as effective as radiofrequency ablation in the treatment of artificial liver metastases in a pig model. *J Surg Oncol* 2008;**98**(2): 135-138.
40. Raman SS, Lu DS, Vodopich DJ, Sayre J, Lassman C. Creation of radiofrequency lesions in a porcine model: correlation with sonography, CT, and histopathology. *AJR Am J Roentgenol* 2000;**175**(5): 1253-1258.
41. Lee JD, Lee JM, Kim SW, Kim CS, Mun WS. MR imaging-histopathologic correlation of radiofrequency thermal ablation lesion in a rabbit liver model: observation during acute and chronic stages. *Korean J Radiol* 2001;**2**(3): 151-158.
42. Scudamore CH, Buczkowski A, Nagy A et al. . Possible injuries to intrahepatic and perihepatic structures with radiofrequency probe. *Surgical Endoscopy* 1997;**11**: 193.
43. Lu DS, Raman SS, Vodopich DJ, Wang M, Sayre J, Lassman C. Effect of vessel size on creation of hepatic radiofrequency lesions in pigs: assessment of the "heat sink" effect. *AJR Am J Roentgenol* 2002;**178**(1): 47-51.
44. Scudamore CH, Lee SI, Patterson EJ, Buczkowski AK, July LV, Chung SW, Buckley AR, Ho SG, Owen DA. Radiofrequency ablation followed by resection of malignant liver tumors. *Am J Surg* 1999;**177**(5): 411-417.
45. Frich L, Mala T, Gladhaug IP. Hepatic radiofrequency ablation using perfusion electrodes in a pig model: effect of the Pringle manoeuvre. *Eur J Surg Oncol* 2006;**32**(5): 527-532.
46. Morimoto M, Sugimori K, Shirato K, Kokawa A, Tomita N, Saito T, Tanaka N, Nozawa A, Hara M, Sekihara H, Shimada H, Imada T, Tanaka K. Treatment of hepatocellular carcinoma with radiofrequency ablation: radiologic-histologic correlation during follow-up periods. *Hepatology* 2002;**35**(6): 1467-1475.
47. Gazelle GS, Goldberg SN, Solbiati L, Livraghi T. Tumor ablation with radio-frequency energy. *Radiology* 2000;**217**(3): 633-646.
48. Bilchik AJ, Wood TF, Allegra DP. Radiofrequency ablation of unresectable hepatic malignancies: lessons learned. *Oncologist* 2001;**6**(1): 24-33.

CHAPTER 5: Hsp 70

5. Chapter 5: Hsp 70	123
5.1. Introduction	123
5.2. Heat shock protein 70.....	124
5.3. Immunohistochemistry results	127
5.3.1. Radiofrequency ablation	131
5.3.2. Microwave ablation	134
5.4. Comparing microwave and radiofrequency	136
5.5. Discussion	137
5.6. Conclusion.....	141
Figure 5-1. Hsp expression at margin x100	128
Figure 5-2 Hsp expression at margin x200	128
Figure 5-3. Hsp x400	129
Figure 5-4. No Hsp expression x400	130
Figure 5-5. Radiofrequency and Hsp expression n=5 at each time point	132
Figure 5-6. HSP 70 expression with microwave ablation. n=5 at each time point.....	135

5. Chapter 5: Hsp 70

5.1. Introduction

Haematoxylin and Eosin staining of the ablation revealed previously unreported findings, namely ablation edge and extra-lesional apoptosis. It also highlighted the importance of the transition zone in particular changes at the ablated/unablated tissue interface. As mentioned in Chapter 1, the majority of tumour recurrences occur adjacent to major vessels at the tissue-vessel interface where flowing blood thermally protects perivascular tissue and tumour cells and allow them to recover¹⁻³. In addition, tumours in the vicinity of large blood vessels may undergo inadequate ablation and may account for the increased rate of local recurrence observed at these sites. Liver parenchyma and primary and secondary liver tumours are water rich and invariably have an extensive vascular supply.

It was clear from the H&E studies that whilst some cells at the ablation margin underwent apoptosis, others survived. Firstly, this suggests that not all cells at a fixed radius from the probe receive equal degrees of cytotoxic temperatures. Secondly surviving cells adjacent to those which have undergone apoptosis or necrosis must have been subjected to sub-lethal thermal doses yet have an inherent protective mechanism which, although recognises they are damaged, allows them to recover and regain function. H&E does not distinguish between cells that may

have incurred thermal damage yet survived or the effect of surrounding vasculature on ablation morphology, therefore a more sensitive marker is necessary.

5.2. Heat shock protein 70

Heat shock protein 70 (Hsp70) was originally discovered by Ritossa in the 1960's when a lab worker in Italy accidentally increased the temperature of an incubator containing *Drosophila* (fruit flies). The following day when the salivary gland chromosomes were examined a "puffing pattern" was observed which indicated transcription of an unknown protein due to an unusual pattern of gene expression^{4, 5}. These new proteins were subsequently called heat shock proteins (Hsps) and they are a group of related molecules with myriad functions which are known to be strongly upregulated by heat stress, toxic chemicals (particularly heavy metals), oxidative stress, ischaemia, inflammation and infection and reperfusion^{6, 7}. Hsp70 proteins are a family of heat shock proteins with an average molecular weight of 70kDa (highly related protein isoforms ranging in size from 66-78 kDa). Hsps are highly conserved and ubiquitous, being found in animals, plants (in the chloroplast) and bacteria. There are Hsps with widely differing molecular weights (including 10, 25, 40, 60, 70, 90 and 100 kDa) and they perform a bewildering range of functions⁸. In most species there are many proteins which belong to the Hsp70 family and although some of these are only expressed in response to stress (strictly inducible) some are present in cells under normal conditions (constitutive or cognate). When a cell is not stressed these Hsps make up approximately 2% of the cells contents but under conditions of stress a remarkable 20% of the cells soluble protein content is provided by these Hsps⁹. The cognate proteins are found within major intracellular compartments and the highly inducible isoforms are predominately cytoplasmic or nuclear in distribution¹⁰. Hsp70 proteins function as molecular

chaperones and are involved in a number of cellular functions including protein folding, transport, maturation and degradation and operate in an ATP-dependant manner ¹¹. The molecular chaperones of the Hsp70 family recognise and bind to nascent polypeptide chains or partially folded intermediates of proteins, preventing their aggregation or misfolding, and the binding of ATP triggers a critical conformational change leading to the release of the bound substrate protein. Hsp70 also aids in transmembrane transport of proteins by stabilising them in a partially folded state and can act to protect cells from thermal or oxidative stress. Low ATP is characteristic of heat shock and sustained binding suppresses aggregation, while recovery from heat shock involves substrate binding and nucleotide recycling ⁸.

In addition to improving overall protein integrity, Hsp70 directly inhibits apoptosis by interacting directly with key components of the apoptotic pathway ¹². One of the main features of apoptosis is the release of cytochrome c which recruits Apaf-1 and dADT/ATP into an apoptosome complex. This complex then cleaves procaspase-9 which eventually induces apoptosis via caspase-3 activation. Hsp70 inhibits this process by blocking the recruitment of procaspase-9 to the Apaf-1/dATP/cytochrome c apoptosome complex ¹². It does not bind directly to the procaspase-9 binding site but probably induces a conformational change that renders procaspase-9 binding less favourable ¹². Other studies suggest that Hsp70 may also play an anti-apoptotic role at other stages and therefore not only protects important components of the cell (proteins) but also protects the whole cell ^{13, 14}.

Hsp70 appears to be able to participate in the disposal of damaged or defective proteins. Hsps load peptide detritus onto major histocompatibility complex (MHC) molecules. A loaded MHC molecule moves towards the cell surface where it can be monitored by roving sentry cells of the immune system. These cells react vigorously if they sense any peptides which should not be there such as fragments of viral proteins or altered constituents of a malignant cell. In this way Hsp70 proteins bind tumour peptides and chaperone these antigenic tumour structures to host antigen presenting cells, which subsequently present them to cytotoxic T cell lymphocytes ⁷.

As well as being involved in recognition by the immune system Hsps are over-expressed in a wide range of human cancers and are implicated in tumour cell proliferation, differentiation, invasion, metastasis and death. Although they are not useful at the diagnostic level they are valuable biomarkers for carcinogenesis in some tissues and signal the degree of differentiation and aggressiveness of some cancers. Several Hsps are implicated in the prognosis of specific cancers most notably Hsp27 in stomach, liver, and prostate cancer and osteosarcomas and Hsp70 which correlates with poor prognosis in breast, endometrial, uterine, cervical and bladder cancer. Increased Hsp70 expression may also predict the response to some anticancer treatments and Hsp70 is implicated in the resistance of some breast and pancreatic cancers to chemotherapy ¹⁵,
¹⁶.

Hsps are also upregulated when necrotic tissue is present ¹⁷ and as a consequence may have a role to play in modulating the evolution of the ablation zone produced following liver tumour ablation. This may also be exacerbated by the ability of Hsp70 to enhance ‘acquired

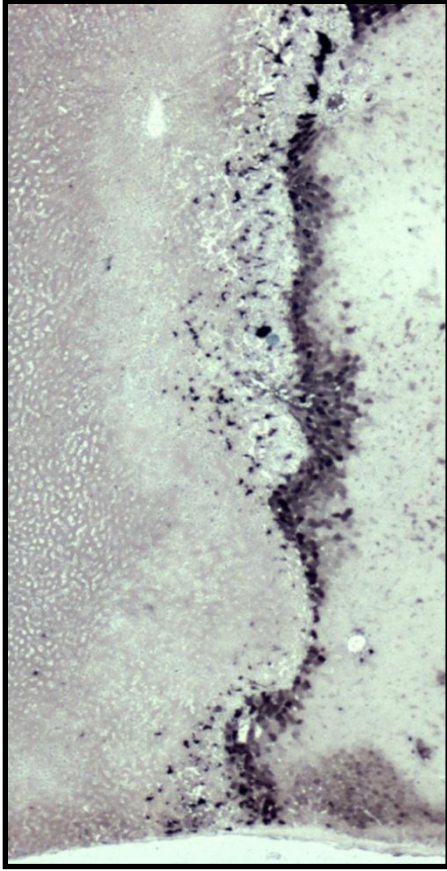


Figure 5-1. Hsp expression at margin x100

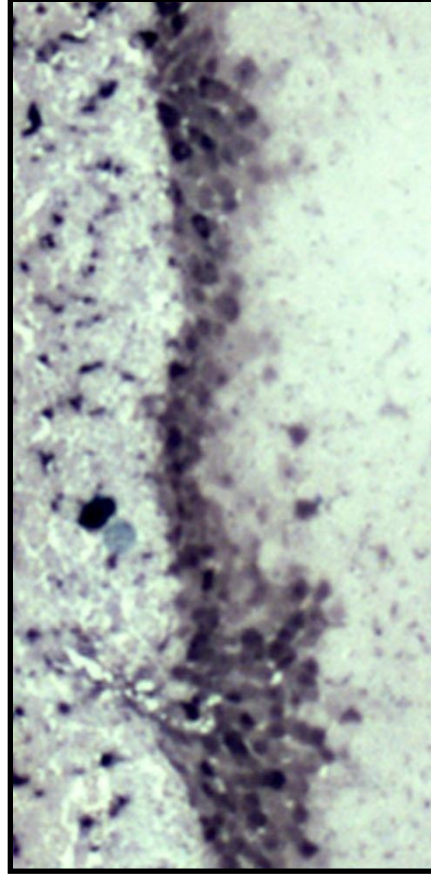


Figure 5-2 Hsp expression at margin x200

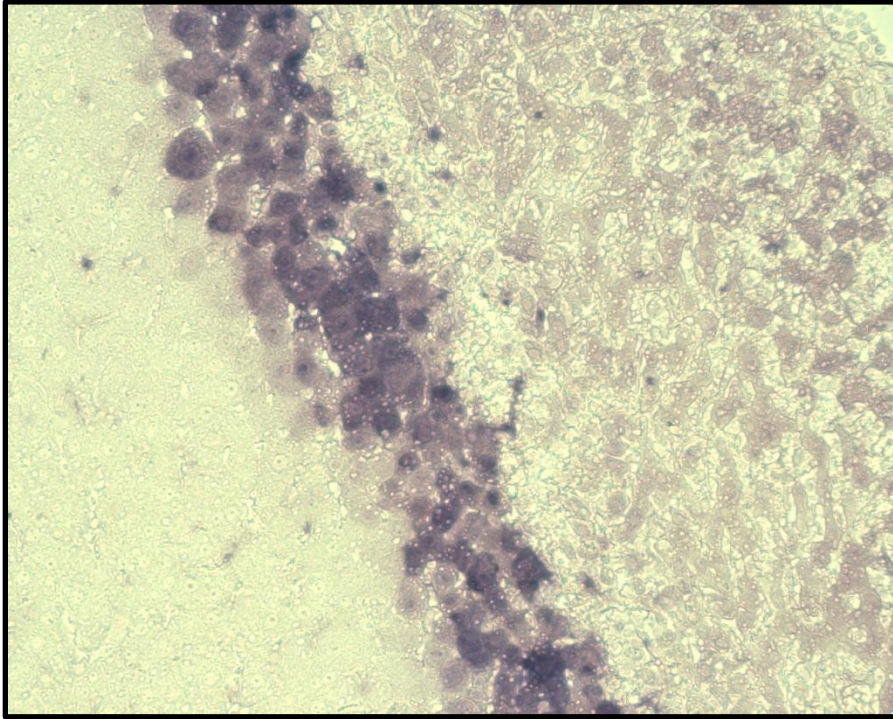


Figure 5-3. Hsp x400

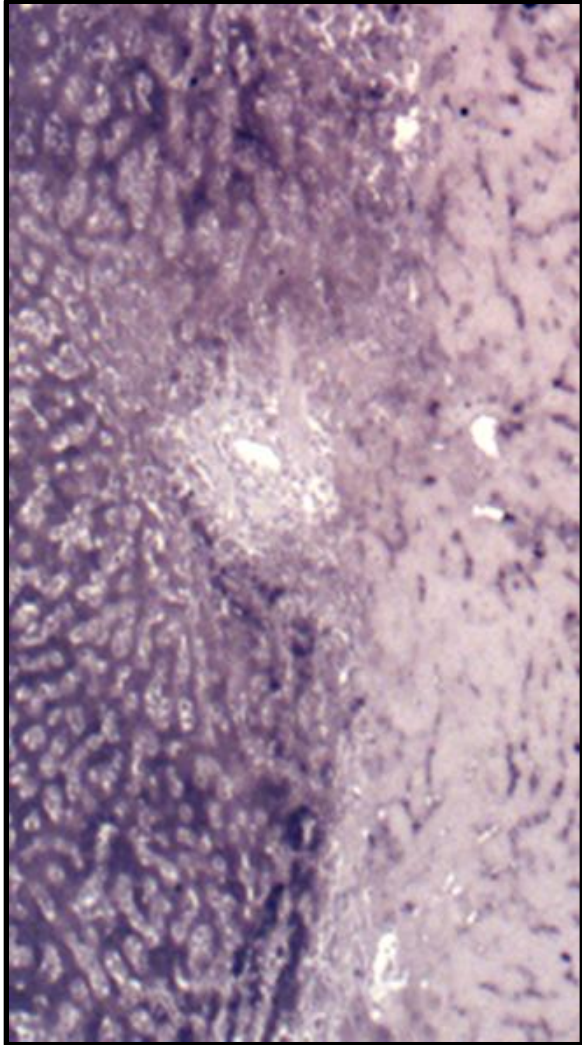


Figure 5-4. No Hsp expression x400

5.3.1. Radiofrequency ablation

Five rats at each time point (0,4hrs, 24hrs, 48 hrs and 2 weeks) were analysed and a mean number of cells calculated for each rat at various distances from the hilum. No Hsp was detected in the ablated or normal liver tissue or in any tissue at time zero and week 2. (Table 5-1. Mean number of cells in transition zone in each rat treated with RF ablation).

5 rats at each time point	Mean number of cells in each rat at various distance from the hilum		
	Proximal	Intermediate	Distal
Time 0			
Rat 1	0	0	0
Rat 2	0	0	0
Rat 3	0	0	0
Rat 4	0	0	0
Rat 5	0	0	0
Time 4 hours			
Rat 1	6.2	3.8	2.1
Rat 2	5.8	2.7	1.9
Rat 3	6.1	3.2	1.7
Rat 4	6.8	3.8	3.1
Rat 5	6.4	4.1	2.4
Time 24 hours			
Rat 1	13.1	10	8.2
Rat 2	12	10.6	8.2
Rat 3	12.4	10.9	9.8
Rat 4	12	10.3	8.3
Rat 5	14.1	11.1	9.2
Time 48 hours			
Rat 1	5.4	4.9	1.4
Rat 2	4.2	2.2	1.8
Rat 3	4.1	3.2	1.5
Rat 4	3.9	2.9	1.8
Rat 5	5.2	4.8	1.7

Table 5-1. Mean number of cells in transition zone in each rat treated with RF ablation

These results are presented graphically (Figure 5-5. Radiofrequency and Hsp expression n=5 at each time point). Time zero and 2 weeks have been excluded as no cells were expressed in the ablated, normal or hilar tissues.

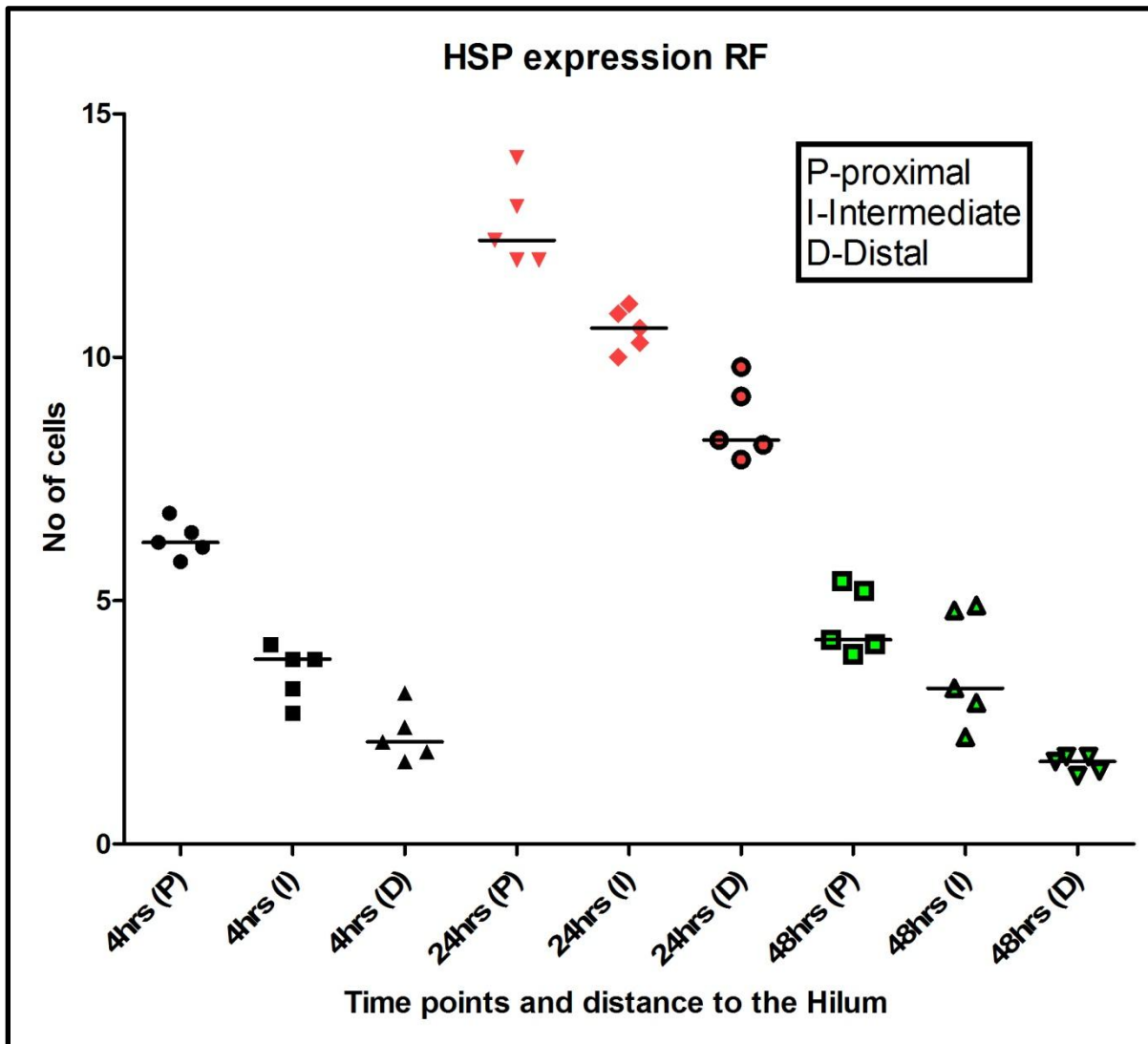


Figure 5-5. Radiofrequency and Hsp expression n=5 at each time point

Four hours:

By four hours a clear band of Hsp70 was detected occupying the transition zone (between the ablated and normal liver tissue interface). Proximal ablations had the widest zone of Hsp expression followed by the intermediate and finally distal ablations ($p=0.0024$). No Hsp was detected in the ablated or normal liver tissue.

Twenty four hours:

At twenty four hours the band of Hsp was still localised to the interface between the ablated and normal liver tissue but occupied a wider area compared to the tissue examined at 4 hours. The proximal ablations again had the widest band, followed by the intermediate and finally the distal ablations ($p=0.0019$).

Forty eight hours:

The band was narrower at forty eight hours compared to the findings at 4 and 24 hours and again the proximal tissue had the widest band compared to the intermediate and distal sections ($P=0.006$). No Hsp expression occurred in the ablated or normal tissue.

5.3.2. Microwave ablation

The results were very similar to RF. Again no Hsp expression was detected at time 0 and 2 weeks (Table 5-2. Mean number of cells at each time point in rats treated with microwave ablation) and (Figure 5-6. HSP 70 expression with microwave ablation. n=5 at each time point.

5 rats at each time point	Mean number of cells in each rat relative to distance from the hilum		
	Proximal	Intermediate	Distal
Time 0			
Rat 1	0	0	0
Rat 2	0	0	0
Rat 3	0	0	0
Rat 4	0	0	0
Rat 5	0	0	0
Time 4 hours			
Rat 1	4.3	3.1	1.1
Rat 2	3.8	2.8	1.4
Rat 3	4.1	2.4	1.5
Rat 4	3.5	2.5	1.8
Rat 5	3.9	2.2	1.9
Time 24 hours			
Rat 1	10	6.7	4.3
Rat 2	9.4	6.5	3.8
Rat 3	7.3	3.2	2.1
Rat 4	7.1	4.8	3.3
Rat 5	6.9	4.3	2.9
Time 48 hours			
Rat 1	3.2	2.2	1.9
Rat 2	4.8	3.2	1.5
Rat 3	4.6	3.4	1.8
Rat 4	5.1	4.2	2.1
Rat 5	4.8	3.7	2.3

Table 5-2. Mean number of cells at each time point in rats treated with microwave ablation

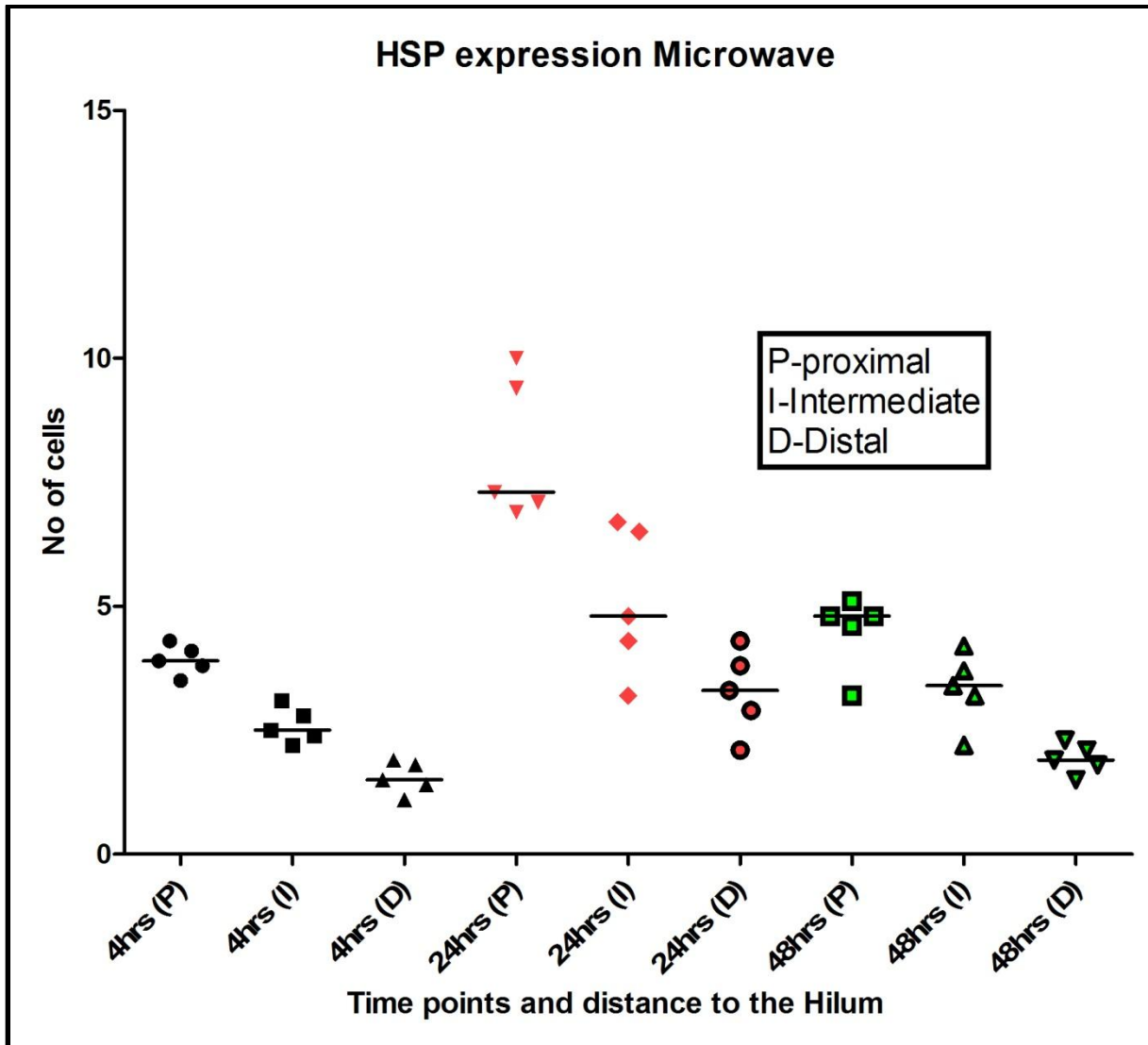


Figure 5-6. HSP 70 expression with microwave ablation. n=5 at each time point.

Four hours:

A clear band was detected occupying the transition zone (between the ablated and normal liver tissue interface). Proximal ablations had the widest zone of Hsp expression followed by the intermediate and finally distal ablations ($p=0.0019$).

Twenty four hours:

A wider area compared to the tissue examined at 4 hours was visible at the interface. The proximal ablations again had the widest band, followed by the intermediate and finally the distal ablations ($p=0.0041$).

Forty eight hours:

The band was narrower at forty eight hours compared to the findings at 4 and 24 hours and again the proximal tissue had the widest band compared to the intermediate and distal sections ($P=0.0053$). No Hsp expression occurred in the ablated or normal tissue.

5.4. Comparing microwave and radiofrequency

At all time point, 4, 24 and 48 hours, RF had a greater degree of Hsp expression at proximal distances ($p=0.0079$), ($p=0.0079$) and ($p=0.9683$), respectively compared to microwave (Wilcoxon exact test). This was also the case at intermediate distances at 4, 24, and 48 hours; ($p=0.0317$), ($p=0.0079$) and ($p=0.9683$), respectively and at distal distances at times 4, 24 and 48 hours; ($p=0.0397$), ($p=0.0079$) and ($p=0.1111$), respectively

5.5. Discussion

Few studies have investigated the expression of Hsp70 in ablated tissue and no study to date has investigated the effects of the surrounding vasculature on Hsp expression following ablation or investigated Hsp 70 expression post microwave ablation or cryotherapy. As previously described, Hsp 70, in the inducible form, is upregulated when cells undergo any degree of stress; heat, toxic chemicals (particularly heavy metals), oxidative stress, ischaemia and reperfusion, inflammation and infection ^{6, 7}. It is surprising that hepatocytes subjected to sub-lethal temperatures at the periphery of the ice-ball during cryotherapy did not express any Hsp 70. This suggested that ablated/unablated interface is extremely sharp and consists of necrotic/normal hepatocytes respectively with no transition zone. However, this seems unlikely as H&E analysis confirmed that there is a transition zone, which was wide and irregular with a mix of necrotic and viable cells. Perhaps Hsp 70 is not upregulated in hypothermic conditions; this again seems unlikely as there are studies which have studied Hsp 70 expression in kidney tubules of subjects who have died due to hypothermia ²¹. Although it must be stressed that this study did not distinguish between hsp 70 expression solely due to hypothermia or whether any necrosis secondary to hypoxia (as would be expected in cells dying of hypothermia) was responsible for Hsp 70 expression.

As mentioned previously no studies have reported Hsp 70 expression in liver tissue subjected to cryotherapy or microwave ablation. Studies that have investigated the expression of Hsp70 in ablated tissue have reached different conclusions. *Rai et al* ablated pig liver with radiofrequency

found increased Hsp 70 expression in the transition zone subjected to sub-lethal temperatures at day 5 and concluded that as Hsp70 expression is known to enhance the immunogenicity of cells, it could be a potential target for the delivery of therapeutic drugs ²². Yang *et al* ablated subcutaneous implanted human colon cancer cells at different temperatures, (42°C, 45°C and 50°C) and found tumour growth at sub-lethal temperatures but complete ablation at high temperatures. They suggested that Hsp70 induction played a role in cell survival after sub-lethal RF ablation although unfortunately they did not quantify Hsp70 expression at the different temperatures ¹⁸. Nikfarjam *et al* investigated the effects of laser thermal ablation in a murine model of colorectal metastases and expression of HSP 70 in tumour cells was demonstrated which peaked at day 2 and was enhanced greatly following ablation compared to normal liver tissue. They concluded that a protective role for Hsp70 may be implicated in tumour recurrence or inadequate ablation and down regulation of Hsp expression would be beneficial therapeutically ²³. Finally a RF study investigated the expression of Hsp70 after 24 hours in the rabbit liver subjected to basic ultrasound, contrast enhanced ultrasound (CEUS), RF and RF+CEUS. They reported expression of Hsp70 at the ablation margin following RF treatment and a lower level with RF+CEUS. They acknowledged the contradictory cellular effects of Hsp70 reported in the literature but concluded that their findings suggested that CEUS may have future therapeutic benefits as an adjunct to RF ablation ⁶.

Thermal tumour destruction occurs in two distinct phases. The initial *direct* phase is multifactorial and depends on the total energy applied, tumour biology and microenvironment ³. It is only possible to influence these variables in a limited fashion as the total energy which can be effectively delivered by radiofrequency and microwave generators and probes is limited by

the effects of tissue charring and the consequently increased tissue impedance ¹. Tumour cells are more sensitive to the damaging effects of heat compared to normal tissue but unfortunately it is extremely difficult to manipulate the tumour microenvironment. The *indirect* phase occurs after the application of the heat energy and is responsible for the progression of tissue damage. This is a balance of several factors, including microvascular damage, ischaemia-reperfusion injury, induction of apoptosis, Kupffer cell activation, altered cytokine expression and modulation of the immune response ³.

Hsp70 was detected in the transition zone, with no HSP expression in the completely ablated zone or in the normal liver of the ablated lobe and the chosen slides (above) highlight this with greatest clarity. The Hsp70 expression showed statistically significant differences with time and peaked at 24 hours and was undetectable by week 2 in both modalities. Necrotic cells in the transition zone showed increased Hsp expression and this is to be expected as Hsp70 has been known to be upregulated in necrotic tissue ¹⁷. In addition several ablative studies have confirmed this finding ^{6, 22, 23} although in none of these studies have the effects of surrounding vasculature been examined or described. The degree of Hsp70 expression varied depending upon the distance of the transition zone from the hilum at each time point in this study. The ‘heat sink’ phenomenon is the Achilles heel of all ablative techniques and limits their success due to the consequence of tumour recurrence. Manipulation of hepatic blood flow has been shown to improve ablation diameter, but is also associated with increased side effects such as venous thromboses ^{24,25}. Cells at the centre of the ablation zone undergo rapid destruction and are therefore probably unable to upregulate Hsp70 expression. Peripherally placed cells however, are subjected to lower temperatures than at the centre due to the fall of current density at increasing

distances from the probe and therefore have more time to upregulate Hsp70 expression. This study also suggests that ablations closer to relatively larger blood vessels have a wider transition zone (as evidenced by the increased level of Hsp70 expression) and therefore provide a larger volume where lower temperatures provide cells with sufficient time to express Hsp70.

The bandwidth of Hsp 70 expression was greater with RF compared to microwave at 4 and 24 hours in proximal, intermediate and distal ablated lesions, which was statistically significant. This trend continued at all hilar distances at 48 hours, though this was not statistically significant. As the actual macroscopic ablation size at 24 and 48 hours (as described in chapter 3) was similar between microwave and RF and dead cells are unable to express Hsp 70, this suggests that central zone of coagulative necrosis must be smaller and the transition zone must be wider in RF. Microwave has a broader field of power density surrounding the applicator, thus creating a larger and more uniform zone. In comparison, as described in chapter 1, active RF heating is limited to a few mm around the applicator with reliance on conduction of cytotoxic temperatures through the tissues in order to create an ablation zone ²⁶⁻²⁸. As a consequence the final delivered current at the periphery of tissues and subsequent thermal energy with RF is inversely proportional to the square of the distance from the electrode ²⁹ and as a consequence allows cells in the transition zone sufficient time to up-regulate Hsp expression.

A wider transition zone at 24 hours also suggests indirectly that there is some mechanism conferring a degree of protection from the cytotoxic temperatures to the cells which survive the initial insult. This is significant in the clinical setting as the highest blood flow in tumours is at

the periphery, near the tissue-liver interface ³, which is often the area subjected to lower temperatures and this problem is highlighted by the fact that recurrences occur at this site. Ablative techniques produce effects which are more complex than they initially appear. The success of these treatments depends on the interaction between a number of factors. These include some that have previously been studied extensively such as probe and generator design, the method of deployment and choice of ablative modality and some that have been examined more recently including tumour biology, influence of the micro-environment, local and systemic immunological modulation. It is now also clear that, in addition to Hsps, there are a significant number of very complex interactions involving cytokines and immunomodulatory chemicals eluted from tumour cells.

Essentially, the final fate of the cells in the transition zone will ultimately dictate the success or failure of the ablation. Previous studies have reported conflicting results concerning the influence of Hsp70 on the fate of damaged cells. There are a number of reports suggesting that it enhances immunogenicity ^{7, 17} whilst others suggest that it confers ‘acquired thermotolerance’ and inhibits apoptosis in tumour cell lines which potentially leads to greater heat resistance of some malignant tumour strains ^{3, 14, 18-20}.

5.6. Conclusion

This study examined Hsp70 expression in the transition zone in relation to surrounding vasculature and found a statistically significant influence of blood flow on Hsp70 expression in

microwave and RF ablated tissue. It also revealed that extremes of temperatures, as induced by cryotherapy does not cause cells to upregulate Hsp 70. In addition, it found a statistically significant difference in Hsp expression between RF and microwave. In conclusion, although the exact role of Hsp70 in aiding survival of some of the cells in the transition zone that have been subjected to sub-lethal temperatures remains unclear, this study does report new findings. Further work was then undertaken in order to quantify apoptosis in at the ablation margin as revealed in H&E studies and to see if there is a correlation with Hsp 70 expression.

1. Wright AS, Sampson LA, Warner TF, Mahvi DM, Lee FT, Jr. Radiofrequency versus microwave ablation in a hepatic porcine model. *Radiology*. Jul 2005;236(1):132-139.
2. Tungjitkusolmun S, Staelin ST, Haemmerich D, et al. Three-Dimensional finite-element analyses for radio-frequency hepatic tumor ablation. *IEEE Trans Biomed Eng*. Jan 2002;49(1):3-9.
3. Nikfarjam M, Muralidharan V, Christophi C. Mechanisms of focal heat destruction of liver tumors. *J Surg Res*. Aug 2005;127(2):208-223.
4. Ritossa F. Discovery of the heat shock response. *Cell Stress Chaperones*. Jun 1996;1(2):97-98.
5. Ritossa F. A new puffing pattern induced by heat shock and DNP in *Drosophila*. *Experientia*. 1962;18:571-573.
6. Liu GJ, Moriyasu F, Hirokawa T, Rexiati M, Yamada M, Imai Y. Expression of heat shock protein 70 in rabbit liver after contrast-enhanced ultrasound and radiofrequency ablation. *Ultrasound Med Biol*. Jan;36(1):78-85.
7. Matzinger P. Tolerance, danger, and the extended family. *Annu Rev Immunol*. 1994;12:991-1045.
8. Mayer MP, Bukau B. Hsp70 chaperones: cellular functions and molecular mechanism. *Cell Mol Life Sci*. Mar 2005;62(6):670-684.
9. Crevel G, Bates H, Huikeshoven H, Cotterill S. The *Drosophila* Dpit47 protein is a nuclear Hsp90 co-chaperone that interacts with DNA polymerase alpha. *J Cell Sci*. Jun 2001;114(Pt 11):2015-2025.
10. Tavarina M, Gabriele T, Kola I, Anderson RL. A hitchhiker's guide to the human Hsp70 family. *Cell Stress Chaperones*. Apr 1996;1(1):23-28.
11. Mallouk Y, Vayssier-Taussat M, Bonventre JV, Polla BS. Heat shock protein 70 and ATP as partners in cell homeostasis (Review). *Int J Mol Med*. Nov 1999;4(5):463-474.
12. Beere HM, Wolf BB, Cain K, et al. Heat-shock protein 70 inhibits apoptosis by preventing recruitment of procaspase-9 to the Apaf-1 apoptosome. *Nat Cell Biol*. Aug 2000;2(8):469-475.
13. Takayama S, Reed JC, Homma S. Heat-shock proteins as regulators of apoptosis. *Oncogene*. Dec 8 2003;22(56):9041-9047.
14. Mosser DD, Caron AW, Bourget L, et al. The chaperone function of hsp70 is required for protection against stress-induced apoptosis. *Mol Cell Biol*. Oct 2000;20(19):7146-7159.
15. Aghdassi A, Phillips P, Dudeja V, et al. Heat shock protein 70 increases tumorigenicity and inhibits apoptosis in pancreatic adenocarcinoma. *Cancer Res*. Jan 15 2007;67(2):616-625.
16. Sherman M, Multhoff G. Heat shock proteins in cancer. *Ann N Y Acad Sci*. Oct 2007;1113:192-201.
17. Schueller G, Paolini P, Friedl J, et al. Heat treatment of hepatocellular carcinoma cells: increased levels of heat shock proteins 70 and 90 correlate with cellular necrosis. *Anticancer Res*. Jan-Feb 2001;21(1A):295-300.
18. Yang WL, Nair DG, Makizumi R, et al. Heat shock protein 70 is induced in mouse human colon tumor xenografts after sublethal radiofrequency ablation. *Ann Surg Oncol*. Apr 2004;11(4):399-406.

19. Samali A, Cotter TG. Heat shock proteins increase resistance to apoptosis. *Exp Cell Res.* Feb 25 1996;223(1):163-170.
20. Calderwood SK, Asea A. Targeting HSP70-induced thermotolerance for design of thermal sensitizers. *Int J Hyperthermia.* Nov-Dec 2002;18(6):597-608.
21. Preuss J, Dettmeyer R, Poster S, Lignitz E, Madea B. The expression of heat shock protein 70 in kidneys in cases of death due to hypothermia. *Forensic Sci Int.* Apr 7 2008;176(2-3):248-252.
22. Rai R, Richardson C, Flecknell P, Robertson H, Burt A, Manas DM. Study of apoptosis and heat shock protein (HSP) expression in hepatocytes following radiofrequency ablation (RFA). *J Surg Res.* Nov 2005;129(1):147-151.
23. Nikfarjam M, Muralidharan V, Su K, Malcontenti-Wilson C, Christophi C. Patterns of heat shock protein (HSP70) expression and Kupffer cell activity following thermal ablation of liver and colorectal liver metastases. *Int J Hyperthermia.* Jun 2005;21(4):319-332.
24. Kim SK, Lim HK, Ryu JA, et al. Radiofrequency ablation of rabbit liver in vivo: effect of the pringle maneuver on pathologic changes in liver surrounding the ablation zone. *Korean J Radiol.* Oct-Dec 2004;5(4):240-249.
25. Mulier S, Mulier P, Ni Y, et al. Complications of radiofrequency coagulation of liver tumours. *Br J Surg.* Oct 2002;89(10):1206-1222.
26. Organ LW. Electrophysiologic principles of radiofrequency lesion making. *Appl Neurophysiol.* 1976;39(2):69-76.
27. Simon CJ, Dupuy DE, Mayo-Smith WW. Microwave ablation: principles and applications. *Radiographics.* Oct 2005;25 Suppl 1:S69-83.
28. Skinner MG, Iizuka MN, Kolios MC, Sherar MD. A theoretical comparison of energy sources--microwave, ultrasound and laser--for interstitial thermal therapy. *Phys Med Biol.* Dec 1998;43(12):3535-3547.
29. McKay A, Dixon E, Taylor M. Current role of radiofrequency ablation for the treatment of colorectal liver metastases. *Br J Surg.* Oct 2006;93(10):1192-1201.

CHAPTER 6: CASPASE 3

6. Chapter 6: Caspase 3.....	146
6.1. Introduction: Apoptosis.....	146
6.2. Caspase 3.....	146
6.2.1. Intrinsic or mitochondrial pathway.....	148
6.2.2. Extrinsic or death receptor pathway.....	148
6.2.3. Caspase 3 and ablation.....	149
6.3. Aims of this study.....	149
6.4. Caspase analyses.....	150
6.5. Results.....	154
6.5.1. Normal unablated liver.....	154
6.5.2. Microwave ablation.....	154
6.5.3. Radiofrequency.....	160
6.5.4. Cryotherapy.....	166
6.6. Discussion.....	172
6.7. Conclusion.....	175

Figure 6-1. Summary of intrinsic and extrinsic apoptotic pathway leading to activation of Caspase 3 (adapted from Harrington HA, Ho KL, Ghosh S, Tung KC. Construction and analysis of a modular model of caspase activation in apoptosis. <i>Theor Biol Med Model.</i> 2008;5:26). ..	147
Figure 6-2. Caspase expression x 400.....	151
Figure 6-3. Caspase expression at transition zone, area on the right is ablated tissue x 20.....	152
Figure 6-4. Caspase expression at the transition zone, the area on the right is ablated tissue x 100.....	153
Figure 6-5 Caspase expression 4 hours post microwave ablation; median values and range plotted.....	156
Figure 6-6. Caspase expression 24 hours post microwave ablation; median values and range plotted.....	158
Figure 6-7 Caspase expression 4 hours post RF ablation; median values and range plotted.....	162
Figure 6-8 Caspase expression 24 hours post RF ablation; median values and range plotted ...	164
Figure 6-9. Caspase expression 4 hours post cryotherapy ablation; median values and range plotted.....	168
Figure 6-10. Caspase expression 24 hours post cryotherapy ablation; median values and range plotted.....	170

6. Chapter 6: Caspase 3

6.1. Introduction: Apoptosis

Apoptosis is a genetically programmed, morphologically distinct form of cell death that can be triggered by a variety of physiological and pathological stimuli such as cytokines, hormones, viruses and toxic insults ¹. Apoptosis is defined morphologically as having distinct features; cytoplasm shrinkage, active membrane blebbing, chromatin condensation and typically fragmentation into membrane-enclosed vesicles ². These are accompanied by changes on the cell surface that promote the recognition of phagocytes and intracellular changes including, degradation of chromosomal DNA into high molecular weight and oligonucleosomal fragments along with cleavage of a specific subset of cellular polypeptides. This cleavage is accomplished by a specialised family of Cysteine-dependent *AS*Partate-directed prote~~ASES~~ termed caspases, so called as they are all proteases which cleave protein (usually each other) at the *Asp* residue ¹.

6.2. Caspase 3

There are 2 main caspase dependent methods of apoptosis; intrinsic or mitochondrial pathway and extrinsic or death receptor pathway which converge on Caspase 3, commonly known as the “executioner” caspase. It is the conversion of procaspase 3 to caspase 3 which exposes a novel peptide end and it is this neoepitope that is detected by immunocytochemistry. Caspase 3 then

creates an expanding cascade of proteolytic activity, much like the complement or clotting cascade. This leads to digestion of structural proteins in the cytoplasm, degradation of chromosomal DNA and eventually phagocytosis of the cell (Figure 6-1. Summary of intrinsic and extrinsic apoptotic pathway leading to activation of Caspase 3).

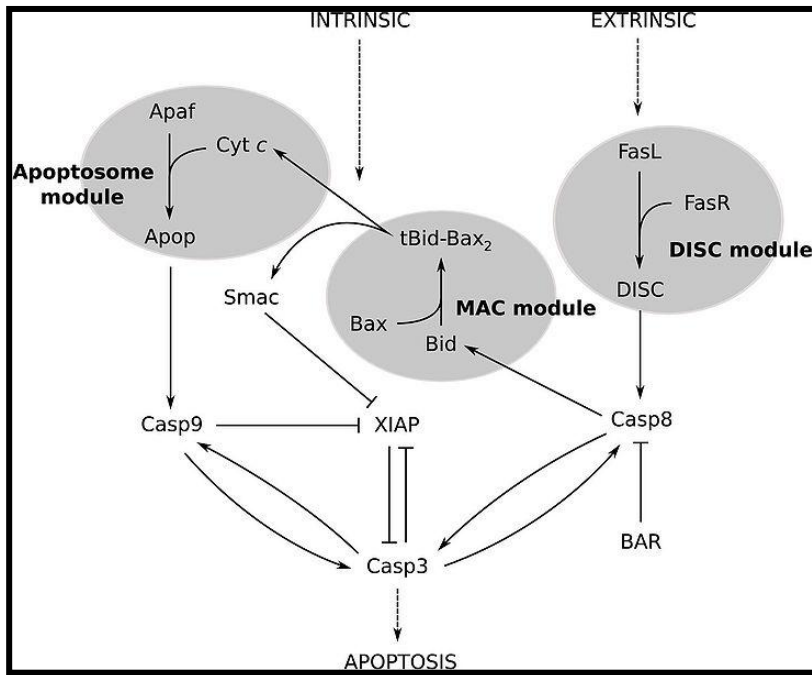


Figure 6-1. Summary of intrinsic and extrinsic apoptotic pathway leading to activation of Caspase 3 (adapted from Harrington HA, Ho KL, Ghosh S, Tung KC. Construction and analysis of a modular model of caspase activation in apoptosis. *Theor Biol Med Model.* 2008;5:26).

6.2.1. Intrinsic or mitochondrial pathway

In a healthy cell, the outer membranes of its mitochondria display the *Bcl-2* protein on their surface, which inhibits apoptosis. Internal damage to the cell causes a related protein, *Bax*, to migrate to the surface of the mitochondria, where it inhibits the protective effect of Bcl-2 and punches holes into the surface, causing *Cytochrome c* to leak into the cytoplasm. This binds to Apaf-1 (Apoptotic Protease Activating Factor-1) and forms the apoptosome. This then binds and activates caspase-9, which subsequently cleaves and activates caspase 3.

6.2.2. Extrinsic or death receptor pathway

The death inducing signalling pathway (DISC) is formed by the ligation of transmembrane death receptors such as Tumour Necrosis Factor (TNF) Receptor family, TNFR1 such as Fas with extracellular death ligands like FasL. This complex recruits procaspase-8 through proximity-induced self-cleavage, hence activating caspase-8. This subsequently activates caspase 3 downstream. The extrinsic initiator caspase (caspase 8) initiates the mitochondrial apoptosis-induced channel (MAC), which leads to activation of the intrinsic pathway; thereby coupling the two pathways.

6.2.3. Caspase 3 and ablation

Several studies in the rat liver have demonstrated caspase 3 expression to be a far more sensitive marker of apoptosis than H&E ³⁻⁵. It is also superior to traditional methods of apoptosis detection such as terminal deoxynucleotide transferase-mediated dUTP nick end labelling (TUNEL) technique, particularly as TUNEL is unable to distinguish DNA strand breakages due to apoptotic, necrosis or over-fixation artefacts ⁶⁻⁸.

Caspase 3 expression has been studied post microwave ⁹ and radiofrequency ablation ¹⁰ in the rat liver. The study by Ohno et al, measures caspase 3 activity by flow cytometry in the transition zone immediately, 2, 6, 12, 24,72 and 168 hours post microwave ablation and reports peak activity at 2 hours ⁹. The study by Vanagas et al confirmed caspase activity 1 hour post radiofrequency ablation in the transition zone by immunoblotting and immunocytochemical methods, however they did not measure caspase 3 expression at any other time point ¹⁰. Both studies agree that apoptosis is confined to the transition zone and no intra-lesional (applicator and central zone) apoptosis occurs. They believe that this ongoing apoptotic activity post ablation causes expansion of the ablation site and subsequently influences the final ablation size. Neither of the two studies investigated the influence of surrounding vasculature on caspase 3 expression. There are no published studies of caspase 3 expression post cryotherapy ablation.

6.3. Aims of this study

This aims are to;

-Quantify the degree of apoptosis in ablated or the transition zone for each modality at different time points and determine peak caspase 3 activity.

-Determine if caspase 3 expression is influenced by the distance between the ablation edge and the hilum.

-Determine if there is a difference in apoptosis expression between microwave, radiofrequency ablation and cryotherapy.

6.4. Caspase analyses

Haematoxylin and Eosin analyses in Chapter 4 described edge apoptosis extending to normal parenchyma visible in all modalities at up to 48 hours post ablation. The purpose of this study is to analyse and quantify the degree of apoptosis by measuring caspase expression. The method for caspase detection is described in Chapter 2. Only whole cytoplasmic staining was counted and any weak background granular staining was ignored. This was quite rare due to the specific unambiguous binary nature of caspase expression (Figure 6-2. Caspase expression x 400). Analyses were performed by viewing the slides under high power (x 100) light microscope fitted with a graticule containing 100 squares. Caspase cell expression was counted in 10 fields moving in a perpendicular line away from the ablated/central area towards normal tissue. At this magnification, a 1cm x 1cm graticule, covers 1mm of tissue, thus allowing a count to be made every millimetre (Figure 6-3. Caspase expression at transition zone, area on the right is ablated tissue x 20 and Figure 6-4. Caspase expression at the transition zone, the area on the right is

ablated tissue x 100). Tissue samples and time points were the same as those used for H&E and HSP 70 analyses i.e. 0, 4, 24, 48 hours, 2 weeks and 1 month. Five rats were sacrificed at each time point and each rat had undergone similar ablations to those in H&E and HSP 70 analyses. This provided 5 proximal, 5 intermediate and 5 distal samples to analyse for each modality at each of the time points. In addition, unablated normal liver tissue was also included in each run, thereby providing a background ‘turnover’ rate of apoptosis that takes place in the normal liver.

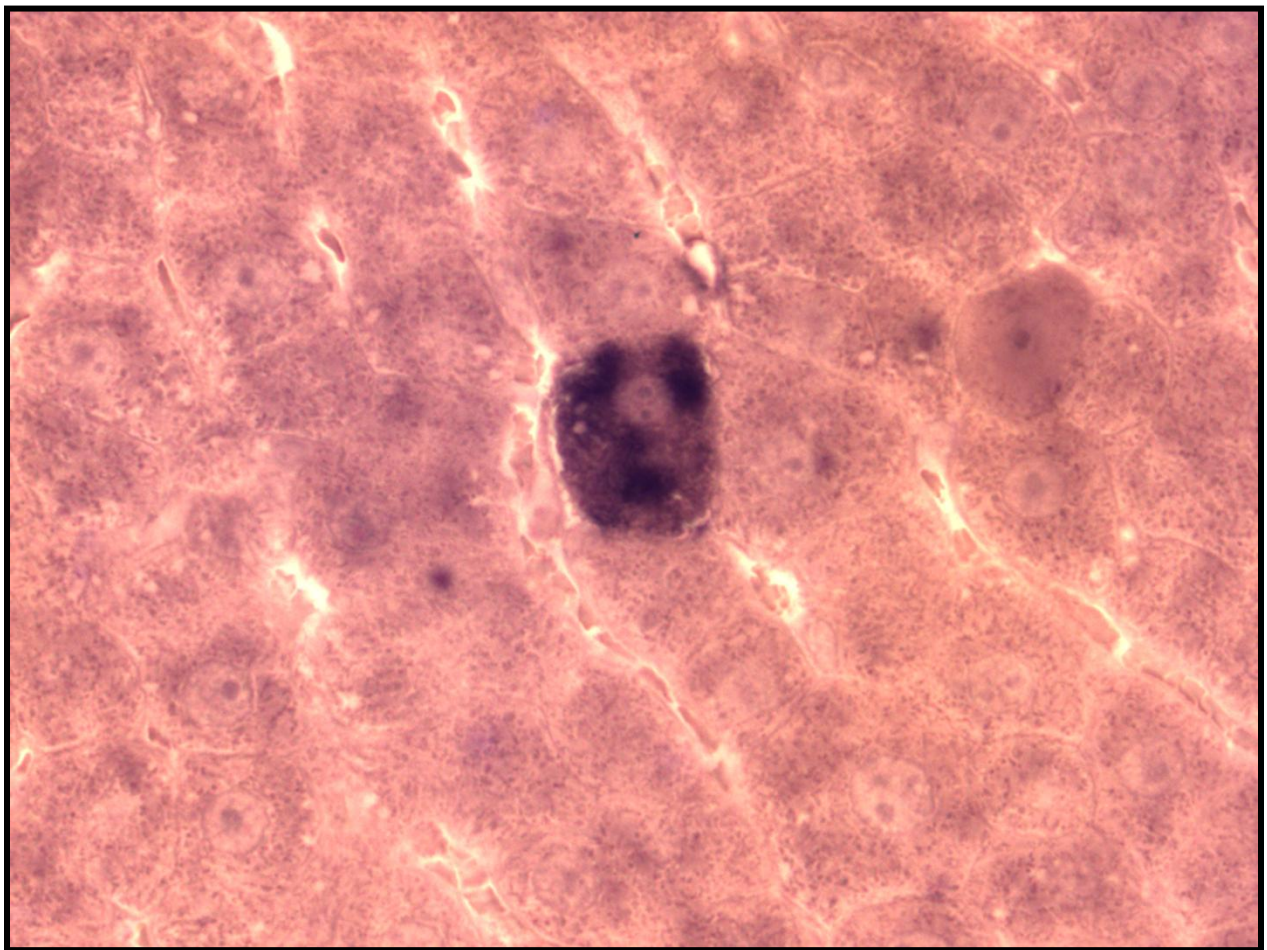


Figure 6-2. Caspase expression x 400



Figure 6-3. Caspase expression at transition zone, area on the right is ablated tissue x 20

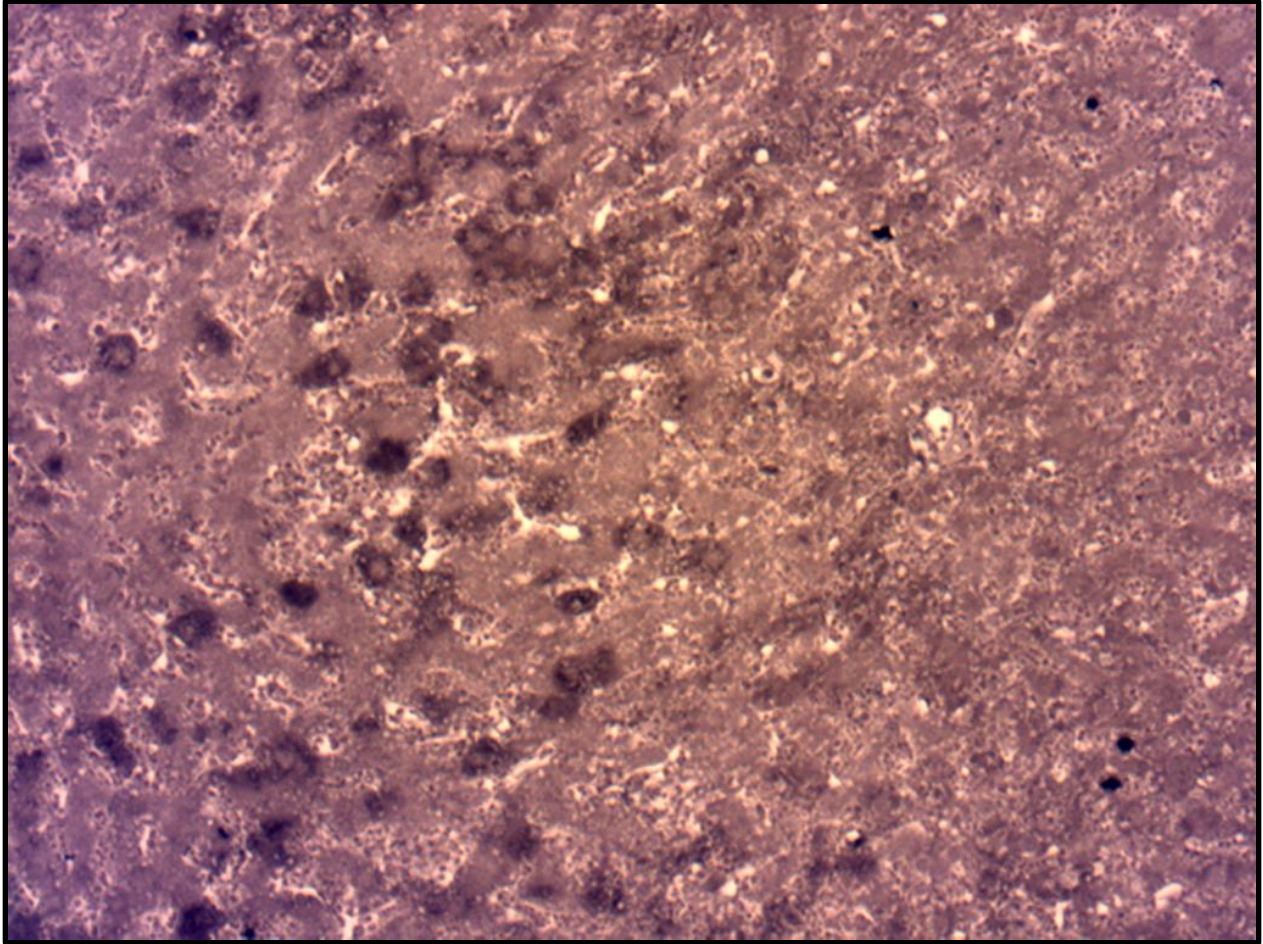


Figure 6-4. Caspase expression at the transition zone, the area on the right is ablated tissue x 100

6.5. Results

6.5.1. Normal unablated liver

Normal liver had a median background apoptotic rate of 3 cells (range 0-4 cells) per graticule area of apoptotic activity. This was the case in all random liver samples taken from unablated liver.

6.5.2. Microwave ablation

No Caspase 3 expression was detected in the ablated applicator or central zone at any of the time points and was first detected 4 hours post ablation in the transition zone (Table 6-1. Caspase expression 4 hours post Microwave ablation and Figure 6-5 Caspase expression 4 hours post microwave ablation; median values and range plotted). Maximum activity was found at the burn edge, which was regular, in the transition zone which reduced moving further away from the transition zone and closer towards the hilum. Caspase activity was detectable at 24 hours, albeit decreased compared to activity at 4 hours ($p=0.018$) (Table 6-2. Caspase expression 24 hours post Microwave ablation and Figure 6-6. Caspase expression 24 hours post microwave ablation; median values and range plotted) and was sporadic at 48 hours (Table 6-3. Caspase expression 48 hours post Microwave ablation). No significant difference in caspase expression was found between distal, intermediate and proximal ablations.

Hilar Distances	Distal					Intermediate					Proximal				
	Time 4 hours														
Distance from edge of ablation in millimetres	No of cells in each of the 5 rats														
	1	2	3	4	5	1	2	3	4	5	1	2	3	4	5
1	29	27	26	25	30	25	25	24	19	17	27	28	27	25	23
2	23	24	21	18	22	21	21	19	18	19	19	18	22	21	22
3	17	13	15	19	16	15	13	15	14	15	12	13	14	12	12
4	12	10	14	13	12	11	12	10	10	9	14	13	12	15	12
5	10	10	12	11	9	8	8	9	7	8	10	8	11	12	9
6	6	7	8	4	5	3	5	5	6	5	6	5	6	10	9
7	6	5	2	3	4	4	2	2	3	3	4	4	4	2	3
8	5	4	5	4	3	4	3	4	3	2	3	5	6	4	3
9	3	1	2	1	4	2	1	2	3	2	3	4	5	5	2
10	3	1	1	3	1	4	1	1	0	3	3	2	3	6	2

Table 6-1. Caspase expression 4 hours post Microwave ablation

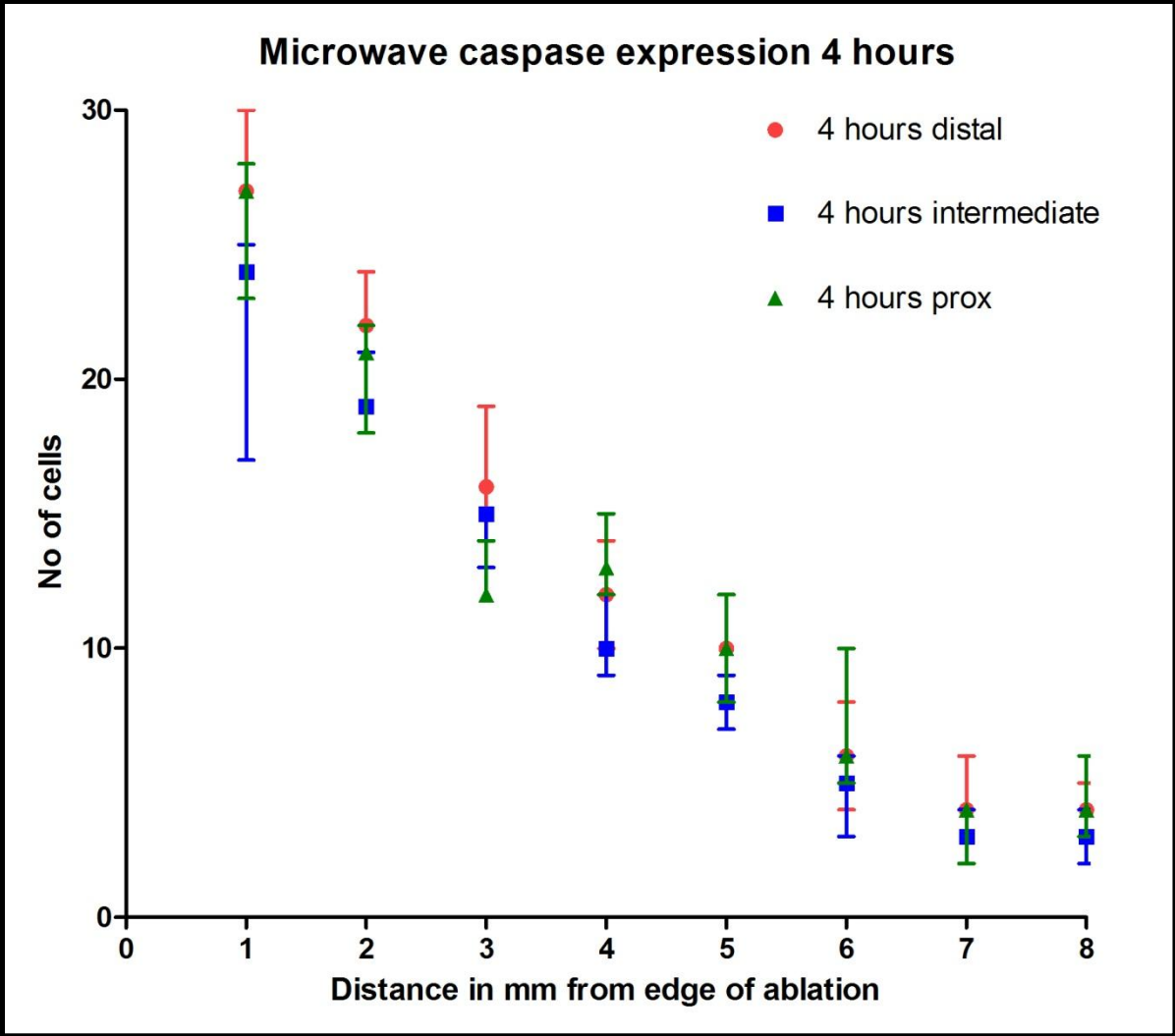


Figure 6-5 Caspase expression 4 hours post microwave ablation; median values and range plotted

Hilar Distances	Distal					Intermediate					Proximal				
	Time 24 hours														
Distance from edge of ablation in millimetres	No of cells in each of the 5 rats														
	1	2	3	4	5	1	2	3	4	5	1	2	3	4	5
1	14	13	14	13	12	12	12	13	13	12	12	13	14	12	11
2	10	10	12	11	9	10	10	12	11	9	10	10	11	12	11
3	12	12	11	11	8	10	8	9	9	9	11	12	9	9	10
4	10	10	10	9	8	9	10	8	8	7	6	5	10	8	7
5	5	4	4	3	5	5	5	5	4	4	4	4	6	6	6
6	3	3	2	2	3	3	4	2	1	3	3	3	2	2	3
7	4	2	2	2	1	5	2	2	2	1	4	2	2	2	1
8	4	2	1	2	1	4	2	1	2	1	4	2	1	2	1
9	2	3	3	4	2	2	3	3	4	1	2	3	3	4	2
10	1	2	1	2	2	1	1	1	2	2	1	2	1	2	2

Table 6-2. Caspase expression 24 hours post Microwave ablation

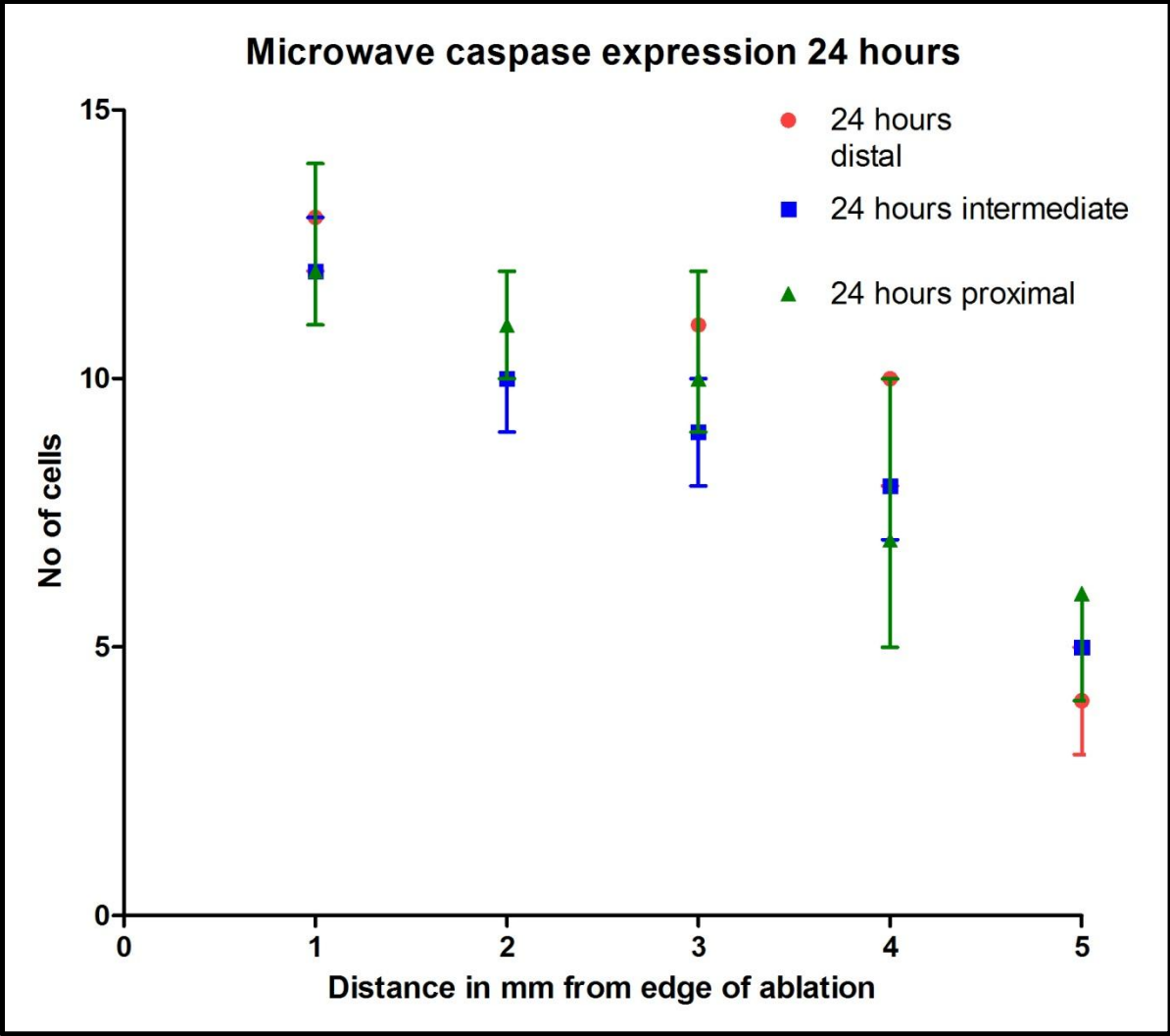


Figure 6-6. Caspase expression 24 hours post microwave ablation; median values and range plotted

Hilar Distances	Distal					Intermediate					Proximal				
	Time 48 hours														
Distance from edge of ablation in millimetres	No of cells in each of the 5 rats														
	1	2	3	4	5	1	2	3	4	5	1	2	3	4	5
1	3	3	2	2	3	3	3	2	2	3	3	3	2	2	3
2	4	2	2	2	1	5	2	2	2	3	3	2	2	2	1
3	4	2	1	2	1	3	2	4	3	1	4	4	1	2	3
4	2	3	3	4	2	3	3	3	3	2	2	3	2	4	1
5	1	2	1	2	2	2	3	1	4	2	1	2	1	2	2
6	3	3	2	2	3	4	3	2	1	3	3	3	4	3	3
7	4	2	2	2	1	2	2	4	2	1	4	2	2	2	4
8	4	2	1	2	1	3	5	1	2	3	3	4	2	4	1
9	2	3	3	4	2	4	4	3	2	2	3	2	3	4	4
10	1	2	1	2	2	1	2	1	2	2	1	2	1	2	2

Table 6-3. Caspase expression 48 hours post Microwave ablation

6.5.3. Radiofrequency

No Caspase 3 expression was detected in the ablated applicator or central zone at any of the time points and similar to microwave ablation was first detected 4 hours post ablation in the transition zone. It was detectable at a lower level 24 hours post ablation compared to activity at 4 hours ($p=0.02$) but expression was sporadic at 48 hours (Table 6-4. Caspase expression 4 hours post Radiofrequency ablation, Table 6-5. Caspase expression 24 hours post radiofrequency ablation and Table 6-6. Caspase expression 48 hours post Radiofrequency ablation). The greatest amount of activity was found adjacent to the edge of the burn in the transition zone and this reduced as the distance from the edge increased (Figure 6-7 Caspase expression 4 hours post RF ablation; median values and range plotted and Figure 6-8 Caspase expression 24 hours post RF ablation; median values and range plotted). Again no significant differences were detected between proximal, intermediate and distal ablations. At 48 hours, normal background apoptosis was detected (Table 6-6. Caspase expression 48 hours post Radiofrequency ablation), this continued in a sporadic fashion at up to 1 month post ablation.

Hilar Distances	Distal					Intermediate					Proximal				
	Time 4 hours														
Distance from edge of ablation in millimetres	No of cells in each of the 5 rats														
	1	2	3	4	5	1	2	3	4	5	1	2	3	4	5
1	24	26	23	22	23	20	20	22	20	20	21	21	20	18	24
2	19	18	17	19	18	16	18	16	19	18	18	17	16	16	16
3	15	14	15	15	11	14	13	11	14	11	10	13	10	10	9
4	13	15	13	11	10	10	12	11	12	10	10	8	10	8	9
5	8	9	10	9	7	9	8	7	8	6	9	8	7	6	6
6	9	10	10	7	9	8	8	10	8	6	8	9	10	9	8
7	8	9	7	7	6	5	6	7	8	8	9	8	7	6	6
8	4	4	5	5	4	5	5	4	4	5	6	5	5	6	5
9	3	3	2	1	3	3	2	1	3	4	2	4	3	2	1
10	1	2	3	2	1	1	2	1	2	2	1	2	1	2	2

Table 6-4. Caspase expression 4 hours post Radiofrequency ablation

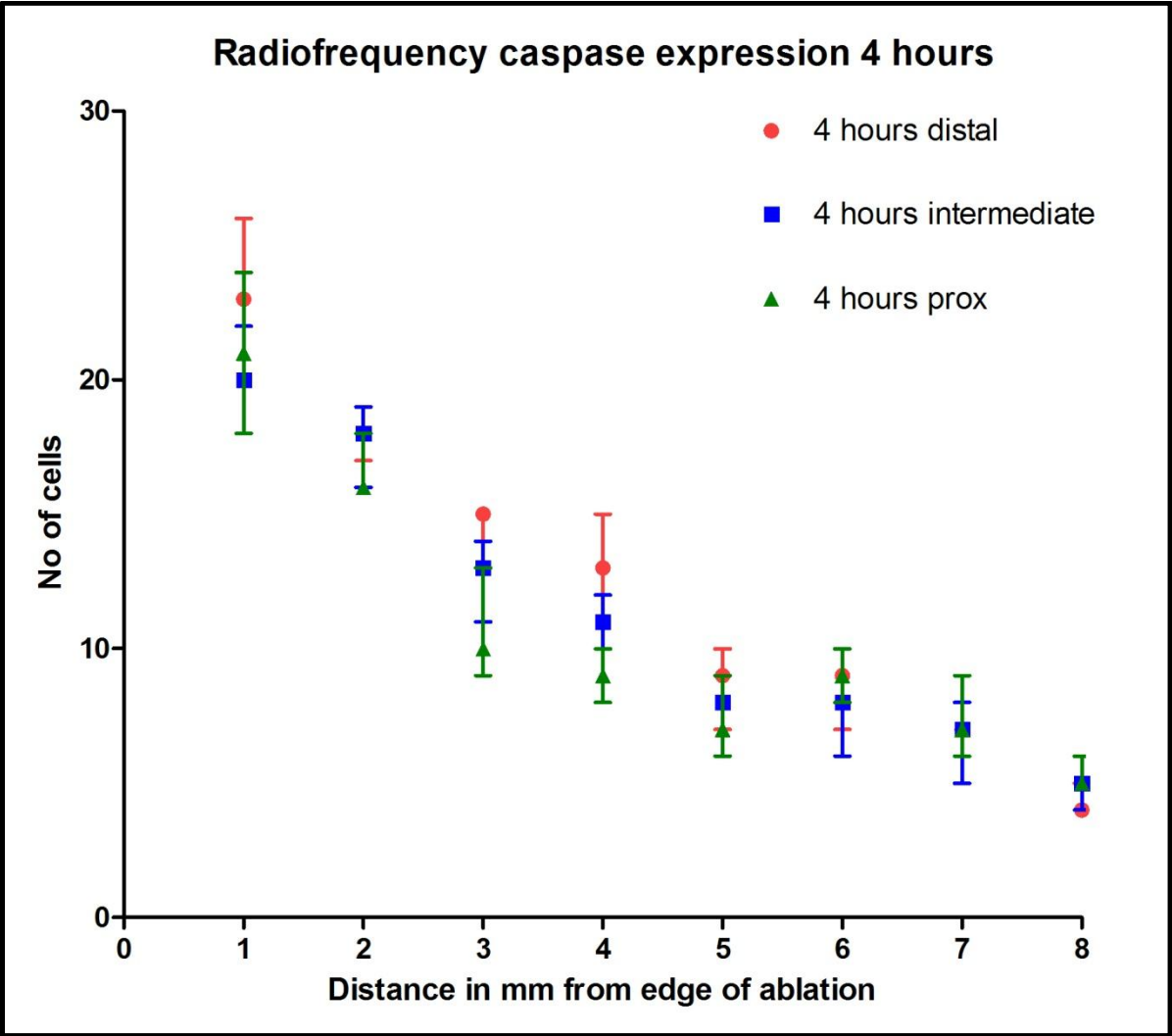


Figure 6-7 Caspase expression 4 hours post RF ablation; median values and range plotted

Hilar Distances	Distal					Intermediate					Proximal				
	Time 24 hours														
Distance from edge of ablation in millimetres	No of cells in each of the 5 rats														
	1	2	3	4	5	1	2	3	4	5	1	2	3	4	5
1	12	12	13	10	10	12	10	9	9	9	10	9	10	10	9
2	13	12	10	11	9	9	8	9	9	9	9	8	9	9	8
3	7	7	6	8	6	6	7	6	5	4	5	5	6	5	4
4	4	5	6	6	6	2	4	5	4	4	5	4	4	4	4
5	5	4	4	6	5	4	5	6	5	4	5	4	4	6	5
6	4	4	5	5	4	3	4	3	3	4	4	4	3	3	4
7	4	3	3	2	3	4	3	2	3	3	3	3	4	3	3
8	3	4	2	4	1	3	4	2	4	1	3	5	1	2	3
9	3	2	3	4	4	3	2	3	4	4	4	4	3	2	2
10	1	2	1	2	2	1	2	1	2	2	1	2	1	2	2

Table 6-5. Caspase expression 24 hours post radiofrequency ablation

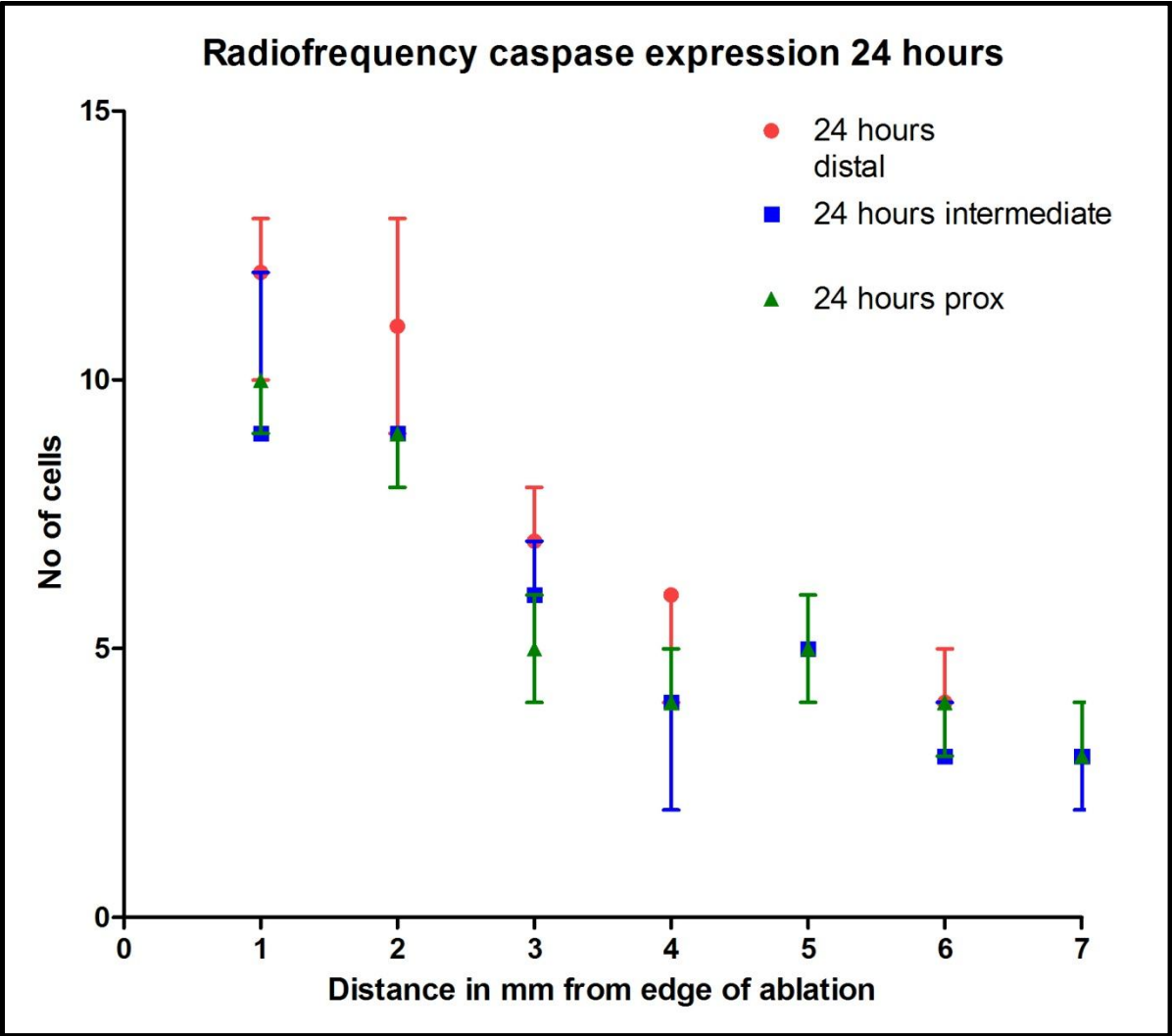


Figure 6-8 Caspase expression 24 hours post RF ablation; median values and range plotted

Hilar Distances	Distal					Intermediate					Proximal				
	Time 48 hours														
Distance from edge of ablation in millimetres	No of cells in each of the 5 rats														
	1	2	3	4	5	1	2	3	4	5	1	2	3	4	5
1	3	3	2	2	3	4	3	3	2	2	3	3	2	3	1
2	2	3	1	2	1	5	2	4	2	3	2	2	2	2	2
3	2	4	2	2	1	5	2	2	3	2	5	4	1	2	4
4	1	2	4	4	2	2	3	1	3	2	3	3	2	4	2
5	3	3	4	2	2	1	3	3	4	2	1	2	1	2	5
6	2	1	3	2	3	3	3	2	1	3	3	6	4	2	4
7	2	4	4	2	1	6	2	4	2	2	4	2	2	2	4
8	1	2	3	2	1	2	3	1	2	3	3	5	2	1	1
9	2	4	5	4	2	1	4	3	2	4	3	2	3	4	4
10	1	1	6	2	2	1	2	1	2	3	1	3	1	0	2

Table 6-6. Caspase expression 48 hours post Radiofrequency ablation

6.5.4. Cryotherapy

Caspase expression was first detected at 4 hours in the transition zone and non-ablated tissue. Unlike microwave and radiofrequency ablation, apoptotic activity was haphazard and unpredictable (Table 6-7. Caspase expression 4 hours post cryotherapy ablation and Figure 6-9. Caspase expression 4 hours post cryotherapy ablation; median values and range plotted). Similarly at 24 hours, although caspase activity was detected at the transition zone, it was haphazard and irregular (Table 6-8. Caspase expression 24 hours post cryotherapy ablation.). At 48 hours there was sporadic activity (Table 6-9. Caspase expression 48 hours post cryotherapy ablation), which continued at 1 month.

Hilar Distances	Distal					Intermediate					Proximal				
	Time 4 hours														
Distance from edge of ablation in millimetres	No of cells in each of the 5 rats														
	1	2	3	4	5	1	2	3	4	5	1	2	3	4	5
1	22	15	17	15	14	24	18	27	17	16	13	6	12	7	18
2	5	6	16	29	11	22	25	14	16	17	16	11	6	13	24
3	7	11	15	14	6	22	21	21	22	9	12	18	22	14	14
4	5	8	6	22	19	11	12	12	10	9	8	17	23	16	15
5	11	10	12	11	9	13	11	10	9	9	16	15	14	18	19
6	5	5	3	3	4	2	3	4	2	3	6	12	17	4	6
7	6	4	3	5	6	3	4	3	5	6	8	9	9	5	7
8	4	4	5	5	7	2	4	2	3	4	1	2	2	3	7
9	3	4	2	1	3	5	4	3	2	2	3	3	2	4	3
10	2	3	3	4	5	5	5	2	3	4	2	3	4	2	3

Table 6-7. Caspase expression 4 hours post cryotherapy ablation

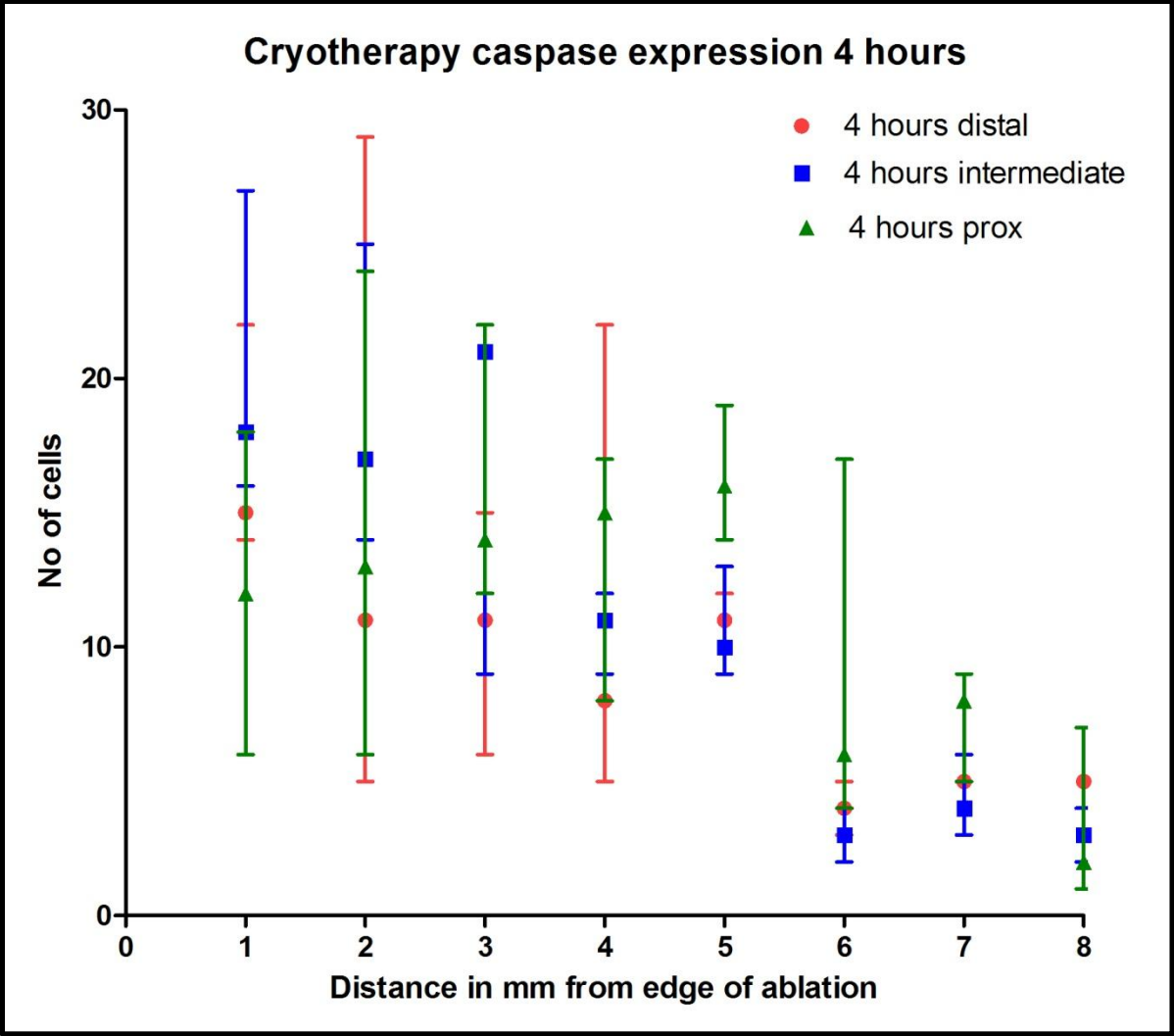


Figure 6-9. Caspase expression 4 hours post cryotherapy ablation; median values and range plotted

Hilar Distances	Distal					Intermediate					Proximal				
	Time 24 hours														
Distance from edge of ablation in millimetres	No of cells in each of the 5 rats														
	1	2	3	4	5	1	2	3	4	5	1	2	3	4	5
1	7	15	10	15	3	7	11	1	8	4	13	6	12	7	1
2	5	6	13	9	11	14	13	14	1	7	10	11	6	13	4
3	7	11	15	14	6	11	4	8	2	9	12	6	5	14	14
4	5	8	6	6	9	11	12	12	10	9	8	4	3	14	15
5	11	10	1	11	9	13	11	10	9	9	6	5	14	4	9
6	5	5	3	3	4	2	3	4	2	3	6	12	3	4	6
7	6	4	3	5	6	3	4	3	5	6	8	9	9	5	7
8	4	4	5	5	7	2	4	2	3	4	1	2	2	3	7
9	3	4	2	1	3	5	4	3	2	2	3	3	2	4	3
10	2	3	3	4	5	5	5	2	3	4	2	3	4	2	3

Table 6-8. Caspase expression 24 hours post cryotherapy ablation.

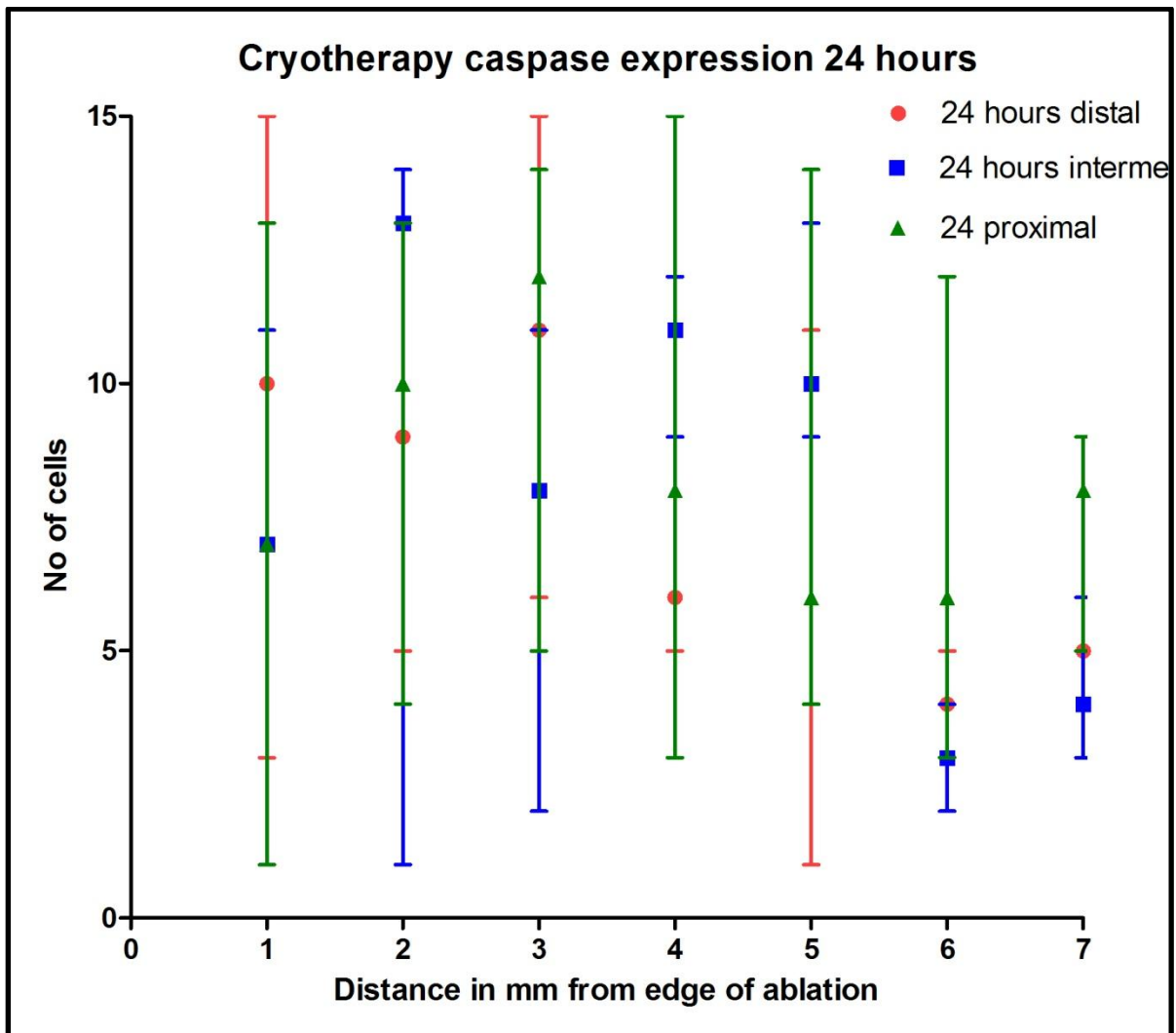


Figure 6-10. Caspase expression 24 hours post cryotherapy ablation; median values and range plotted.

Hilar Distances	Distal					Intermediate					Proximal				
	Time 48 hours														
Distance from edge of ablation in millimetres	No of cells in each of the 5 rats														
	1	2	3	4	5	1	2	3	4	5	1	2	3	4	5
1	2	0	4	1	4	1	2	3	4	3	2	0	3	1	1
2	3	1	3	3	2	2	3	3	2	2	0	0	3	2	3
3	2	3	2	2	2	0	3	3	2	3	2	0	1	3	5
4	1	2	4	2	4	1	2	0	3	1	3	4	2	3	4
5	2	0	1	3	1	3	5	4	2	2	3	1	3	2	1
6	4	3	4	3	3	4	2	3	3	1	0	4	3	3	3
7	2	4	3	2	4	2	4	3	3	4	3	4	3	2	4
8	4	2	3	2	3	1	3	4	1	1	1	2	2	3	3
9	3	3	2	3	3	4	3	4	2	2	1	2	3	4	4
10	1	2	1	3	2	1	2	3	1	3	0	2	2	3	3

Table 6-9. Caspase expression 48 hours post cryotherapy ablation

6.6. Discussion

Haematoxylin & Eosin (H&E) analyses revealed ablation edge apoptosis in the transition zone post ablation in all modalities (Chapter 4) and although the histological features of apoptosis are well described (condensed densely eosinophilic cytoplasm, shrunken homogenous hyperchromatic nuclei but intact nuclear and plasma membranes), it can lead to over- or underestimation as it is subject to inter observer variability. Caspase expression is far more accurate due to its unambiguous binary nature.

This study confirmed the lack of apoptotic activity in the ablated tissue as predicted by the histological appearance of tissue stained with H&E, most likely due to the rapidity with which the cells undergo coagulative necrosis (microwave and radiofrequency) and intracellular freezing (cryotherapy). Lack of apoptotic activity in the transition zone at time 0 is probably due to the fact that very little energy is dissipated outside the immediate applicator and central zone. Caspase expression was first detected 4 hours post microwave, radiofrequency and cryotherapy ablation, in the transition zone. The degree of apoptosis was much more predictable and uniform in radiofrequency and microwave ablated tissue where, the greatest amount of apoptotic activity took place immediately adjacent to the ablated area, with a reduction in activity moving further from the ablation edge and towards the hilum as there is a reduction in temperature gradient away from the site of applicator insertion¹⁰. Peak activity was at 4 hours, reducing at 24 hours

and sporadic at 48 hours. This is in keeping with previous studies mentioned earlier. The background apoptotic rate of normal unablated liver was around 3 cells per graticule area and at 4 hours, radiofrequency and microwave ablation both reached a median of 3 cells at 8 mm and 5 mm respectively from the ablation edge (P=0.03 Wilcoxon analysis). This is significant as it suggests that microwave energy has a smaller transition zone and a sharper cut off compared to radiofrequency ablation. This may be due to rapid coagulation of blood vessels draining the ablated tissue and hence reducing the amount of heat 'transference' distally. In clinical terms this means that microwave only ablates intended tissue and does not damage liver distal to the tumour; an important criteria when ablating large volume primary tumours in cirrhotic livers, where the functional reserve may be limited. It also may account for the lower levels of systemic inflammatory response observed with microwave compared to radiofrequency ablation ¹¹. Cryotherapy ablation was extremely haphazard and difficult to predict at both 4 and 24 hours and therefore cannot be used in any comparative analyses.

Cells undergoing extra-lesional apoptosis post ablation may account for the increase in macroscopic ablation size observed at 4 and 24 hours in tissues ablated with all three modalities (Chapter 4). The increase in size of the transition zone and subsequent final ablated volume has been previously described in liver tissue subjected to microwave ablation, in which peak caspase activity and DNA fragmentation occurred between 2-6 hours and accounted for an increase in the transition zone width and subsequent ablation size ⁹. This phenomenon has also been reported in porcine liver subjected to radiofrequency ablation ^{10, 12} but no reports exist of such an experiment involving cryotherapy ablation. Thermal tumour destruction occurs in two distinct phases. The initial *direct* phase is multifactorial and depends on the total energy applied, tumour biology and

microenvironment. The *indirect* phase occurs after the application of the heat energy and is responsible for the progression of tissue damage^{13, 14}. The indirect mechanism of injury, which continues after cessation of the thermal insult is known to denature important enzymes and may initiate apoptosis^{15, 16} and thus may be ultimately responsible for the completeness of the ablation. This mechanism is of particular clinical significance as often clinicians aim to include a 10mm rim of normal tissue when ablating liver tumours; a 'safety margin'. The characterisation of transition zone apoptosis is thus important as it is often part of this 'normal' rim of tissue and the indirect method of injury can be modulated by a host of factors, including microvascular damage, ischaemia-reperfusion injury, induction of apoptosis, Kupffer cell activation, altered cytokine expression and modulation of the immune response. All ablation were macroscopically 10mm in size and all three modalities showed a macroscopic increase in ablation size at 24 and 48 hours, however this study shows that on a cellular level not all tissue that seems macroscopically abnormal is in fact non-viable. Cells death in the applicator and central zones is unequivocal; however the completeness of cell death in the transition zone is questionable. There is certainly evidence, from Hsp 70 analyses (Chapter 5), that cells in the transition zone are undergoing a stress response and this study further lends itself to the theory that Hsp 70 probably has a role to play in either aiding apoptosis or providing thermotolerance to some cells, thus allowing them to recover. What is difficult to predict however, is which cells in the transition zone will survive and which will succumb to the thermal insult, therefore the transition zone should not be relied upon as providing an effective 'safety margin'

Caspase expression post cryotherapy ablation on the other hand was extremely unpredictable and haphazard. This is in keeping with H&E analyses which describe the ablated/unablated margin as

extremely irregular and scalloped in appearance, thus accounting for the wide variation in apoptotic expression. It is perhaps unsurprising that cryotherapy has over the years declined in its popularity as an ablation modality.

Caspase 3 expression in the transition zone seemed to be unaffected by surrounding vasculature. This is in contrast to Hsp 70 expression which showed a clear variation in expression in relation to the hilar vascular structures. It is difficult to explain the lack of influence of the hilar vascular structures on the degree of apoptosis, however there are several factors which should be considered. The size of the vessels although significantly different between the hilum and the periphery may not be large enough to affect a 10 mm ablation at those sites and RF and microwave may be equal in terms of their potency at that size. Caspase expression in cryotherapy treated tissue was so unpredictable in all ablations that it is difficult to speculate as to the reason why it was unaffected by hilar vessels.

6.7. Conclusion

This study quantified the degree of apoptosis observed in the transition zone at different time points and compared all three modalities. It seems to suggest that microwave tends to cause less collateral damage compared to radiofrequency and establishes cryotherapy ablation as unpredictable and imprecise. Surrounding vasculature does not seem to affect the degree of transition zone apoptosis and further work is required to investigate this in perhaps larger ablations in larger animal models.

1. Earnshaw WC, Martins LM, Kaufmann SH. Mammalian caspases: structure, activation, substrates, and functions during apoptosis. *Annu Rev Biochem* 1999;**68**: 383-424.
2. Wyllie AH, Kerr JF, Currie AR. Cell death: the significance of apoptosis. *Int Rev Cytol* 1980;**68**: 251-306.
3. Eckle VS, Buchmann A, Bursch W, Schulte-Hermann R, Schwarz M. Immunohistochemical detection of activated caspases in apoptotic hepatocytes in rat liver. *Toxicol Pathol* 2004;**32**(1): 9-15.
4. Moronvalle-Halley V, Sacre-Salem B, Sallez V, Labbe G, Gautier JC. Evaluation of cultured, precision-cut rat liver slices as a model to study drug-induced liver apoptosis. *Toxicology* 2005;**207**(2): 203-214.
5. McPartland JL, Guzail MA, Kendall CH, Pringle JH. Apoptosis in chronic viral hepatitis parallels histological activity: an immunohistochemical investigation using anti-activated caspase-3 and M30 cytodetah antibody. *Int J Exp Pathol* 2005;**86**(1): 19-24.
6. Karamitopoulou E, Cioccaro L, Jakob S, Vallan C, Schaffner T, Zimmermann A, Brunner T. Active caspase 3 and DNA fragmentation as markers for apoptotic cell death in primary and metastatic liver tumours. *Pathology* 2007;**39**(6): 558-564.
7. Bantel H, Ruck P, Gregor M, Schulze-Osthoff K. Detection of elevated caspase activation and early apoptosis in liver diseases. *Eur J Cell Biol* 2001;**80**(3): 230-239.
8. Gown AM, Willingham MC. Improved detection of apoptotic cells in archival paraffin sections: immunohistochemistry using antibodies to cleaved caspase 3. *J Histochem Cytochem* 2002;**50**(4): 449-454.
9. Ohno T, Kawano K, Sasaki A, Aramaki M, Yoshida T, Kitano S. Expansion of an ablated site and induction of apoptosis after microwave coagulation therapy in rat liver. *J Hepatobiliary Pancreat Surg* 2001;**8**(4): 360-366.
10. Vanagas T, Gulbinas A, Sadauskiene I, Dambrauskas Z, Pundzius J, Barauskas G. Apoptosis is activated in an early period after radiofrequency ablation of liver tissue. *Hepatogastroenterology* 2009;**56**(93): 1095-1099.
11. Ahmad, F. Gravante, G. Bhardwaj, N. Strickland A. D. Basit, R. West, K. Sorge, R. Dennison, A. R. Lloyd, D. M. . Changes in Interleukin 1 beta and 6 after hepatic microwave tissue ablation compared to radiofrequency, cryotherapy and surgical resections. *American Journal of Surgery* 2010;**in press**.
12. Rai R, Richardson C, Flecknell P, Robertson H, Burt A, Manas DM. Study of apoptosis and heat shock protein (HSP) expression in hepatocytes following radiofrequency ablation (RFA). *J Surg Res* 2005;**129**(1): 147-151.
13. Nikfarjam M, Muralidharan V, Christophi C. Mechanisms of focal heat destruction of liver tumors. *J Surg Res* 2005;**127**(2): 208-223.
14. Nikfarjam M, Malcontenti-Wilson C, Christophi C. Focal hyperthermia produces progressive tumor necrosis independent of the initial thermal effects. *J Gastrointest Surg* 2005;**9**(3): 410-417.
15. Barry MA, Behnke CA, Eastman A. Activation of programmed cell death (apoptosis) by cisplatin, other anticancer drugs, toxins and hyperthermia. *Biochem Pharmacol* 1990;**40**(10): 2353-2362.
16. Benndorf R, Bielka H. Cellular stress response: stress proteins--physiology and implications for cancer. *Recent Results Cancer Res* 1997;**143**: 129-144.

CHAPTER 7: DISCUSSION

7. Chapter 7: Discussion	178
7.1. Aims of the project	178
7.2. Discussion	179
7.3. Unanswered questions	181
7.4. Future directions	181

7. Chapter 7: Discussion

Despite significant advances in pre-operative imaging and anaesthetic optimisation, operative technique and post operative intensive care, the majority of primary and secondary liver tumours are deemed unresectable. However, ablation of these tumours with microwave, radiofrequency and cryotherapy has afforded some patients prolonged survival and therefore represent acceptable alternative treatment modalities. The main drawback with these technologies, as explained in the introduction, is their relatively high rate of recurrence following the treatment of large or peri-vascular tumours. There is a paucity of published evidence comparing all three ablation modalities and there is limited knowledge about the effects of these different ablation modalities on surrounding vasculature. This is not surprising as clinicians will often have a preference for one type of ablation, either due to operator choice or financial constraints.

7.1. Aims of the project

The aim of this study was to compare all 3 modalities and investigate the effect of ablating a set volume of liver in-vivo at various distances from major vascular structures on ablation morphology and surrounding parenchyma, in addition to describing lesion evolution over a

period of time. Ultimately the aim was to enhance our understanding of tumour ablation and work towards the elusive 'ideal' ablation modality.

7.2. Discussion

This project is the only one of its kind which compares pathological changes between all three ablation modalities which also describes lesion evolution over time. All ablations were standardised to 10 mm in size and all experiments were carried out under strict comparable standard laboratory conditions.

Cryotherapy seems to be the least reliable and efficient ablation modality as evidenced by the huge increase in the liver enzyme alanine transaminase (ALT) suggesting extra-lesional hepatocyte damage which was associated with extremely unpredictable and irregular ablation margins as observed by H&E and immuno-cytochemical staining. It is reasonable to conclude that cryotherapy ablation should not be first line therapy for patients with unresectable liver tumours.

The degree of heat-shock protein 70 expression in relation to surrounding vasculature has also never been described before. This is an extremely significant finding as it provides unequivocal evidence that ablation morphology is influenced by surrounding vasculature. In addition, this study also demonstrated that radiofrequency ablation (RFA) has a wider transition zone and a

smaller central zone of coagulative necrosis compared to microwave ablation. This was evident at four and 24 hours. This is significant as it suggests that microwave is more efficient at creating similar volumes of necrotic tissue compared to RFA. It can also be concluded from this study that the ultimate success of an ablation is likely to be influenced by the final fate of the cells in the transition zone.

Radiofrequency and microwave ablation are now well established ablation methods. This project has validated previous experimental data and, moreover, reported several new findings. Very few studies have provided a temporal description of lesion evolution yet this project has established that the majority of significant cellular changes that influence ablation success occur within the first 24 hours. Although apoptosis of cells at the periphery of the ablation zone has been reported before, it has never been quantifiably compared between two techniques. Basic histological staining suggests that RFA and microwave ablation are fairly comparable in terms of their ability to create small volume ablations. However, the higher serum alanine transaminase (ALT) levels observed with RFA, a surrogate marker for hepatocyte damage, and the greater volume of apoptosis observed, further from the ablation margin in the transition zone compared to microwave, suggests that RFA causes greater collateral damage and is less precise than microwave ablation. Unfortunately, there was no evidence that the surrounding vasculature influenced the degree of apoptosis.

As with all health care therapies the financial implications of a technique are a major consideration. The initial expenditure is usually the cost of the machine which can vary

(£20,000-£30,000). In addition, the main on going costs are usually expendables such as the probes, which can cost up to £1000 and in the case of RF the gel pads which cost up to £100. In this project, the microwave machine was the most cost-effective as the probe was re-usable and the main cost was animal husbandry (average £50/animal) and bench fees for consumables (approximately £5000). I was kindly loaned the microwave and cryotherapy machines from the department of surgery at University Hospitals Leicester and the RF machine from the Queens medical centre, University Hospitals Nottingham.

7.3. Unanswered questions

Experimental and clinical evidence suggest that ablation success is dependent on adjacent blood vessels and thus the degree of transition zone apoptosis must be influenced by surrounding blood flow as it is the only part of an ablation which is considered to be significantly variable. The exact nature of this relationship is still not fully understood. In addition the exact role of HSP 70 on the fate of cells in the transition zone, and the subsequent final ablation size and morphology is yet to be determined.

7.4. Future directions

Larger ablations in larger animal models may help answer some of these questions. The rat model, although very useful in this project and economical, is not suitable for ablations over 3cm in diameter. A larger animal model using pigs, although would be more expensive, would provide an opportunity to undertake snap-frozen analyses of tissues at different time frames

following several ablation modalities utilising immuno-histochemical techniques which may be more superior to analysing tissue fixed in paraffin. In addition, larger animals have larger livers so the increase cost per animal may be offset by the ability to create more ablations per animal. Larger blood vessels easily seen on ultrasound means ablations can be monitored under direct ultrasound guidance. In this way, perhaps the effect of heat-sink and blood flow near the ablation can be assessed more accurately.